Supporting Information for

Synthesis and metalation of polycatechol nanohoops derived from fluorocycloparaphenylenes

Ashlyn A. Kamin,[1] Tara D. Clayton,[2] Claire E. Otteson,[2] Paige M. Gannon,[1] Sebastian Krajewski,[1] Werner Kaminsky,[1] Ramesh Jasti,[2] Dianne J. Xiao.[1,*]

[1]Department of Chemistry, University of Washington, Seattle, Washington 98195, United States
[2]Department of Chemistry and Biochemistry, Materials Science Institute, and Knight Campus for Accelerating Scientific Impact, University of Oregon, Eugene, Oregon 97403, United States

*Correspondence to: djxiao@uw.edu

Table of Contents

1. General Materials and Methods:

Reagents and solvents were purchased from commercial vendors (Millipore Sigma, TCI America, Alfa Aesar, Fisher Scientific, Oakwood Chemical, Combi-Blocks) and used without further purification unless otherwise noted. Deuterated solvents were purchased from Cambridge Isotope Laboratories. Oxygen- and moisture-sensitive reactions were performed using standard Schlenk or glovebox procedures under a nitrogen atmosphere. Workups were performed in air unless otherwise specified.

Silica column chromatography was conducted with Zeochem Zeoprep n60 Eco 40-63 μm silica gel. Alumina column chromatography was conducted with SorbTech basic alumina (pH 10), Act. II-III, 50-200 μm. Preparative TLC was performed using Millipore Sigma 200 μm silica gel 60 matrix F_{254} TLC plates.

NMR spectra were acquired using 500 MHz Bruker spectrometers. ^{1}H spectra were referenced to TMS (δ 0.00 ppm) or residual solvent peaks ($CDCl_3$ δ 7.26 ppm, DMSO-d_6 δ 2.50 ppm, and tetrachloroethane-d_2 δ 6.00 ppm). ^{13}C NMR spectra were referenced to residual $CDCl_3$ (δ 77.16 ppm). ^{19}F NMR spectra were indirectly referenced to $CFCl_3$ (δ 0.00 ppm) using a hexafluorobenzene standard (δ –164.9 ppm) or via the Bruker TopSpin 3.5 software suite.

Solution-phase UV-vis spectra were collected on an Agilent Cary 100 UV-vis or Shimadzu UV-3600i Plus UV-vis-NIR spectrophotometer using a 1 cm quartz cuvette.

Standard ESI-MS data were collected on a Bruker Esquire Ion Trap mass spectrometer in positive ion mode. GC-MS data were collected on an Agilent 9573 mass spectrometer in positive ion mode.

High-resolution ESI-MS data for **4MeO-CPP**, **12MeO-CPP**, **12iPrS-CPP**, **12HO-CPP**, **Ru_2(Ph$_2$dhbq)**, and **Ru_2(4O-CPP)** were collected on an LTQ-Orbitrap XL mass spectrometer in positive ion mode. High-resolution ESI-MS data for **4HO-CPP** was collected on the same instrument in negative ion mode.

High-resolution MALDI-TOF data for **4F-MC-OTES** and **4F-CPP** were collected on a Bruker Autoflex Speed LRF mass spectrometer in positive ion mode. High resolution MALDI-TOF data for **Ru_2(4O-CPP)** and **Ru_6(12O-CPP)** were collected on a Waters Synapt XS mass spectrometer in positive ion mode. All samples were prepared in DCM with *trans*-2-[3-(4-*tert*-butylphenyl)-2-methyl-2-propenylidene]malononitrile (DCTB) as a matrix.

2. Synthetic Procedures:

The starting material, **12F-CPP**, was prepared according to published methods by Jasti and coworkers.[1,2] The intermediates, **S1** and **S2**, used in the preparation of **4F-CPP** were prepared according to previously published methods by Jasti and coworkers.[2,3] The terphenyl model ligand, **H_4Ph_2dhbq**, was prepared according to published methods by Xiao and coworkers.[4]

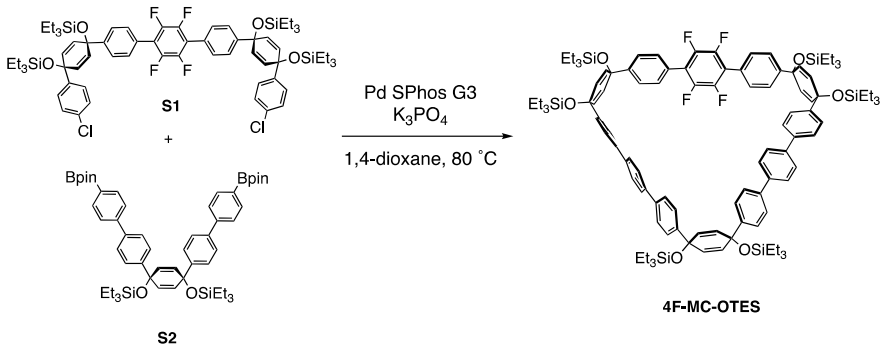

Synthesis of 4F-MC-OTES. To a flame-dried 1 L round-bottom flask equipped with a stir bar was added **S1** (0.6 g, 0.5 mmol, 1.0 equiv), **S2** (0.493 g, 0.55 mmol, 1.1 equiv), and Pd SPhos G3 (78 mg, 0.1 mmol, 0.2 equiv). The flask was placed under high vac for one hour, and subsequently evacuated and backfilled with nitrogen three times. Starting materials were dissolved in 1,4-dioxane (333 mL) and the mixture was sparged with nitrogen for 30 minutes. The mixture was then lowered into a preheated oil bath at 80 ˚C and allowed to stir for 30 minutes. A 2M aqueous solution of K_3PO_4 (33 mL) that had been sparged for 30 minutes prior was added dropwise. The solution was allowed to stir at 80 ˚C overnight. In the morning, the solution was cooled to room temperature, poured over a fritted funnel filled with celite and sodium sulfate, and eluted with ethyl acetate. The eluent was collected, and the solvent was removed *via* rotary evaporation. The resulting brown oil was extracted with ethyl acetate (3 × 100 mL), washed with water (3 × 100 mL), brine (1 × 100 mL), and finally dried over sodium sulfate. After removal of sodium sulfate and solvent, the crude oil was dissolved in DCM, adsorbed onto silica, and purified via silica column chromatography from 0-100% DCM in hexanes. Concentration of fractions afforded **4F-MC-OTES** as an off-white solid (0.28 g, 31%).

^{1}H NMR (500 MHz, $CDCl_3$) δ 7.67 (s, 8H), 7.58 (d, *J* = 8.4 Hz, 8H), 7.52 (d, *J* = 8.5 Hz, 4H), 7.49–7.41 (m, 12H), 6.09 (d, *J* = 10.2 Hz, 4H), 6.06–6.01 (m, 8H), 0.97 (td, *J* = 7.9, 3.8 Hz, 54H), 0.70-0.62 (m, 36H). ^{13}C{^{1}H} NMR (126 MHz, $CDCl_3$) δ 139.66, 131.89, 130.13, 127.48, 126.86, 126.83, 126.52, 126.25, 7.24, 7.22, 7.21, 6.66, 6.62. ^{19}F NMR (471 MHz, $CDCl_3$) δ –144.37 (s). HRMS (MALDI) *m*/*z*: $[M]^+$ calculated for $C_{108}H_{134}F_4O_6Si_6$, 1770.8732; found, 1770.8672.

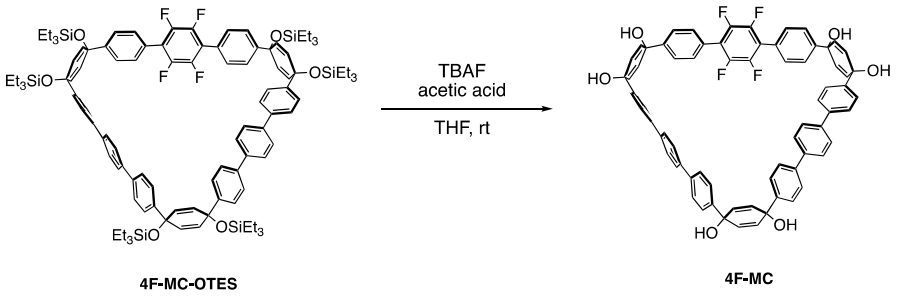

4F-MC-OTES **4F-MC**

Synthesis of 4F-MC. To a flame-dried 250 mL round bottom flask equipped with a stir bar was added **4F-MC-OTES** (0.54 g, 0.305 mmol, 1.0 equiv). This was placed under high vac for an hour and subsequently dissolved in tetrahydrofuran (anhydrous/degassed; 101 mL), resulting in a clear solution. Glacial acetic acid (0.870 mL, 15.2 mmol, 50 equiv) was added quickly dropwise, followed by the slow dropwise addition of tetrabutylammonium fluoride (1M in THF, 7.62 mL, 7.62 mmol, 25 equiv). The colorless solution was allowed to stir under nitrogen overnight at room temperature. The next day, water (50 mL) was added to the reaction mixture, resulting in a white suspension, and THF was removed *via* rotary evaporation. The suspension was poured over a fritted vacuum funnel, resulting in **4F-MC** as a white powder that was washed with water, dried under high vac, and moved on without further purification (0.510 g, 96%).

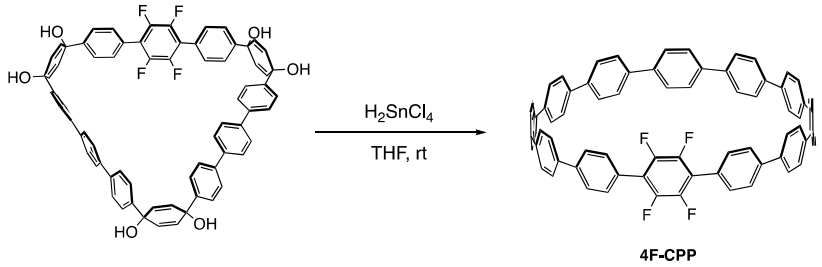

4F-MC **4F-CPP**

Synthesis of 4F-CPP. To a flame-dried 100 mL round bottom flask equipped with a stir bar was added **4F-MC** (0.167 g, 0.154 mmol, 1.0 equiv), which was placed under high vac for an hour and then dissolved in tetrahydrofuran (anhydrous/degassed; 26 mL, 0.006 M). In a separate 100 mL flame dried round bottom flask equipped with a stir bar was added $SnCl_2 \cdot 2H_2O$ (0.181 g, 0.154 mmol, 1.0 equiv) followed by concentrated aqueous HCl (0.133 mL, 0.308 mmol, 2.0 equiv). This was dissolved in tetrahydrofuran (20 mL, 0.040 M) and allowed to stir for 30 minutes at room temperature. The prepared H_2SnCl_4 solution (8.46 mL, 0.040 M, 2.2 equiv) was added to the **4F-MC** solution dropwise resulting in a cloudy yellow-white mixture that was allowed to stir overnight at room temperature. In the morning, a 1M aqueous NaOH solution (30 mL) was added followed by the removal of THF *via* rotary evaporation. The suspension was extracted with DCM (3 × 100 mL), washed with water (3 × 100 mL), brine (1 × 100 mL), and dried over sodium sulfate. After removal of the sodium sulfate and solvent, the crude yellow solid was dissolved in DCM, adsorbed onto alumina, and purified via alumina column chromatography from 0-100% DCM/hexanes. Concentration of fractions afforded **4F-CPP** as a blue-fluorescent yellow solid (36 mg, 24% yield). Single crystals suitable for X-ray diffraction were obtained by vapor diffusion of *n*-heptane into trichloroethylene.

^{1}H NMR (500 MHz, $CDCl_3$) δ 7.67–7.59 (m, 40H), 7.55 (d, J = 8.3 Hz, 4H). ^{13}C{^{1}H} NMR (126 MHz, $CDCl_3$) δ 140.99, 138.99, 138.76, 138.62, 138.59, 138.54, 138.42, 138.32, 130.93, 127.74, 127.48, 127.44, 127.38, 127.00, 126.68. ^{19}F NMR (471 MHz, $CDCl_3$) δ –143.79 (s). HRMS (MALDI) *m*/*z*: $[M]^+$ calculated for $C_{72}H_{44}F_4$, 984.3379; found, 984.3390.

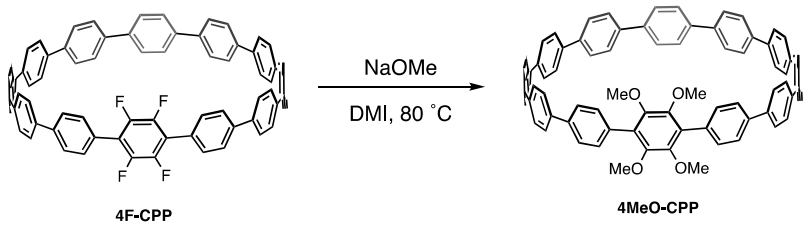

4F-CPP **4MeO-CPP**

Synthesis of 4MeO-CPP. In a nitrogen-filled glovebox, **4F-CPP** (22.8 mg, 23.1 µmol), sodium methoxide (20.3 mg, 0.376 mmol, 16 equiv), and DMI (0.8 mL) were divided evenly between two, 4 mL scintillation vials. The vials were sealed and stirred at 80 ˚C for 16 hr. The contents of both vials were combined. The mixture was removed from the glovebox, diluted with water (20 mL), acidified with 2M aqueous HCl (~15 drops), and the solution was verified to be acidic by pH paper. The resulting white precipitate was collected by vacuum filtration, washed with H_2O, and dried under reduced pressure to give **4MeO-CPP** as an off-white solid (20.7 mg, 87%). Residual DMI (*ca.* 5% by mass) was observed in the ^{1}H NMR spectrum of isolated **4MeO-CPP**, the contribution of which was already removed from the previously stated mass and yield. Further purification could be achieved by preparative TLC (DCM eluent) to give **4MeO-CPP** as off-white solid (17.5 mg, 73%). Single crystals suitable for X-ray diffraction were obtained by vapor diffusion of *n*-heptane into trichloroethylene.

^{1}H NMR (500 MHz, $CDCl_3$) δ 7.67–7.55 (m, 40H), 7.48 (d, J = 8.5 Hz, 4H), 3.50 (s, 12H). ^{13}C{^{1}H} NMR (126 MHz, $CDCl_3$) δ 147.42, 139.33, 138.83, 138.76, 138.70, 138.62, 138.59, 138.50, 138.44, 132.58, 131.43, 128.86, 127.79, 127.61, 127.56, 127.50, 127.48, 127.45, 127.43, 127.37, 127.31, 126.35, 61.18. HRMS (ESI) *m/z*: found 1033.4243 ($[M+H]^+$, calc'd: 1033.4251 for $C_{76}H_{56}O_4H$).

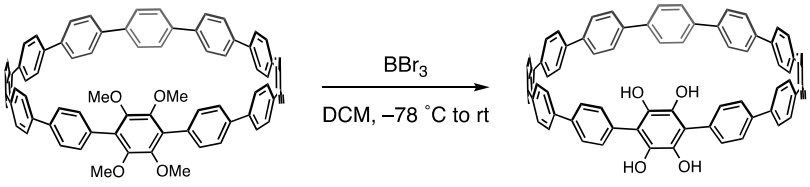

4MeO-CPP **4HO-CPP**

Synthesis of 4HO-CPP. In a Schlenk flask under a nitrogen atmosphere, **4MeO-CPP** (15.8 mg, 15.3 µmol) was dissolved in DCM (degassed/anhydrous, from the glovebox; 4 mL). The solution was cooled to –78 ˚C. A 1M solution of BBr_3 in DCM (0.183 mL, 0.183 mmol, 12 equiv) was added dropwise *via* syringe. The reaction was allowed to return to room temperature over the course of 2-3 hr and stirred overnight without heating. The reaction was cooled to 0 ˚C, quenched carefully by dropwise addition of H_2O (degassed; 10 mL), and stirred for 2 hr. Without exposing the mixture to air, the DCM was removed *in vacuo* and the flask was transferred to a nitrogen-

filled glovebox. Additional H_2O (30 mL) was added, and the mixture was extracted with DCM (3 × 5 mL). The combined organic layers were reduced *in vacuo*, and the resulting solid was washed with pentane to yield **4HO-CPP** as a light yellow/brown solid (13.6 mg, 91%).

^{1}H NMR (500 MHz, $CDCl_3$) δ 7.69–7.54 (m, 44H). ^{13}C NMR (126 MHz, $CDCl_3$) δ 197.23, 193.76, 154.32, 141.95, 140.99, 139.60, 139.46, 139.27, 139.14, 138.97, 138.90, 138.74, 138.64, 138.61, 138.59, 138.49, 138.40, 138.32, 132.07, 131.23, 128.84, 127.81, 127.77, 127.69, 127.63, 127.58, 127.54, 127.50, 127.48, 127.40, 127.38, 127.31, 126.93, 122.20. HRMS (ESI) *m/z*: found 975.3471 ([M-H]$^-$, calc'd: 975.3469 for $C_{72}H_{47}O_4$).

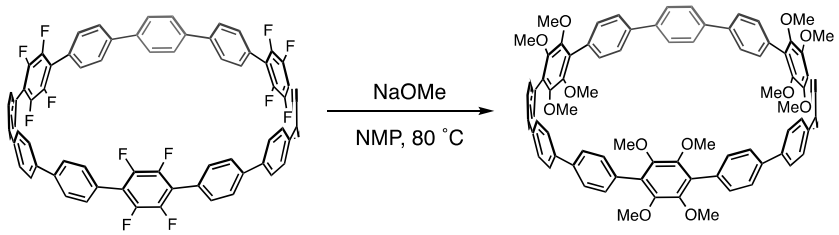

12F-CPP 12MeO-CPP

Synthesis of 12MeO-CPP. In a nitrogen-filled glovebox, **12F-CPP** (99.6 mg, 88.2 µmol), sodium methoxide (229 mg, 4.25 mmol, 48 equiv), and NMP (4 mL) were divided evenly between four, 4 mL scintillation vials. All vials were sealed and stirred at 80 ˚C for 16 hr. The contents of all vials were combined. The mixture was removed from the glovebox and diluted with H_2O (~20 mL). Aqueous 1M HCl (~10 mL) was added, and the solution was verified to be acidic by pH paper. The mixture was then extracted with ethyl acetate (4 × 25 mL). The combined organic layers were washed with H_2O (4 × 30 mL), dried over magnesium sulfate, gravity filtered, and the solvent was removed *in vacuo.* The resulting solid was suspended in minimal cold MeOH, collected via vacuum filtration, and dried *in vacuo* to yield **12MeO-CPP** as an off-white solid (109 mg, 97%). Crystals suitable for X-ray diffraction were grown by slow evaporation out of an acetone/MeOH mixture.

Note: A small degree of premature demethylation may be observed in as-synthesized **12MeO-CPP**. While this is not of concern given our fully demethylated synthetic target, we found that any demethylation could be reversed using the following general procedure. Following heating, the vial(s) were removed from the glovebox, cooled to 0 ˚C, uncapped briefly, and methyl iodide (68 equiv) was added. Once resealed, the vial(s) were stirred at room temperature overnight. The resulting mixture was worked up as previously described, omitting the acidification step, to yield pure **12MeO-CPP** as an off-white solid in 86% yield.

^{1}H NMR (500 MHz, $CDCl_3$) δ 7.66 (s, 12H), 7.59 (d, J = 8.7 Hz, 12H), 7.49 (d, J = 8.7 Hz, 12H), 3.53 (s, 36H). ^{13}C{^{1}H} NMR (126 MHz, $CDCl_3$) δ 147.35, 139.25, 139.19, 132.52, 131.36, 128.77, 127.61, 126.25, 61.07. HRMS (ESI) *m/z*: found 1273.5077 ([M+H]$^+$, calc'd: 1273.5097 for $C_{84}H_{72}O_{12}H$).

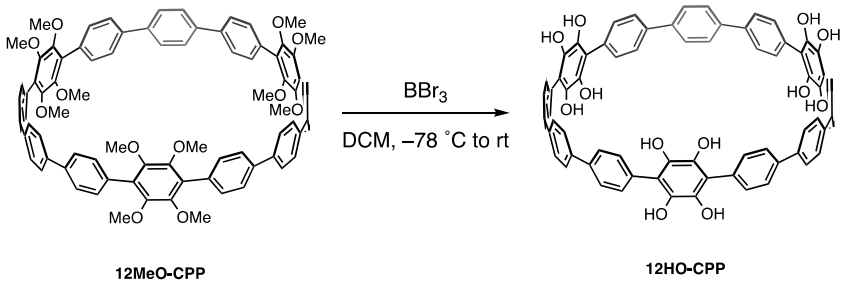

Synthesis of 12HO-CPP. In a Schlenk flask under a nitrogen atmosphere, **12MeO-CPP** (109 mg, 85.4 µmol) was dissolved in DCM (degassed/anhydrous, from the glovebox; 14 mL). The solution was cooled to –78 ˚C. A 1M solution of BBr_3 in DCM (2.05 mL, 2.05 mmol, 24 equiv) was added dropwise via syringe. The reaction was allowed to return to room temperature over the course of 2-3 hr and stirred overnight without heating. The reaction was cooled to 0 ˚C, quenched carefully by dropwise addition of H_2O (degassed; ~55 mL), and stirred for 2 hr. Without exposing the mixture to air, the DCM was removed *in vacuo* and the flask was transferred to a nitrogen-filled glovebox. The precipitate in the flask was recovered by vacuum filtration, washed with H_2O, washed with a minimal amount of MeOH, and dried *in vacuo* to yield **12HO-CPP** as an off-white/brown solid (64.9 mg, 69%).

Note: workups conducted in air resulted in uncontrolled oxidation of the catechol units, as observed by significant peak broadening in the ^{1}H NMR; this oxidation could be partially reversed through reaction with sodium dithionite, however the peaks were significantly less well resolved than for **12HO-CPP** worked up under a nitrogen atmosphere (**Fig. S14**).

^{1}H NMR (500 MHz, DMSO-d_6) δ 7.80 (br), 7.70 (br), 7.58 (br). HRMS (ESI) *m/z*: found 1143.2779 ($[M+K]^+$, calc'd: 1143.2777 for $C_{72}H_{48}O_{12}K$). ^{13}C NMR could not be obtained due to poor solubility.

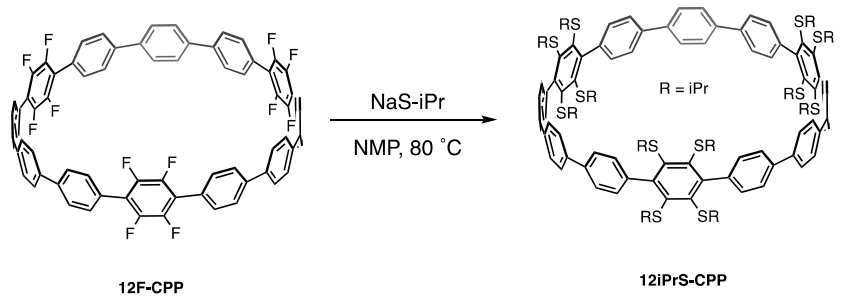

Synthesis of 12iPrS-CPP. An oven-dried Schlenk flask under a nitrogen atmosphere was charged with **12F-CPP** (20.0 mg, 17.7 µmol) and NMP (anhydrous/degassed, from the glovebox; 1.5 mL). Under nitrogen, sodium 2-propanethiolate (68.2 mg, 695 µmol, 39 equiv) was added and the reaction was stirred at 80 ˚C for 12 hr. The reaction was diluted with H_2O (25 mL) and the resulting thiol byproducts were removed *in vacuo*. Additional H_2O (75 mL) was added, and the mixture was extracted with DCM (3 × 20 mL) followed by ethyl acetate (3 × 20 mL). The combined DCM layers were washed with H_2O (5 × 10 mL) and dried over magnesium sulfate. The DCM and ethyl

acetate layers were combined, and the solvent was removed *in vacuo* to yield an oily solid. The solid was suspended in MeOH, filtered, and washed with additional MeOH (~40 mL total) to yield **12iPrS-CPP** as a yellow solid (27.3 mg, 86%). Single crystals could be obtained by slow evaporation out DMSO or a DCM/MeOH mixture, however these crystals were not of suitable quality for X-ray diffraction.

^{1}H NMR (500 MHz, $CDCl_3$) δ 7.56 (s, 12H), 7.41 (d, *J* = 8.1 Hz, 12H), 7.36 (d, *J* = 8.2 Hz, 12H), 3.13 (hept, *J* = 6.7 Hz, 12H), 1.00 (d, *J* = 6.7 Hz, 72H). ^{13}C{^{1}H} NMR (126 MHz, $CDCl_3$) δ 149.82, 140.80, 140.58, 140.37, 140.20, 132.51, 128.22, 126.34, 40.24, 22.81, 1.11. HRMS (ESI) *m/z*: found 1801.6088 ([M+H]$^+$ calc'd: 1801.6111 for $C_{108}H_{120}S_{12}H$).

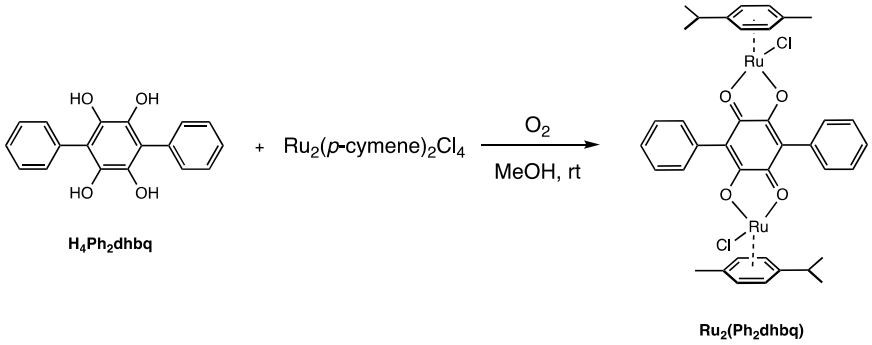

Synthesis of Ru_2(Ph$_2$dhbq). This compound was prepared using a modified procedure from the literature.[5] In a nitrogen-filled glovebox, a 20 mL scintillation vial was charged with **H$_4$Ph$_2$dhbq** (45.0 mg, 0.153 mmol), [Ru(*p*-cymene)Cl_2]$_2$ (95.7 mg, 0.156 mmol, 1 equiv), and MeOH (13 mL). The vial was capped, stirred at room temperature for 10 min, and then removed from the glovebox. The vial was uncapped, and the mixture was stirred while open to air for two days. The resulting dark precipitate was collected by centrifugation and washed with MeOH (3 × 30 mL), diethyl ether (30 mL), and dried *in vacuo* to yield **Ru_2(Ph$_2$dhbq)** as a black solid (89.8 mg, 0.108 mmol, 71%). Slow diffusion of MeOH into DCM gave single crystals suitable for X-ray diffraction.

^{1}H NMR and standard ESI-MS data match the previously reported data for this compound. HRMS (ESI) *m/z*: found 796.0560 ([M–Cl]$^+$ calc'd: 796.0564 for $C_{38}H_{38}O_4ClRu_2$).

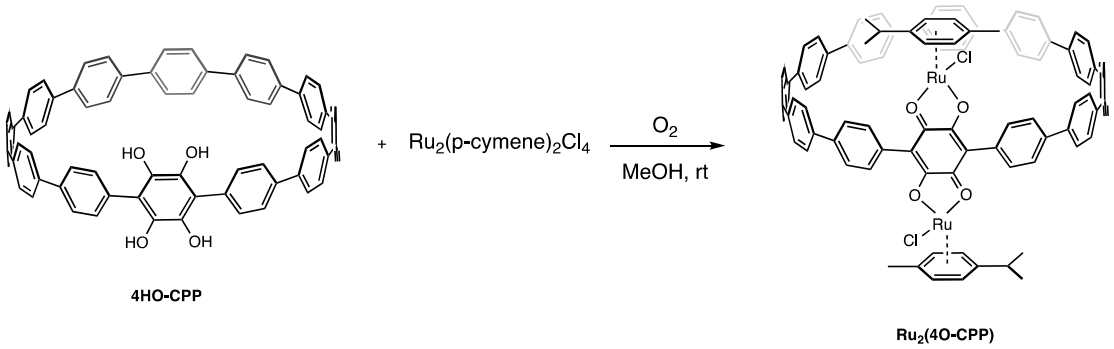

Synthesis of Ru_2(4O-CPP). In a nitrogen-filled glovebox, a 4 mL scintillation vial was charged with **4HO-CPP** (2.8 mg, 2.9 μmol) and MeOH (0.5 mL). While stirring, a solution of [Ru(*p*-

cymene)Cl_2]$_2$ (4.0 mg, 6.5 µmol, 2.2 equiv) in MeOH (0.5 mL) was added dropwise. The vial was capped, stirred at room temperature for 10 min, and then removed from the glovebox. The vial lid was unscrewed by one-quarter turn to facilitate the slow diffusion of oxygen into the vial, and the mixture was stirred at room temperature for five days. The resulting dark precipitate was collected by filtration and washed with MeOH (2 × 1 mL). The precipitate was recovered using $CHCl_3$ and purified by preparative TLC (DCM eluent; TLC plates were pre-treated with 4% NEt_3 in DCM) to yield **Ru$_2$(4O-CPP)** as a dark red solid (0.8 mg, 19%).

Note: due to potential sensitivity of the product to acid, chlorinated solvents were stored over potassium carbonate prior to use.

^{1}H NMR (500 MHz, $CDCl_3$) δ 7.79 (d, *J* = 8.5 Hz, 4H), 7.66–7.57 (m, 36H), 7.50 (d, *J* = 8.5 Hz, 4H), 5.58 (d, *J* = 6.0 Hz, 4H), 5.28 (d, *J* = 5.9 Hz, 4H), 2.89 (hept, 2H), 2.21 (s, 6H), 1.36 (d, *J* = 6.9 Hz, 12H). HRMS (ESI) *m/z*: found 1479.3190 ([M–Cl]$^+$ calc'd: 1479.3236 for $C_{92}H_{72}O_4ClRu_2$). HRMS (MALDI) *m/z*: found 1514.2805 ([M]$^+$ calc'd: 1514.2925 for $C_{92}H_{72}O_4Cl_2Ru_2$).

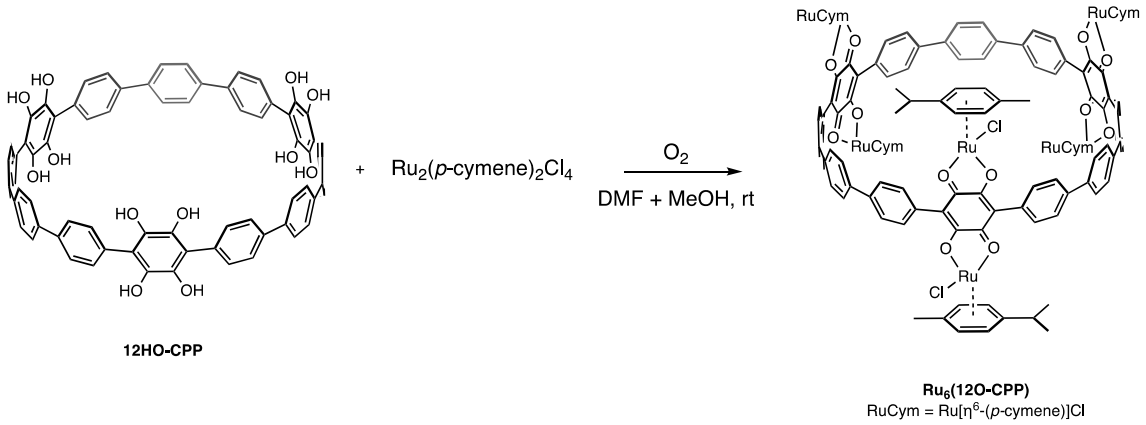

Synthesis of Ru$_6$(12O-CPP). In a nitrogen-filled glovebox, a 4 mL scintillation vial was charged with **12HO-CPP** (2.5 mg, 2.3 µmol) and DMF (0.5 mL). While stirring, a solution of [Ru(*p*-cymene)Cl_2]$_2$ (12.1 mg, 19.7 µmol, 8.6 equiv) in MeOH (0.5 mL) was added dropwise. The vial was capped, stirred at room temperature for 10 min, then removed from the glovebox. The vial was uncapped, and the mixture was stirred open to air at room temperature overnight. The mixture was evaporated to dryness under reduced pressure. The resulting dark solid was suspended in MeOH (10 mL), filtered, and washed with additional MeOH (3 × 2 mL). The precipitate was recovered with $CHCl_3$ and concentrated *in vacuo* to yield **Ru$_6$(12O-CPP)** as a dark red solid (3.3 mg, 54%).

Note: due to potential sensitivity of the product to acid, chlorinated solvents were stored over potassium carbonate prior to use.

^{1}H NMR (500 MHz, $CDCl_3$) δ 7.82–7.47 (m), 5.59 (br), 5.28 (br), 3.94 (br), 2.22 (br), 1.36 (br). HRMS (MALDI) *m/z*: found 2681.1409 ([M–Cl]$^+$ calc'd: 2681.1543 for $C_{132}H_{120}O_{12}Cl_5Ru_6$).

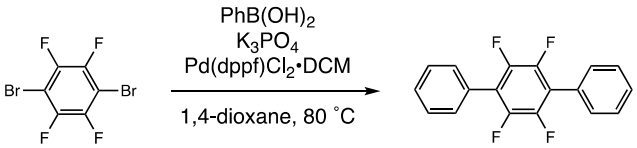

Synthesis of 1,2,4,5-tetrafluoro-3,6-diphenylbenzene. A Schlenk flask was charged with 1,4-dibromo-2,3,5,6-tetrafluorobenzene (6.02 g, 19.6 mmol), phenylboronic acid (6.21 g, 50.9 mmol, 2.6 equiv), and 1,4-dioxane (150 mL). The mixture was sparged with nitrogen for 30 min. A concentrated aqueous solution of K_3PO_4 (22.9 g, 108 mmol, 5.5 equiv) was also sparged with nitrogen for 30 min and transferred to the Schlenk flask *via* cannula. Under nitrogen, $Pd(dppf)Cl_2 \cdot DCM$ (0.301 g, 0.369 mmol, 1.9 mol%) was added and the reaction was heated at 80 ˚C for 24 hours. The solvent was removed *in vacuo* and the resulting solid was suspended in H_2O (400 mL). The solid was collected by vacuum filtration and washed with MeOH (250 mL) to give 1,2,4,5-tetrafluoro-3,6-diphenylbenzene as a fine gray crystalline solid (5.85 g, 99%).

^1H NMR (500 MHz, $CDCl_3$) δ 7.45–7.53 (m, 10H). $^{19}F\{^1H\}$ NMR (471 MHz, $CDCl_3$) δ –147.58. MS (EI) *m/z*: found 302.1 ($[M]^+$ calc'd: 302.1 for $C_{18}H_{10}F_4$). ^{13}C NMR could not be obtained due to poor solubility.

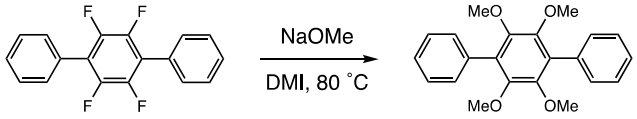

Optimized conditions for the synthesis of 1,2,4,5-tetramethoxy-3,6-diphenylbenzene. In a nitrogen-filled glovebox, a 4 mL scintillation vial was charged with 1,2,4,5-tetrafluoro-3,6-diphenylbenzene (25.0 mg, 82.5 µmol), sodium methoxide (71.3 mg, 132 µmol, 16 equiv), and DMI (1 mL). The vial was sealed and stirred at 80 ˚C for 16 hours. Aqueous 1M HCl (20 mL) was added, and the mixture was extracted with ethyl acetate (2 × 10 mL). The combined organic layers were washed with H_2O (2 × 10 mL), dried over magnesium sulfate, gravity filtered, and the solvent was removed *in vacuo* to give 1,2,4,5-tetramethoxy-3,6-diphenylbenzene as a white crystalline solid (24.9 mg, 86%). ^1H NMR and MS data match the previously reported data for this compound.[6]

Note: Determination of purity was performed by diluting an aliquot of the ethyl acetate extracts in DCM for analysis by GC-MS. Conditions that were too mild yielded a mixture containing partially fluorinated intermediates and conditions that were too harsh lead to partial *in situ* demethylation of one of the methoxy substituents. In both cases, these mixtures would be challenging to purify. The use of DMI as a solvent provided a slight improvement in product purity over NMP (94% *versus* 91%, respectively). However, in both NMP and DMI, as long as no demethylation was observed, resubjecting the worked-up product mixture to a second round of heating with additional sodium methoxide (71.3 mg, 132 µmol, 16 equiv) at 80 ˚C for an additional 16 hr reliably gave complete conversion to the tetrasubstituted product, 1,2,4,5-tetramethoxy-3,6-diphenylbenzene.

3. Single Crystal X-Ray Diffraction

Standard single-crystal X-ray diffraction (SCXRD) data was collected at 100 K on a Bruker APEX II single crystal X-ray diffractometer equipped with a Mo-radiation source and a Miracol X-ray optical collimator. Synchrotron SCXRD data was collected on Beamline 12.2.1 at the Advanced Light Source (ALS), Lawrence Berkeley National Lab (Berkeley, CA, USA).

All data was integrated and scaled using SAINT, SADABS within the APEX2 software package by Bruker.[7] Solution by direct methods using SHELXT produced a complete heavy atom phasing model consistent with the proposed structure.[8,9] The structures were completed by difference Fourier synthesis with SHELXL.[10,11] Scattering factors are from Waasmair and Kirfel.[12] Hydrogen atoms were placed in geometrically idealized positions and constrained to ride on their parent atoms with C–H distances in the range 0.95-1.00 Å. Isotropic thermal parameters U_{eq} were fixed such that they were $1.2U_{eq}$ of their parent atom U_{eq} for CH's and $1.5U_{eq}$ of their parent atom U_{eq} for methyl groups. All non-hydrogen atoms were refined anisotropically by full-matrix least-squares.

Synchrotron SCXRD of 4F-CPP. A colorless needle measuring 0.30 × 0.09 × 0.04 mm^3 was mounted on a loop with oil. Data collection was 98.8% complete to 25.930˚ in θ. The data was integrated as a two-component twin. The twin law is a two-fold rotation about [0 0 1] with a minor twin fraction of 0.258(2), refined from HKLF5 data. A total of 6324 reflections were collected covering the indices, $-24 \leq h \leq 22$, $0 \leq k \leq 10$, $0 \leq l \leq 16$. 6324 reflections were symmetry independent and the R_{int} = 0.0408. Indexing and unit cell refinement indicated a primitive monoclinic lattice. The space group was found to be P $2_1/c$ (No. 14).

The contribution of disordered trichloroethylene molecules to the diffraction pattern was removed with SQUEEZE.[13–15] The tetrafluorophenylene unit is disordered with an unfunctionalized phenylene, and thus there are a total of four fluorine atoms per CPP.

SCXRD of 4MeO-CPP. A yellow needle measuring 0.60 × 0.15 × 0.09 mm^3 was mounted on a loop with oil. Crystal-to-detector distance was 45 mm and exposure time was 180 seconds per frame for all sets. The scan width was 0.5˚. Data collection was 99.2% complete to 25˚ in θ. A total of 101139 merged reflections were collected covering the indices, $-68 \leq h \leq 68$, $-14 \leq k \leq 14$, $-60 \leq l \leq 60$. 15535 reflections were symmetry independent and the R_{int} = 0.1097. Indexing and unit cell refinement indicated an F-centered orthorhombic lattice. The space group was found to be F d d 2 (No. 43).

Due to extensive disorder, the diffraction abruptly fell off at a resolution of about 1Å (**Fig. S44**). This effect is intrinsic to these crystals and a longer exposure time or stronger radiation source would not solve this problem. SQUEEZE analysis showed that a total of 5492 electrons where in solvent accessible voids, the contribution of which to the diffraction pattern was then removed.[13–15] This is more than half of the electrons of the refined structure (F_0 = 9728). One trichloroethylene was found per molecule, but no other solvent molecule could be individually identified. After removal of 116 bad peaks and linking all phenyls with SAME commands in SHELXL, the structure still needed additional restraints. All phenyl-phenyl distance were linked and some thermal displacement parameters were stabilized. A disordered phenyl group was treated accordingly.

Synchrotron SCXRD of 12MeO-CPP. A colorless shard measuring 0.20 × 0.10 × 0.10 mm^3 was mounted on a loop with oil. Data collection was 99.0% complete to 25.709˚ in θ. A total of 25207 reflections were collected covering the indices, $-24 \leq h \leq 23$, $-11 \leq k \leq 11$, $0 \leq l \leq 47$. 13026 reflections were symmetry independent and the $R_{int} = 0.0251$. Indexing and unit cell refinement indicated a primitive monoclinic lattice. The space group was found to be P $2_1/a$ (No. 14).

SCXRD of Ru_2(Ph_2dhbq). A black shard measuring 0.09 × 0.06 × 0.05 mm^3 was mounted on a loop with oil. Crystal-to-detector distance was 40 mm and exposure time was 20 seconds per frame for all sets. The scan width was 0.5˚. Data collection was 100.0% complete to 25˚ in θ. A total of 16214 reflections were collected covering the indices, $-15 \leq h \leq 15$, $-14 \leq k \leq 14$, $-18 \leq l \leq 18$. 4178 reflections were symmetry independent and $R_{int} = 0.0744$. Indexing and unit cell refinement indicated a primitive monoclinic lattice. The space group was found to be P $2_1/n$ (No. 14).

4. Computational Details

Geometry optimization and frequency calculations were performed in the Gaussian 16 suite of software.[16] All calculations were carried out with the B3LYP hybrid functional[17–20] and a split basis of LANL2DZ (Ru atoms)[21–23] and 6-31G* (H, C, O, and Cl atoms)[24–27]. Optimized geometries were verified to be true minima by the absence of imaginary frequencies in vibrational frequency calculations at the same level. For the ease of calculations, η^6-cymene ligands on **Ru$_2$(4O-CPP)** and **Ru$_6$(12O-CPP)** have been modeled as η^6-benzene.

Structural optimization of **Ru$_2$(4O-CPP)** was performed on structures with the following relative positions of Cl atoms:

1. *Trans* (**Fig. S37**)
2. *Cis* with both Cl atoms inside of the ring (**Fig. S38**)
3. *Cis* with both Cl atoms outside of the ring (**Fig. S39**)

Analysis of the resulting structures reveals that the *trans* configuration is the lowest energy of the three configurational isomers.

Structural optimization of **Ru$_6$(12O-CPP)** was performed on structures with the following relative positions of the three Cl atom pairs (within each pair, the Cl atoms were in the *trans* configuration based on results from **Ru$_2$(4O-CPP)**):

1. All Cl atom pairs oriented the same way (contains a C_3 axis of rotation; **Fig. S40**)
2. One Cl atom pair oriented opposite to the two other pairs (no C_3 axis of rotation; **Fig. S41**)

Analysis of the resulting structures reveals that the higher-symmetry configuration is the lower energy of the two configurational isomers.

As discussed in the main text, bond lengths for the optimized structure of **Ru$_2$(4O-CPP)** fall within the range observed in the single crystal structure of **Ru$_2$(Ph$_2$dhbq)**. Similarly, the optimized structure of **Ru$_6$(12O-CPP)** reveals bond lengths that are within the range observed in the single crystal structure of **Ru$_2$(Ph$_2$dhbq)**. The bond lengths in the optimized structure of **Ru$_6$(12O-CPP)** also closely match those of the optimized structure **Ru$_2$(4O-CPP)**, with average bond lengths of 1.2781(3) and 1.2779(8) Å for the C–O bonds and average bond lengths of 2.0794(16) and 2.0799(14) Å for the Ru–O bonds, for **Ru$_6$(12O-CPP)** and **Ru$_2$(4O-CPP)** respectively.

There appears to be slightly more asymmetry in the C–O and Ru–O bond lengths within the Ru–catechol chelate ring in the singe crystal structure of **Ru$_2$(Ph$_2$dhbq)** relative to the optimized structures of **Ru$_2$(4O-CPP)** and **Ru$_6$(12O-CPP)** (**Table S1**). However, this lower degree of bond asymmetry was also observed in the DFT optimized structure of **Ru$_2$(Ph$_2$dhbq)** at the same level of theory (**Fig. S42**). This asymmetry did not appear to increase in **Ru$_2$(Ph$_2$dhbq)** when calculations were performed with larger basis sets (*e.g.* def2-TZVP on all atoms)[28].

Table S1. Bond lengths observed in the single crystal structure of **Ru_2(Ph$_2$dhbq)** compared to the bond lengths observed in the lowest-energy DFT optimized geometries **of Ru_2(Ph$_2$dhbq)**, **Ru_2(4O-CPP)**, and **Ru_6(12O-CPP)**.

	Ru_2(Ph$_2$dhbq) SCXRD	**Ru_2(Ph$_2$dhbq)** DFT	**Ru_2(4O-CPP)** DFT	**Ru_6(12O-CPP)** DFT
C–O Bond Lengths (Å)	1.274(3) 1.278(3)	1.27822 1.27822 1.27865 1.27865	1.27719 1.27736 1.27855 1.27866	1.27785 1.27786 1.27788 1.27789 1.27789 1.27794 1.27830 1.27835 1.27836 1.27845 1.27847 1.27848
Ru–O Bond Lengths (Å)	2.070(2) 2.092(2)	2.08609 2.08609 2.09074 2.09074	2.07860 2.07921 2.08014 2.08174	2.07754 2.07769 2.07797 2.07797 2.07812 2.07824 2.08006 2.08030 2.08050 2.08119 2.08129 2.08162

5. Supplementary Figures:

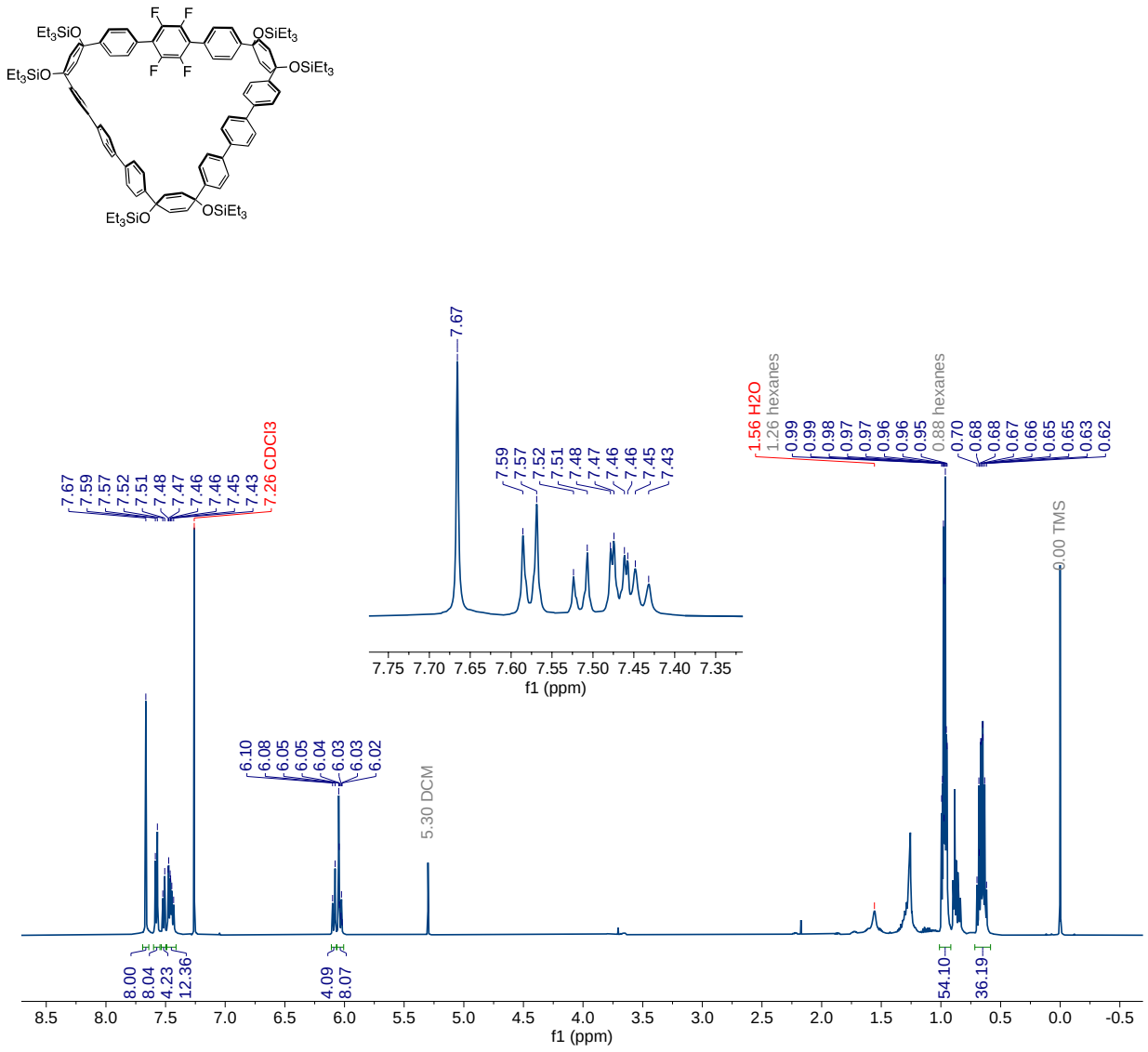

Figure S1. ^{1}H NMR spectrum of **4F-MC-OTES** (500 MHz, $CDCl_3$, 298 K).

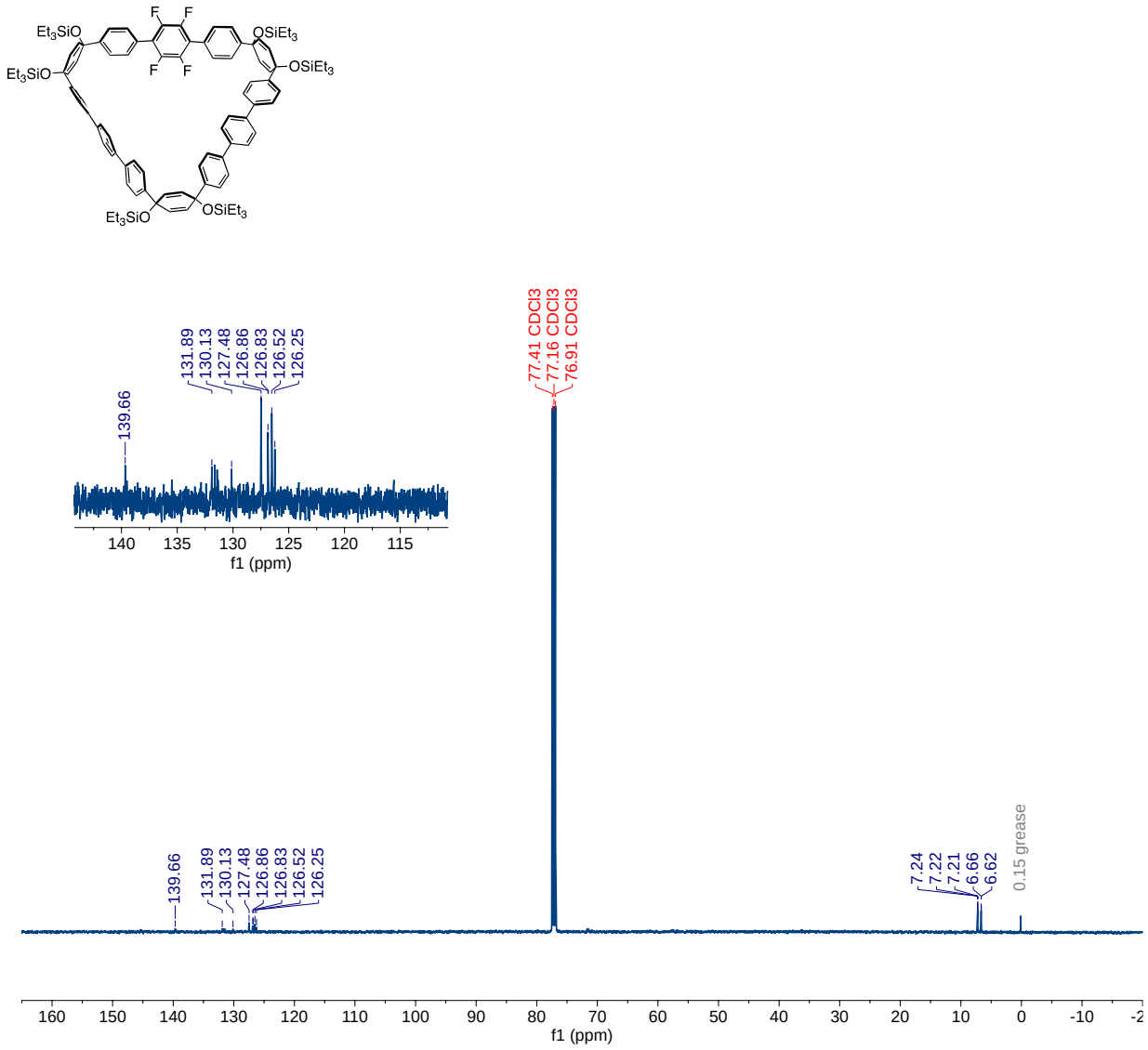

Figure S2. $^{13}C\{^{1}H\}$ NMR spectrum of **4F-MC-OTES** (126 MHz, $CDCl_3$, 298 K).

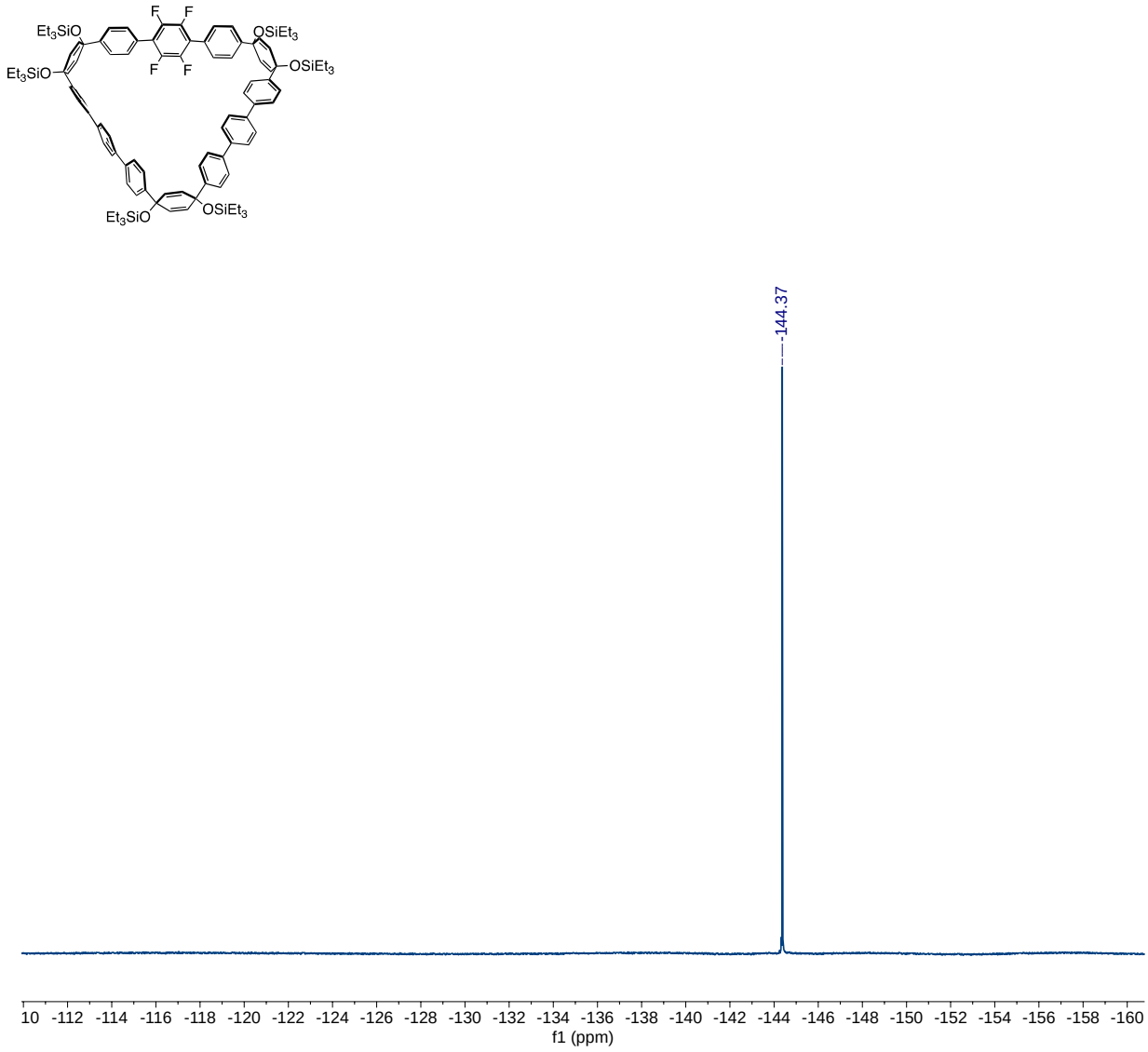

Figure S3. $^{19}F\{^{1}H\}$ NMR spectrum of **4F-MC-OTES** (470 MHz, $CDCl_3$, 298 K).

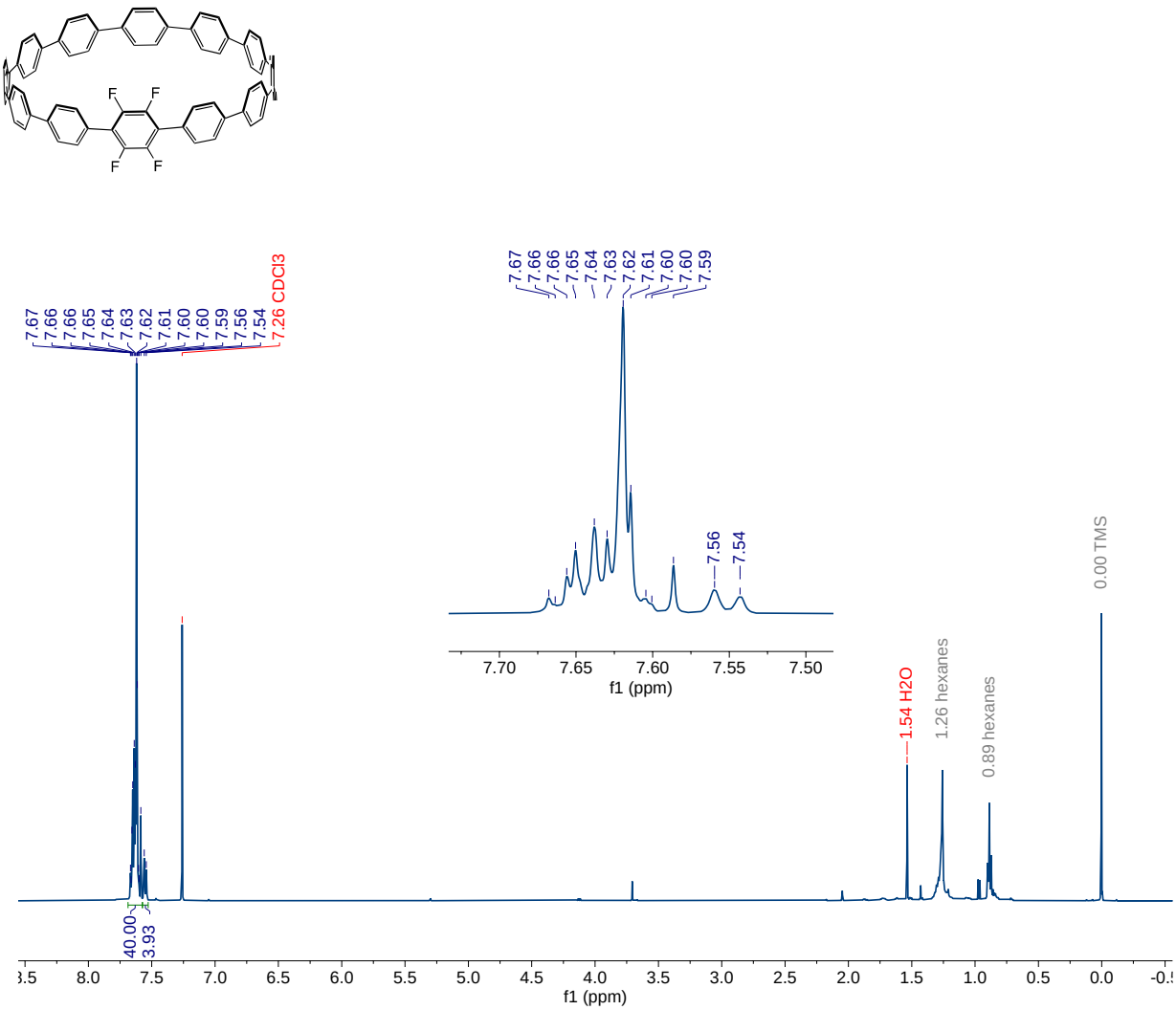

Figure S4. ^{1}H NMR spectrum of **4F-CPP** (500 MHz, $CDCl_3$, 298 K).

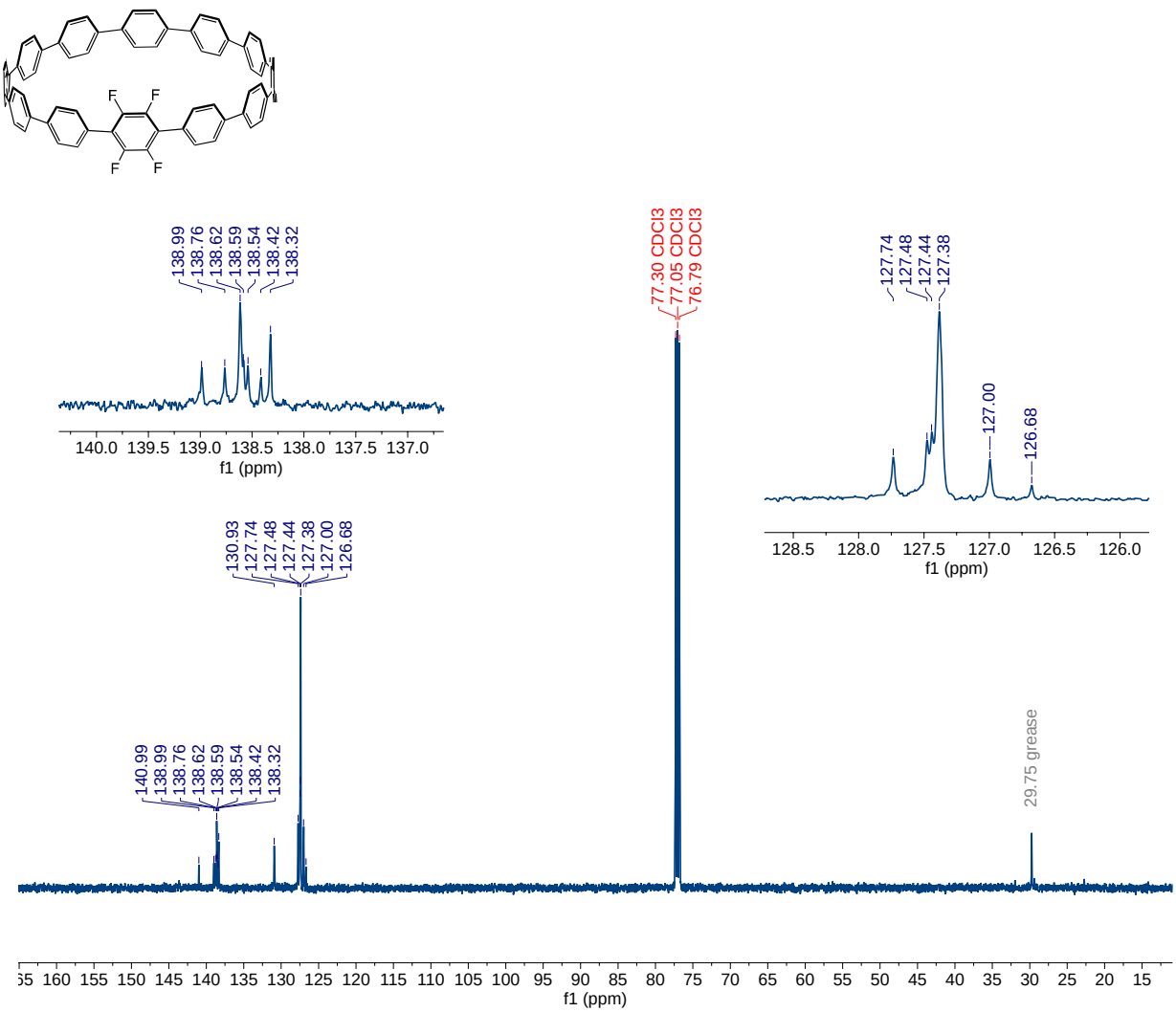

Figure S5. $^{13}C\{^{1}H\}$ NMR spectrum of **4F-CPP** (126 MHz, $CDCl_3$, 298 K).

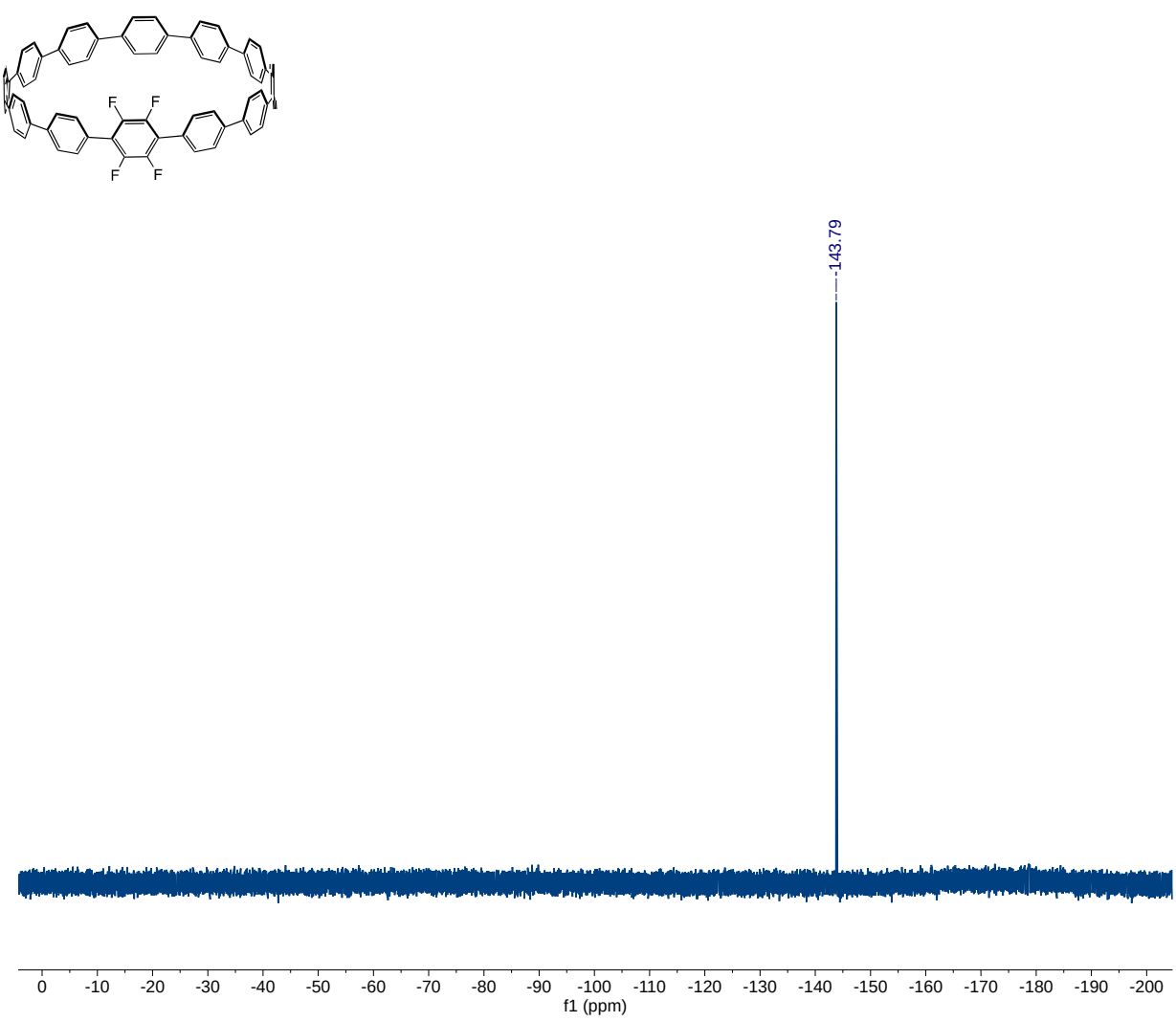

Figure S6. ^{19}F NMR spectrum of **4F-CPP** (470 MHz, $CDCl_3$, 298 K).

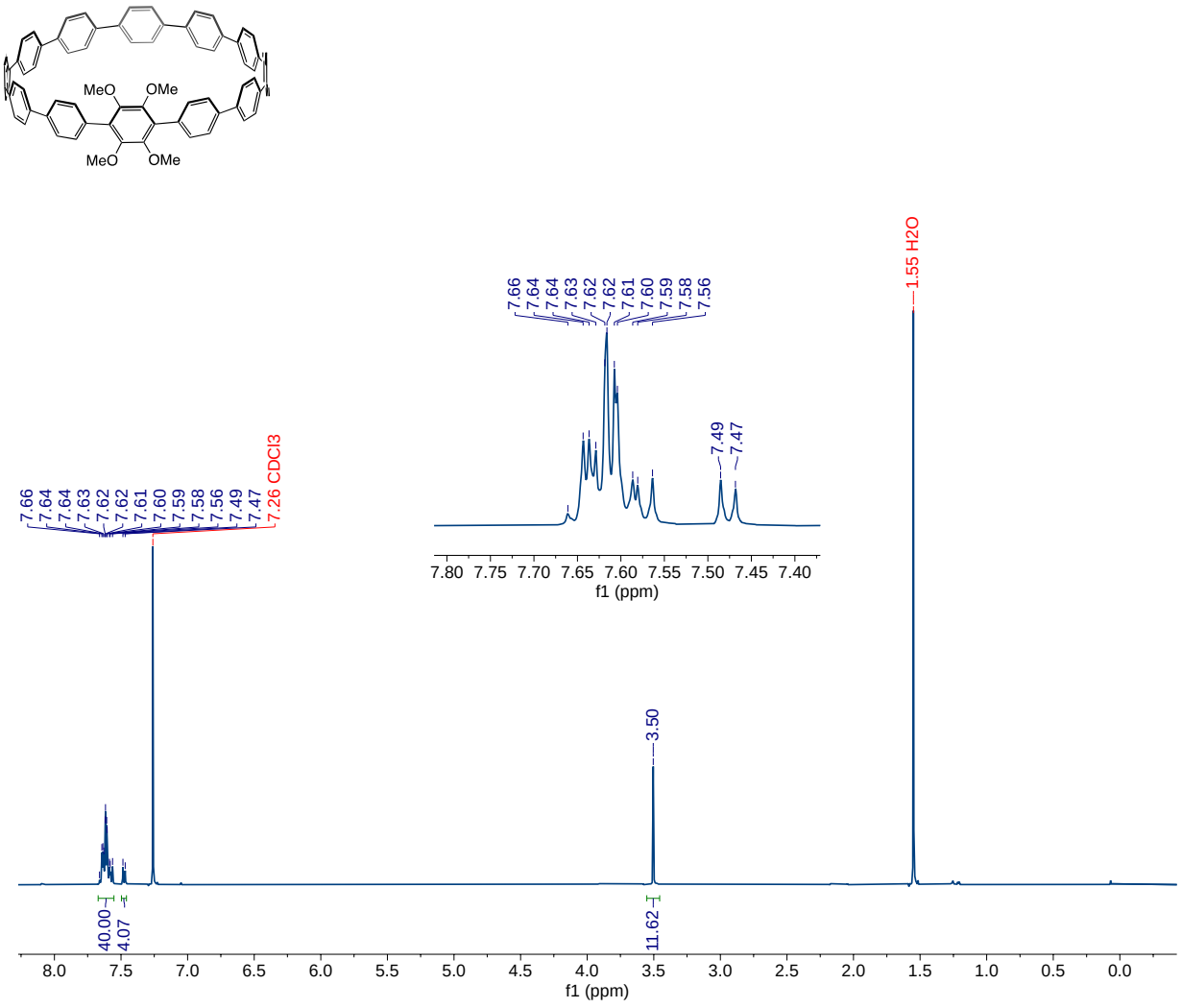

Figure S7. ^{1}H NMR spectrum of **4MeO-CPP** (500 MHz, $CDCl_3$, 298 K).

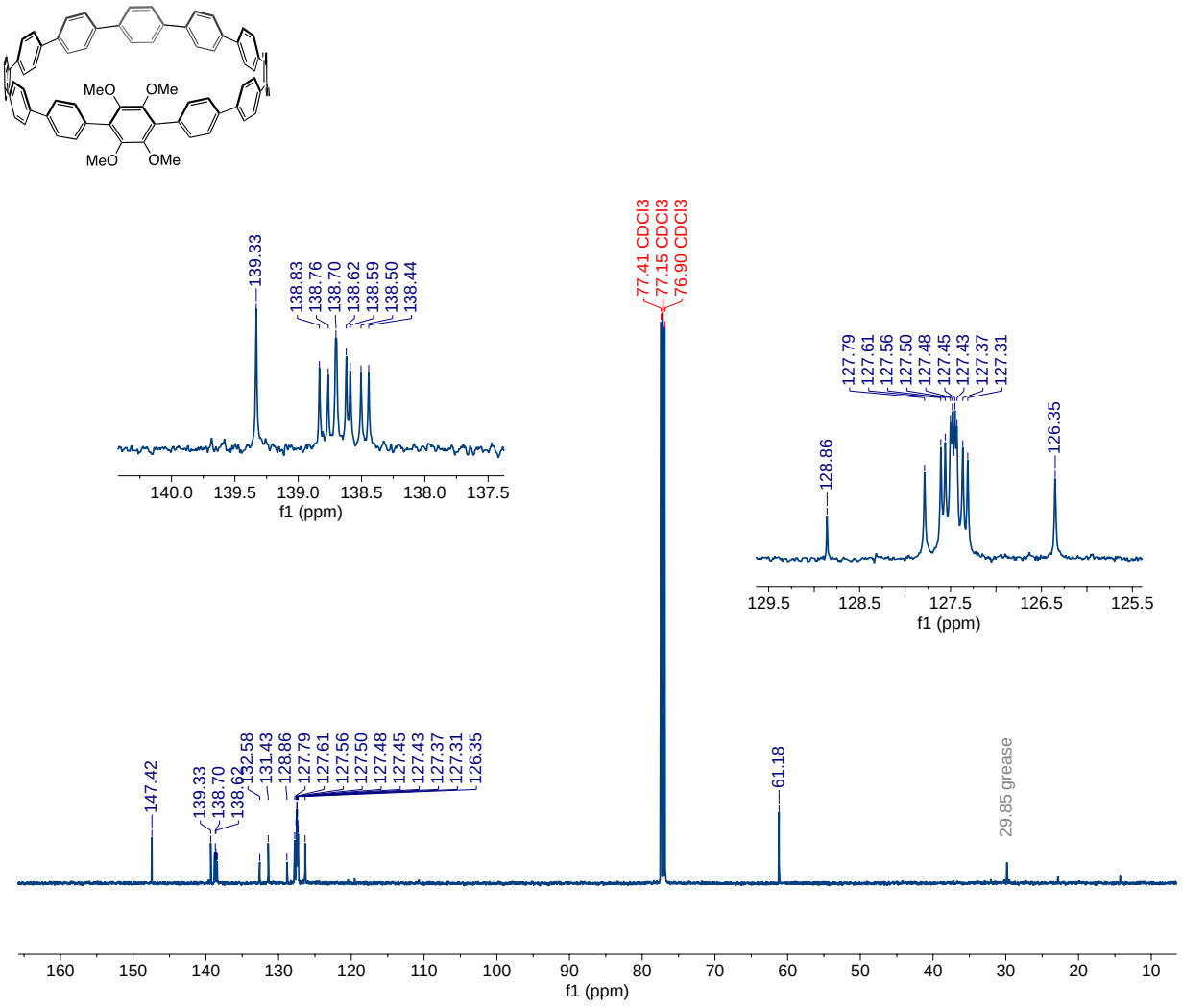

Figure S8. $^{13}C\{^{1}H\}$ NMR spectrum of **4MeO-CPP** (126 MHz, $CDCl_3$, 298 K).

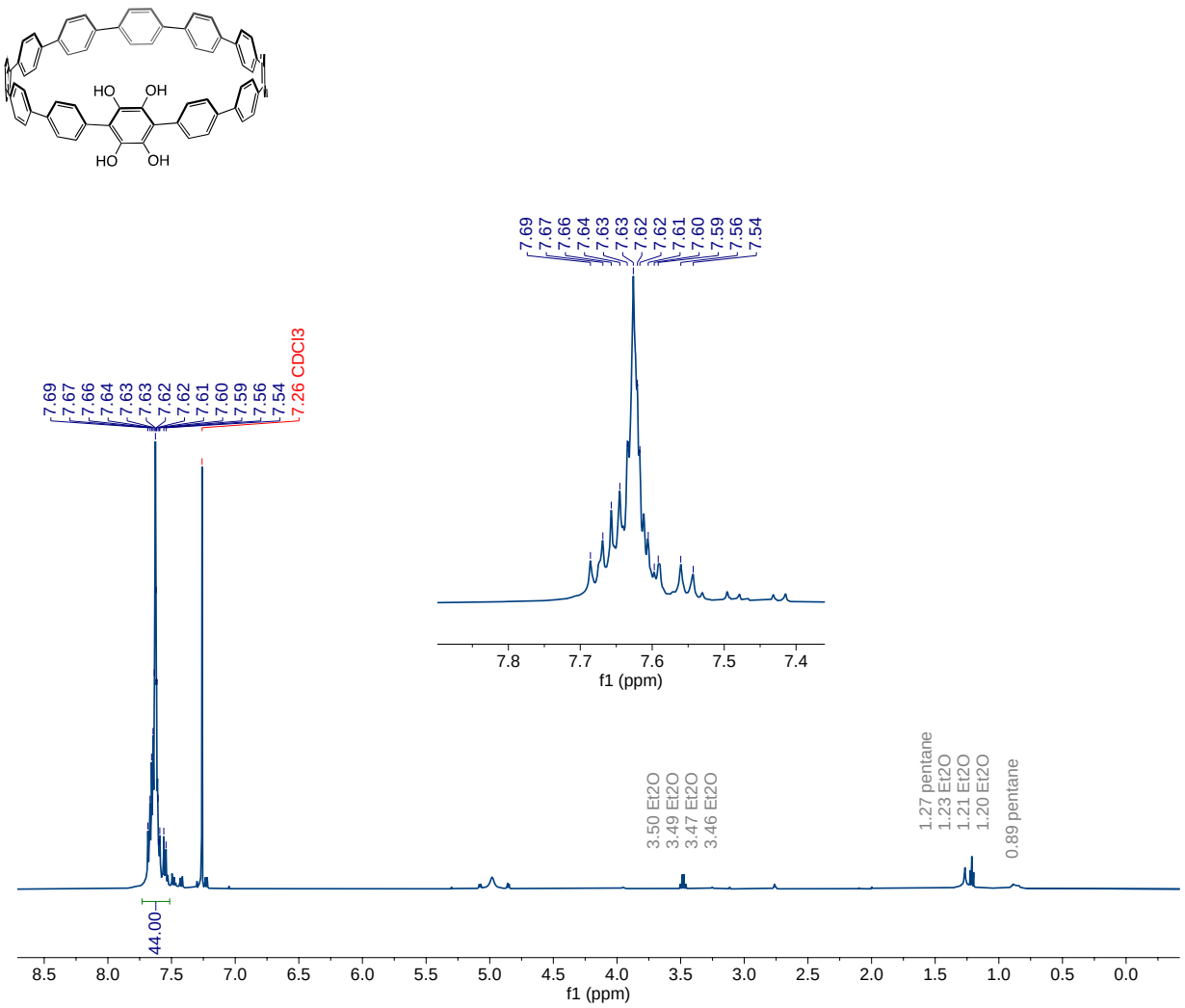

Figure S9. ^{1}H NMR spectrum of **4HO-CPP** (500 MHz, $CDCl_3$, 298 K).

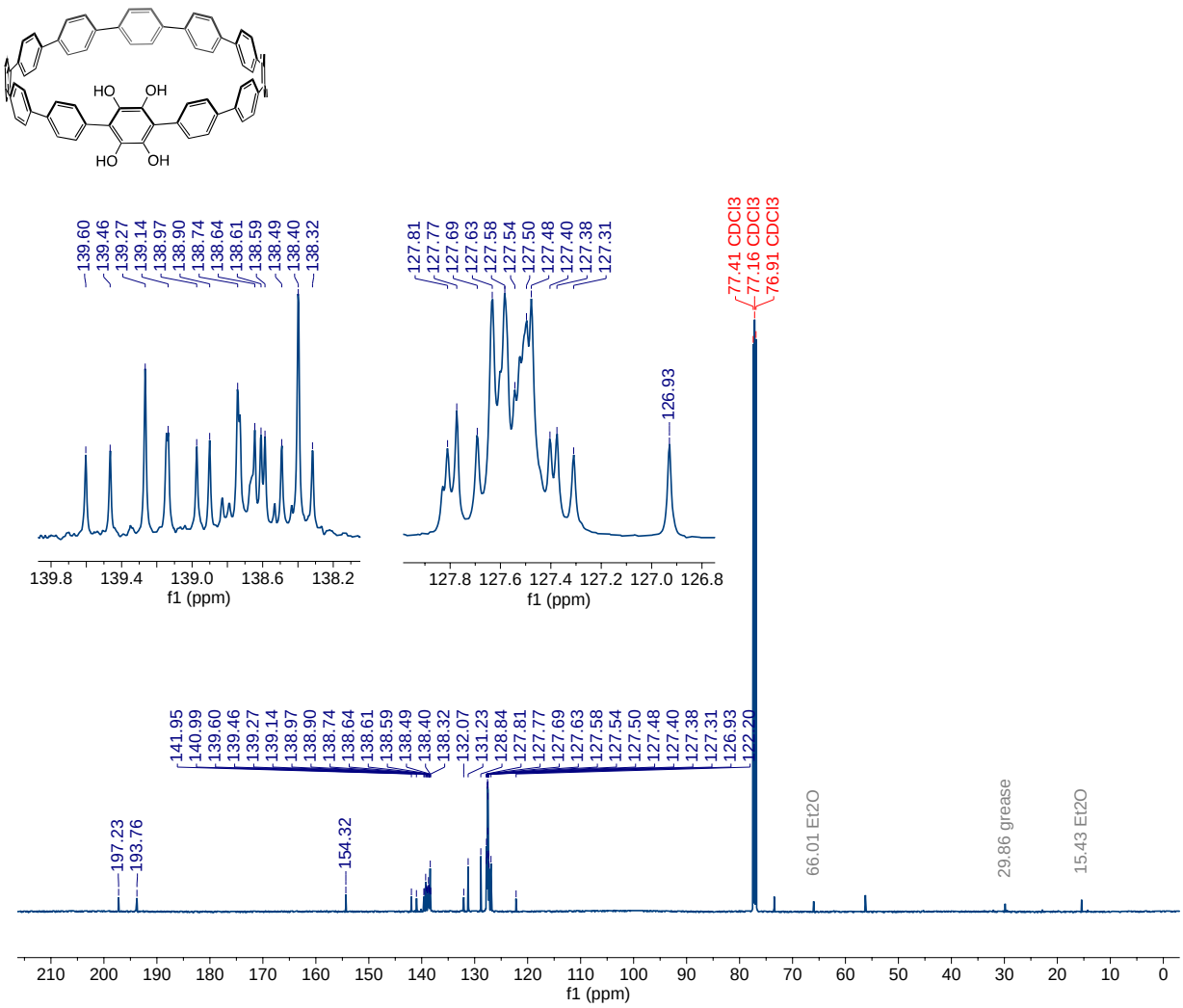

Figure S10. $^{13}C\{^{1}H\}$ NMR spectrum of **4HO-CPP** (126 MHz, $CDCl_3$, 298 K). Note: we expect to observe 24 resonances in the aromatic region of the spectrum for the product in the as-synthesized state. The presence of additional resonances is likely due to partial oxidation of the dicatechol-substituted phenylene unit to the corresponding 2,5-dihydroxy-1,4-benzoquinone. This is further reinforced by the presence of resonances above 160 ppm, which are due to carbonyl-bound carbons, as well as by our high-resolution ESI-MS data, which shows the presence of oxidized species.

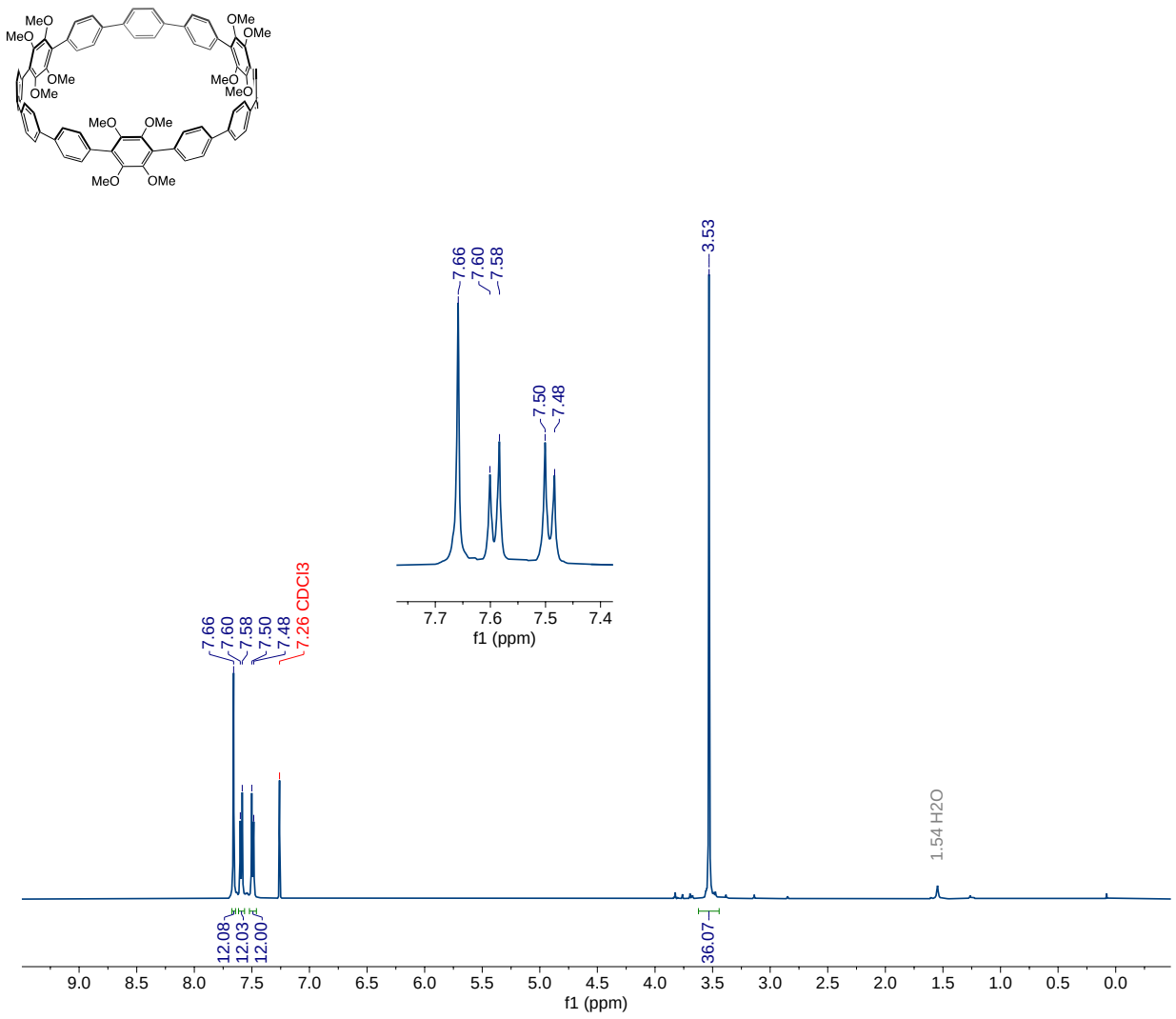

Figure S11. ^{1}H NMR spectrum of **12MeO-CPP** (500 MHz, $CDCl_3$, 298 K).

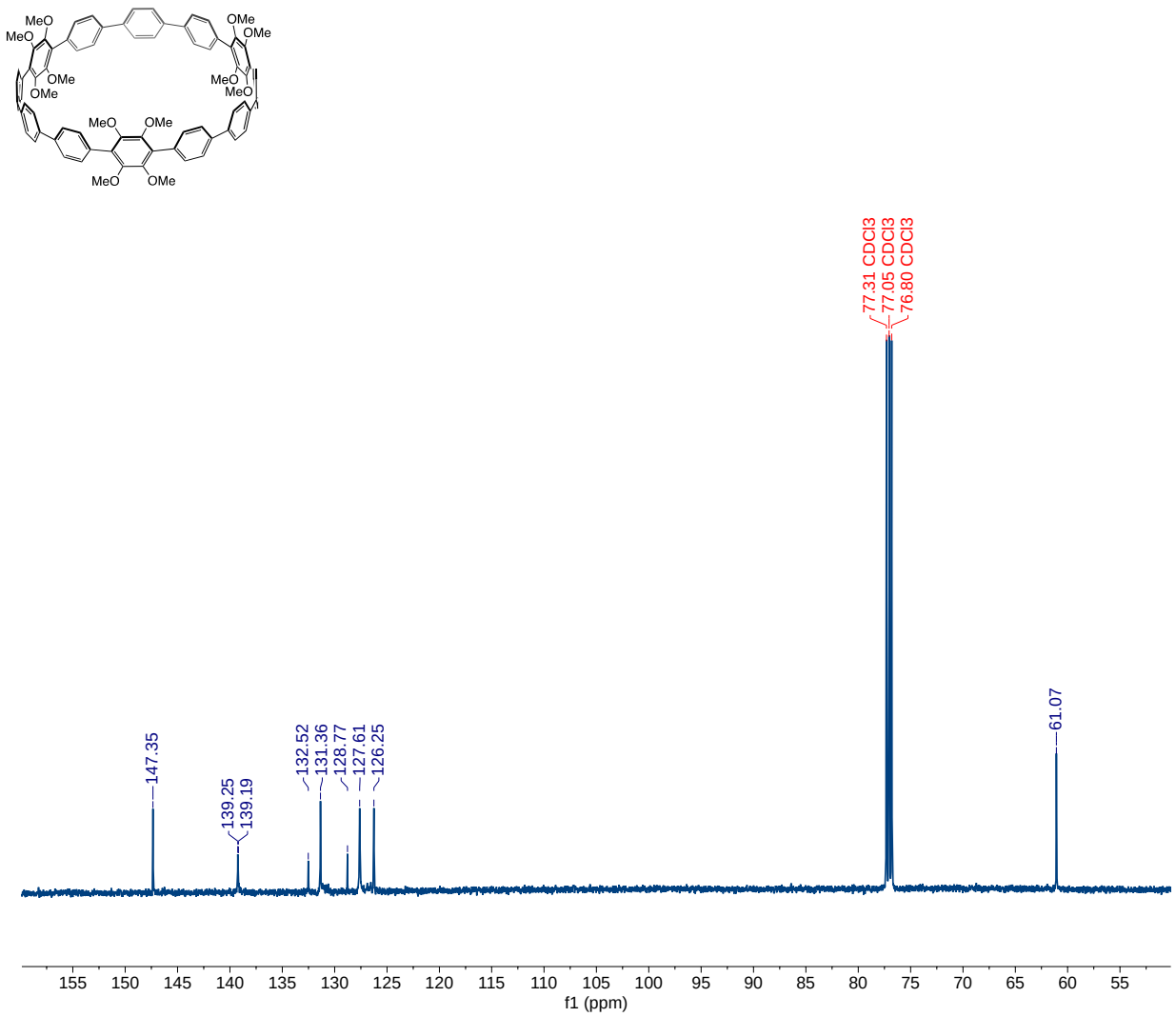

Figure S12. $^{13}C\{^{1}H\}$ NMR spectrum of **12MeO-CPP** (126 MHz, $CDCl_3$, 298 K).

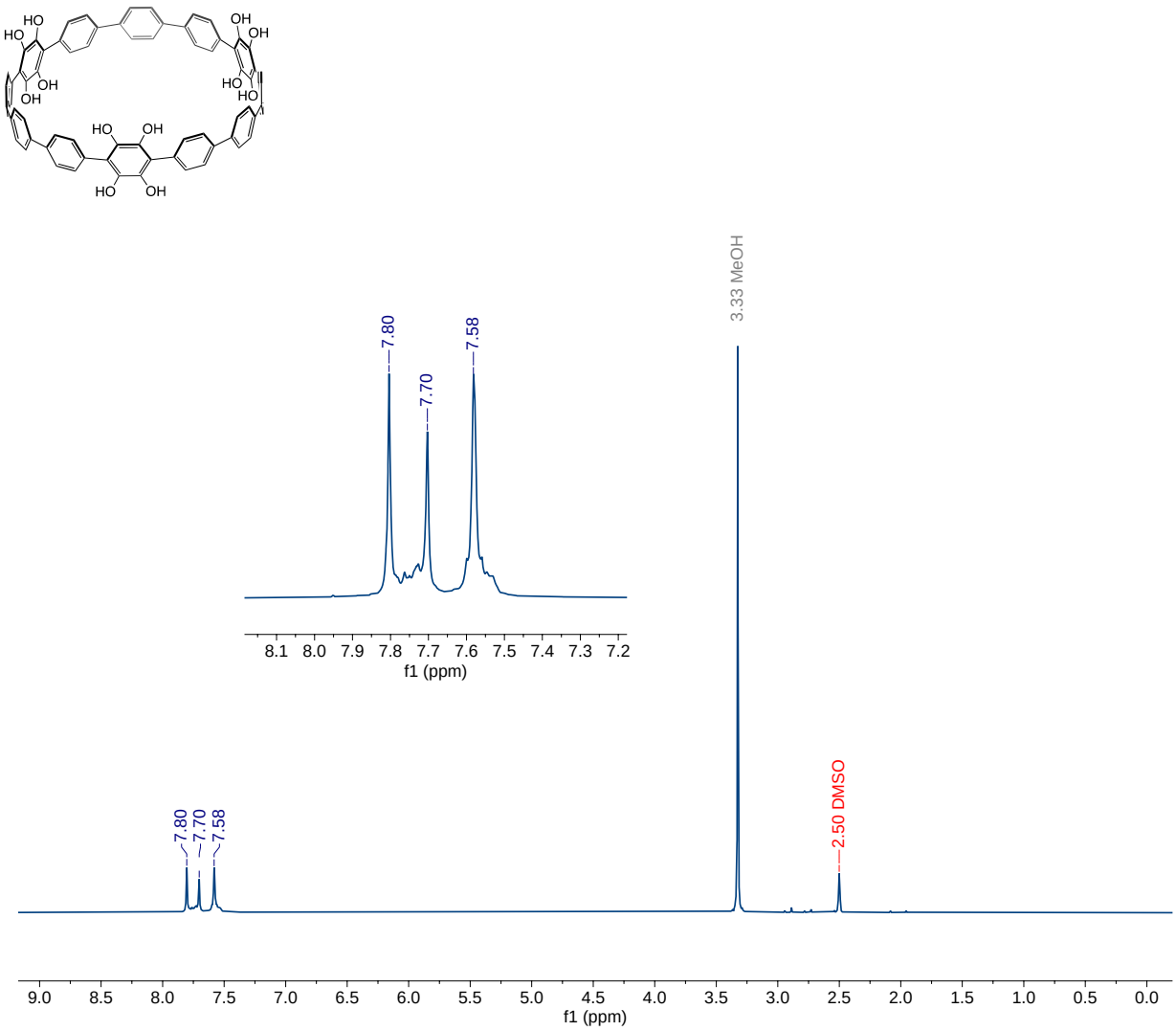

Figure S13. ^{1}H NMR spectrum of **12HO-CPP** (500 MHz, DMSO-d_6, 298 K).

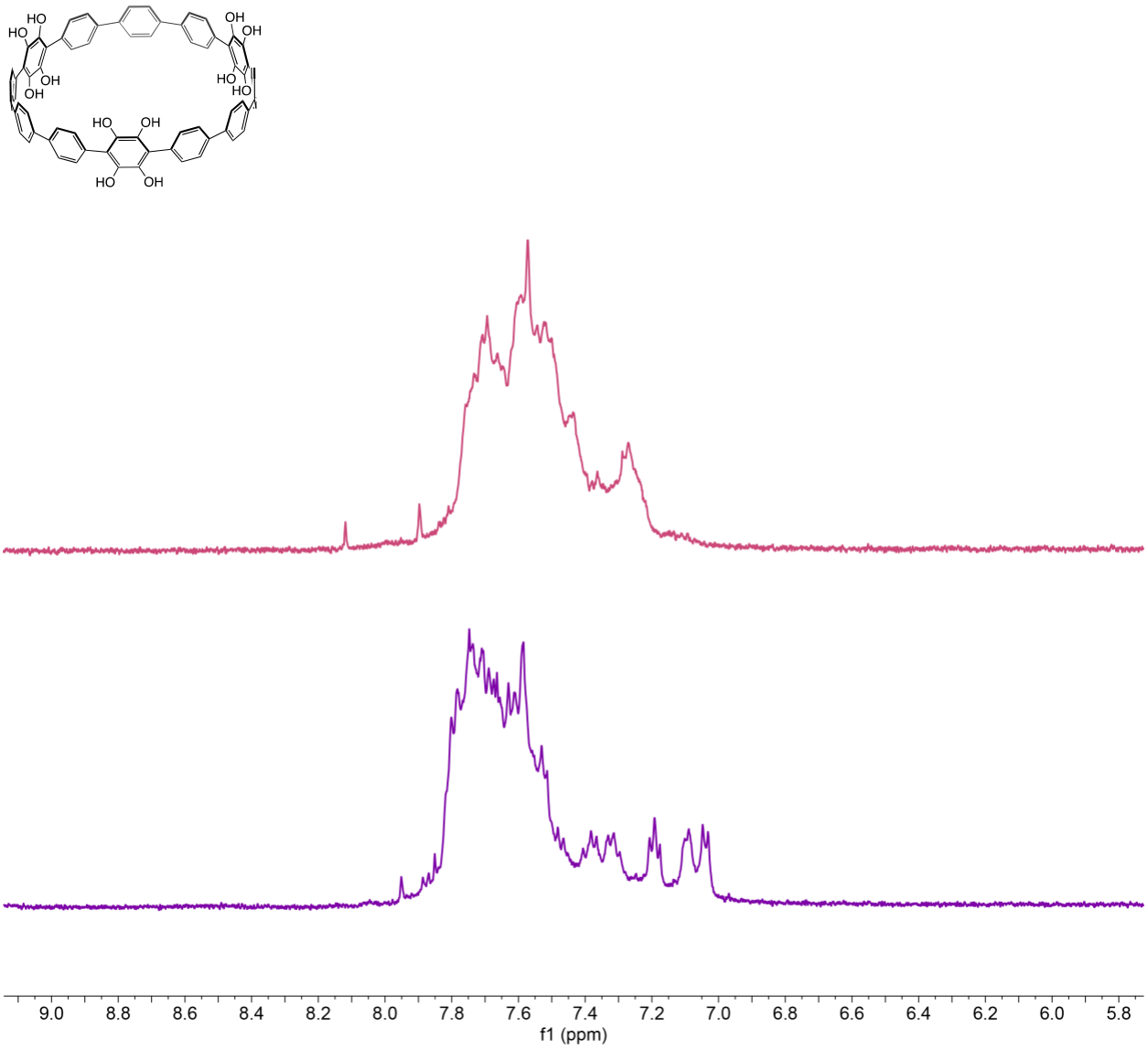

Figure S14. Aromatic region of the ^{1}H NMR spectrum of **12HO-CPP** (500 MHz, DMSO-d_6, 298 K) following workup in air (lower trace) *versus* 4 hr after the addition of a large excess of sodium dithionite while under nitrogen (upper trace).

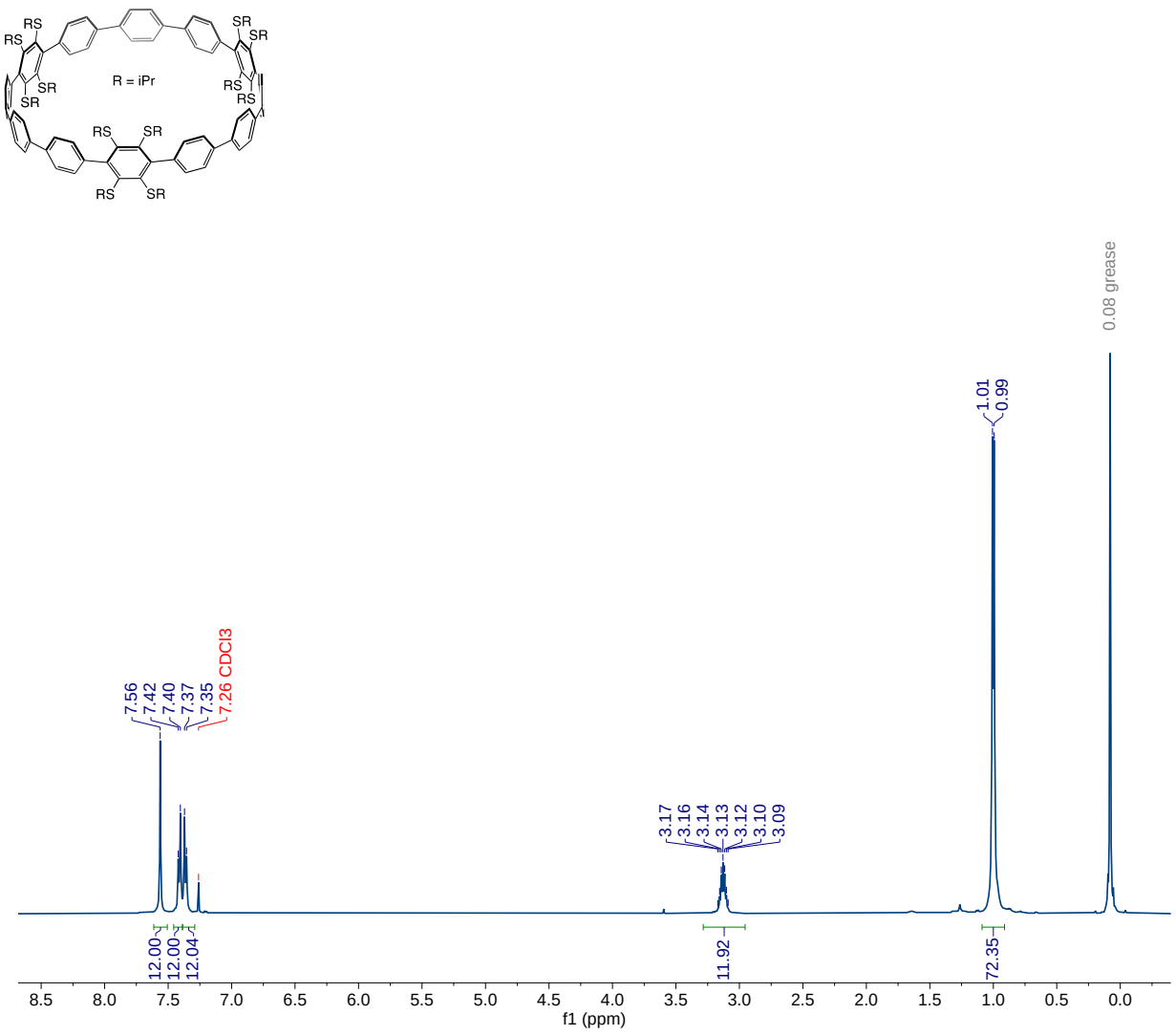

Figure S15. ^{1}H NMR spectrum of **12iPrS-CPP** (500 MHz, $CDCl_3$, 298 K).

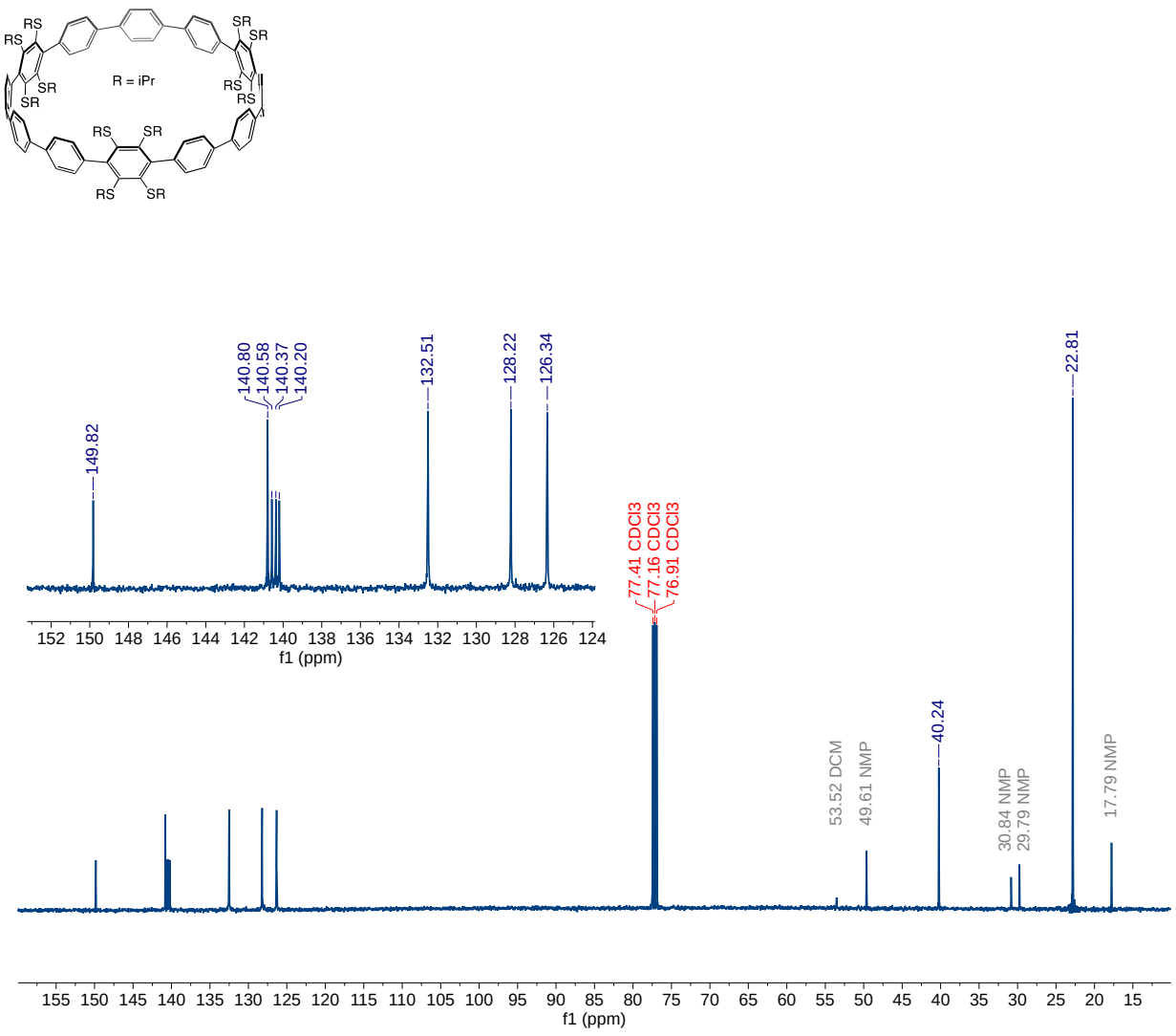

Figure S16. $^{13}C\{^{1}H\}$ NMR spectrum of **12iPrS-CPP** (126 MHz, $CDCl_3$, 298 K).

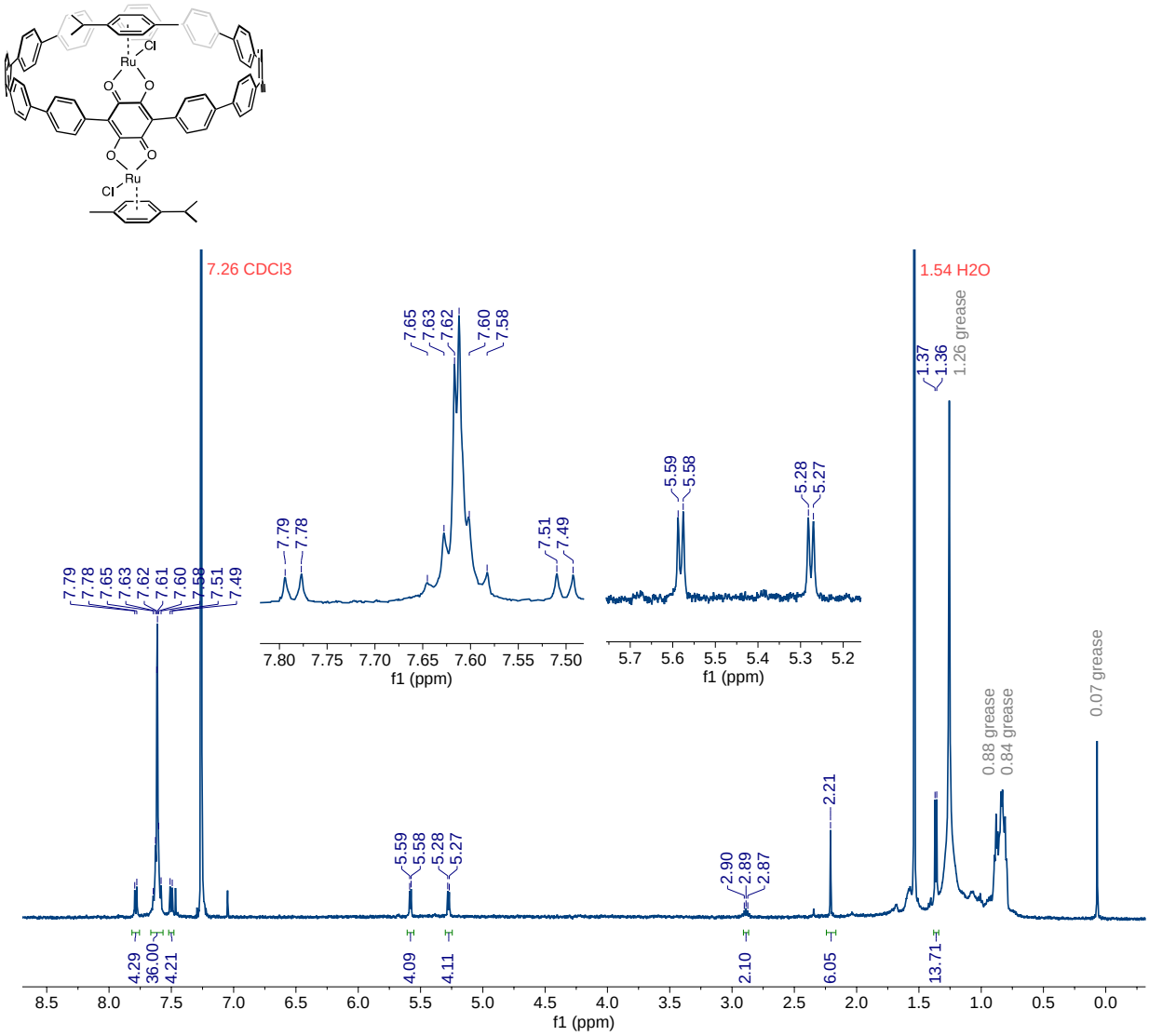

Figure S17. ^{1}H NMR spectrum of **Ru_2(4O-CPP)** (500 MHz, $CDCl_3$, 298 K).

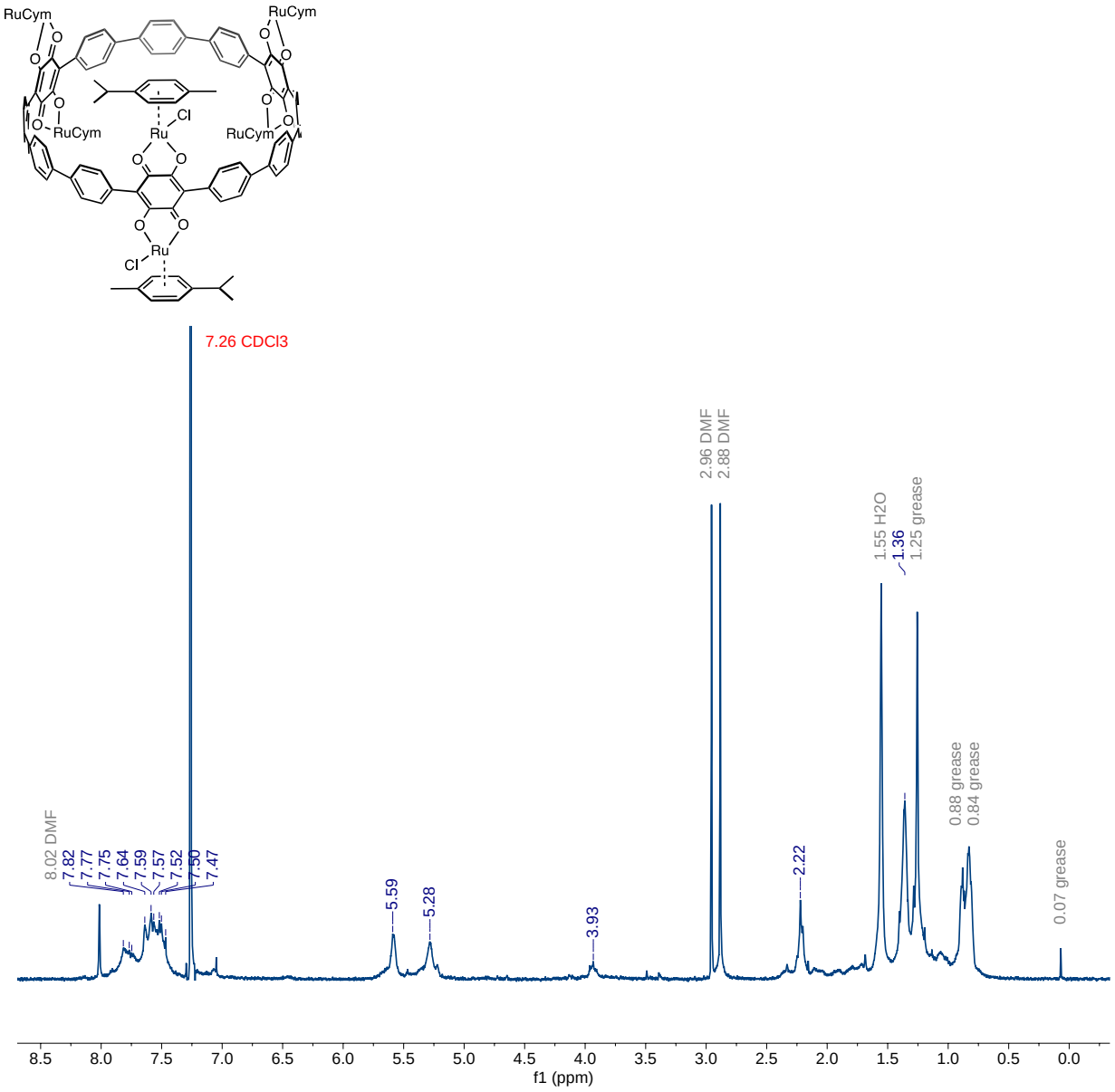

Figure S18. ^{1}H NMR spectrum of **Ru_6(12O-CPP)** (500 MHz, $CDCl_3$, 298 K).

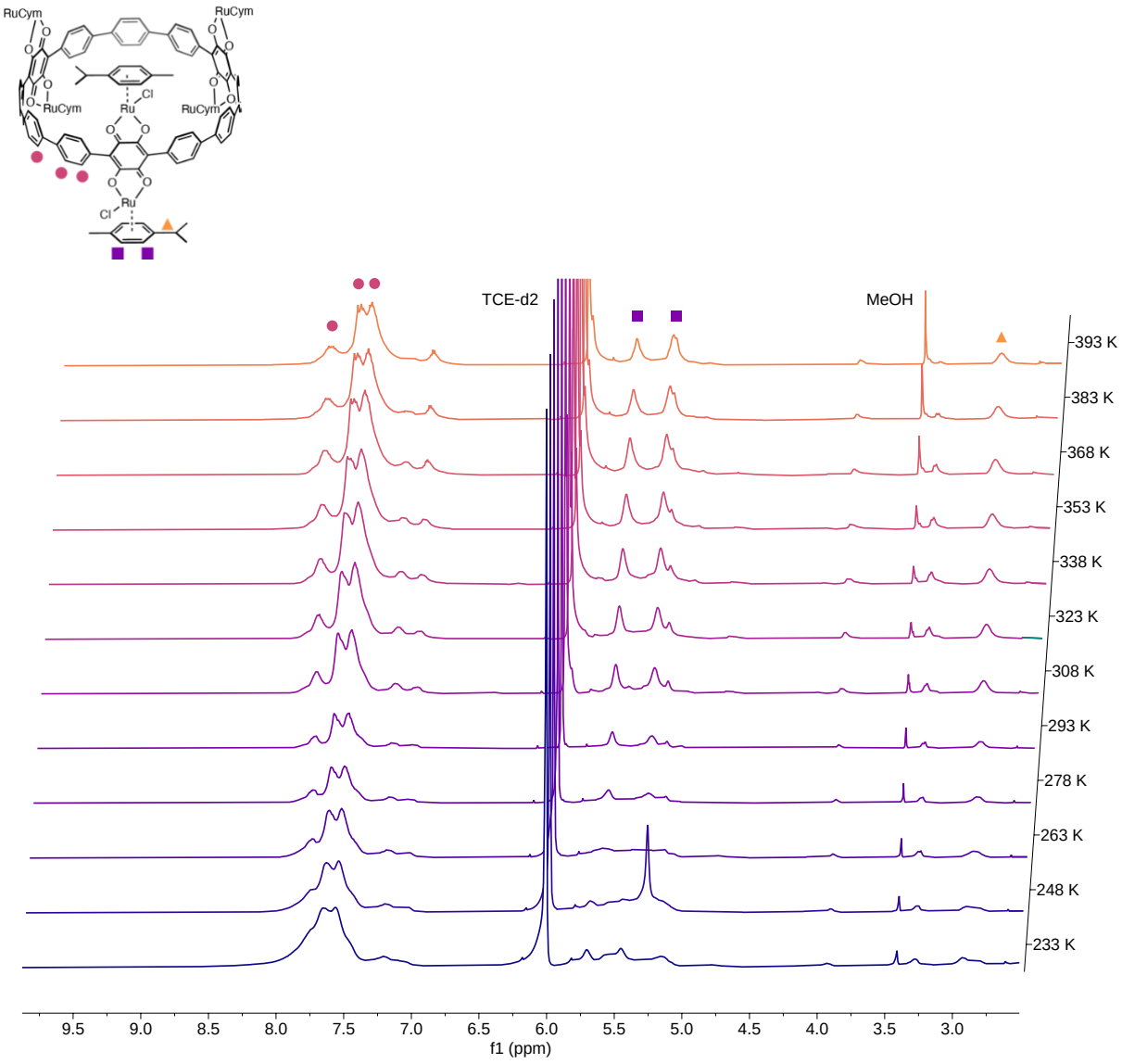

Figure S19. Variable-temperature ^{1}H NMR spectrum of **Ru$_6$(12O-CPP)** (500 MHz, tetrachloroethane-*d*$_2$, 233–393 K). The sample was initially cooled to 233 K and data was collected at successively higher temperatures up to 393 K. Spectra collected at 293 K before and after collecting variable-temperature data looked identical, confirming the absence of temperature-induced decomposition or other changes during the course of the experiment.

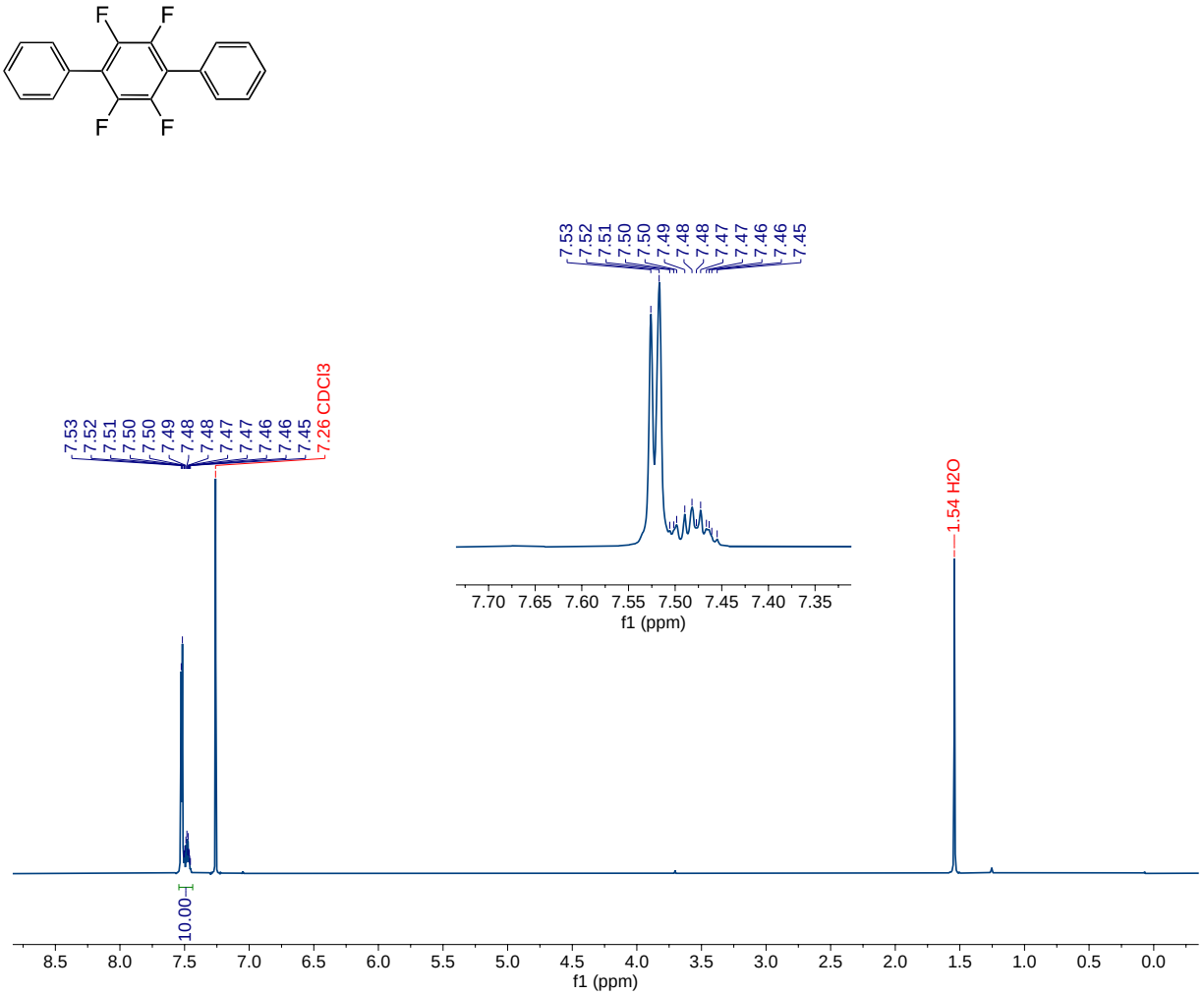

Figure S20. ^{1}H NMR spectrum of 1,2,4,5-tetrafluoro-3,6-diphenylbenzene (500 MHz, $CDCl_3$, 298 K).

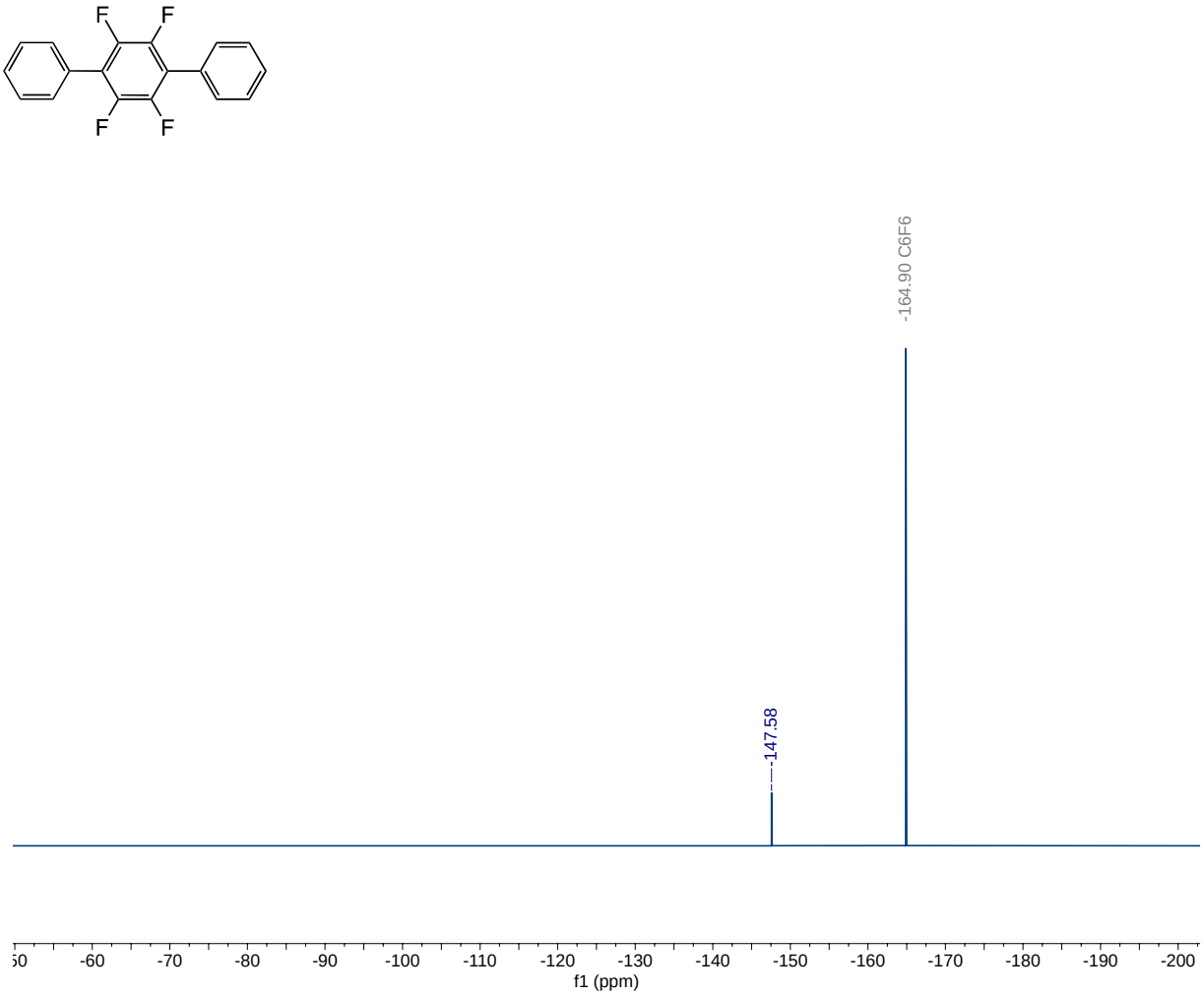

Figure S21. $^{19}F\{^{1}H\}$ NMR spectrum of 1,2,4,5-tetrafluoro-3,6-diphenylbenzene with hexafluorobenzene as an internal chemical shift standard (470 MHz, $CDCl_3$, 298 K).

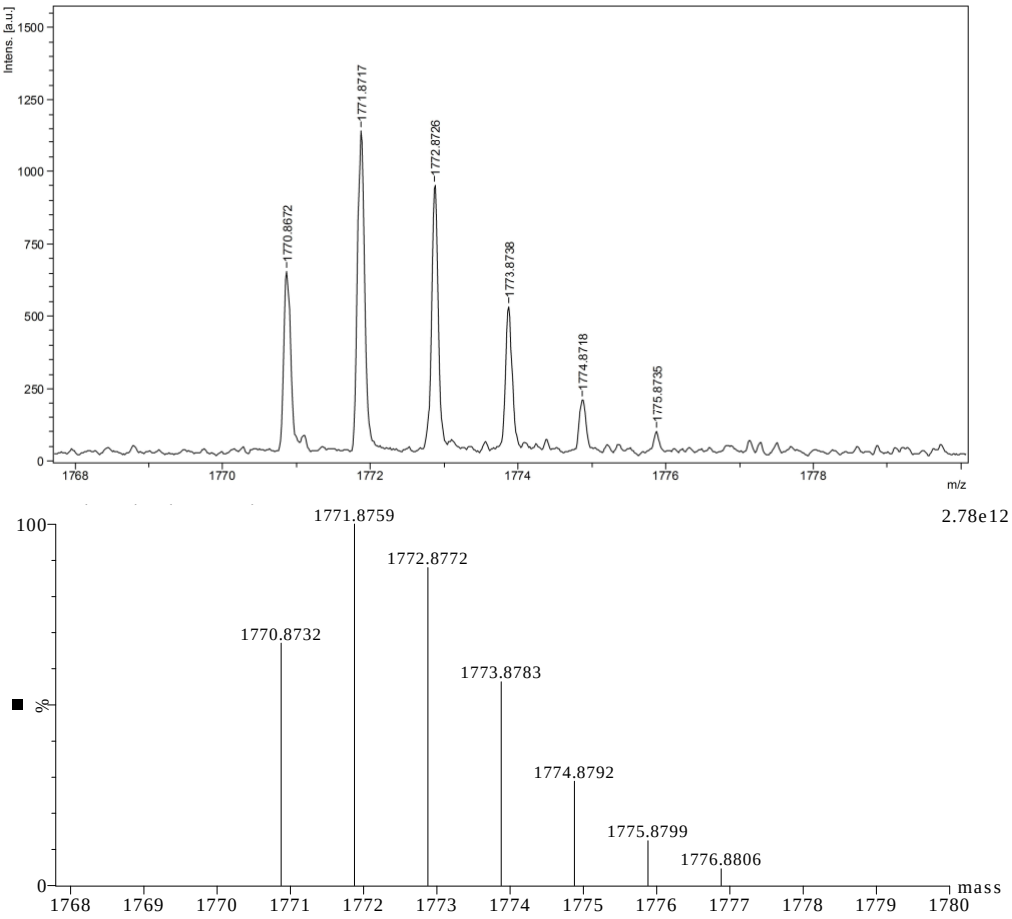

Figure S22. Experimental (top) *versus* simulated (bottom) high-resolution MALDI-TOF mass spectrum for **4F-MC-OTES** ($[M]^+$, $C_{108}H_{134}F_4O_6Si_6$).

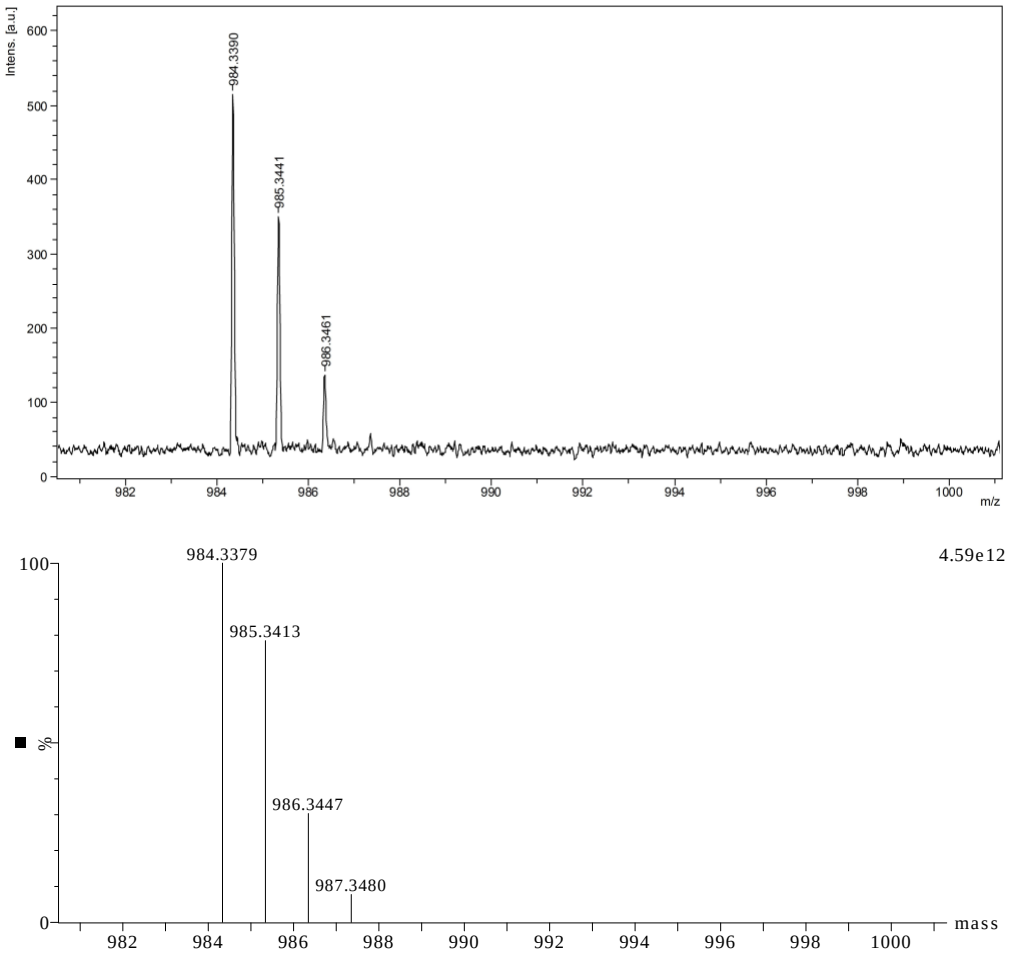

Figure S23. Experimental (top) *versus* simulated (bottom) high-resolution MALDI-TOF mass spectrum for **4F-CPP** ($[M]^+$, $C_{72}H_{44}F_4$).

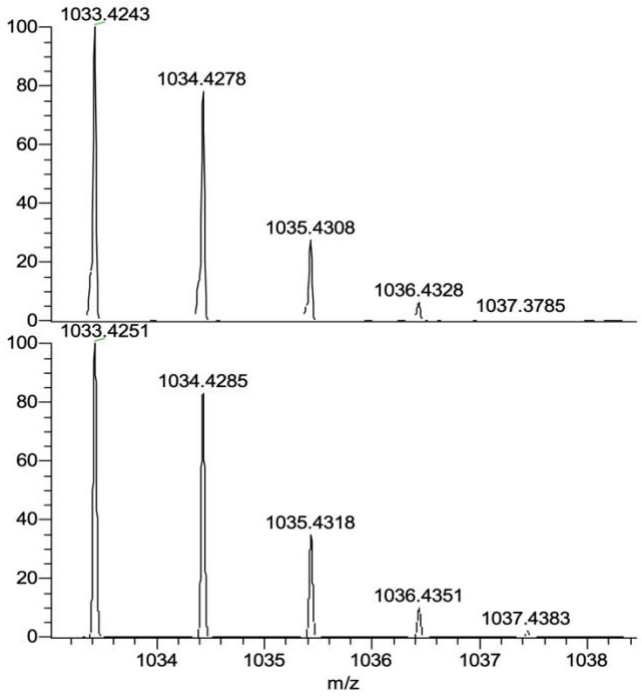

Figure S24. Experimental (top) *versus* simulated (bottom) high-resolution ESI mass spectrum for **4MeO-CPP** ($[M+H]^+$, $C_{76}H_{56}O_4H$).

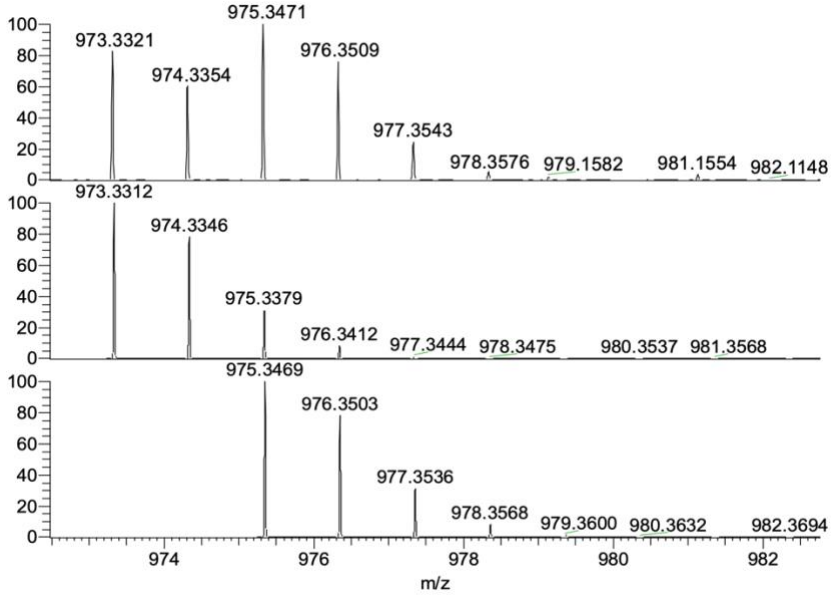

Figure S25. Experimental (top) *versus* simulated high-resolution ESI mass spectrum for **4HO-CPP** with the dicatechol-substituted phenylene unit in the as-synthesized form (bottom) and oxidized by air to the corresponding 2,5-dihydroxy-1,4-benzoquinone form (middle), ($[M_{unox}–H]^–$, $C_{72}H_{47}O_4$; $[M_{ox}–H]^–$, $C_{72}H_{45}O_4$). Data was collected immediately following removal of a solution of as-synthesized **4HO-CPP** from the glovebox.

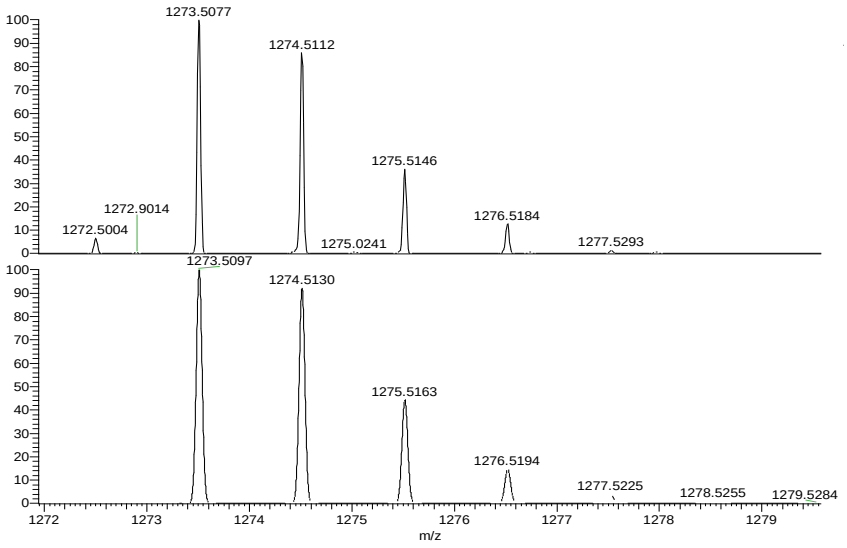

Figure S26. Experimental (top) *versus* simulated (bottom) high-resolution ESI mass spectrum for **12MeO-CPP** ($[M+H]^+$, $C_{84}H_{72}O_{12}H$).

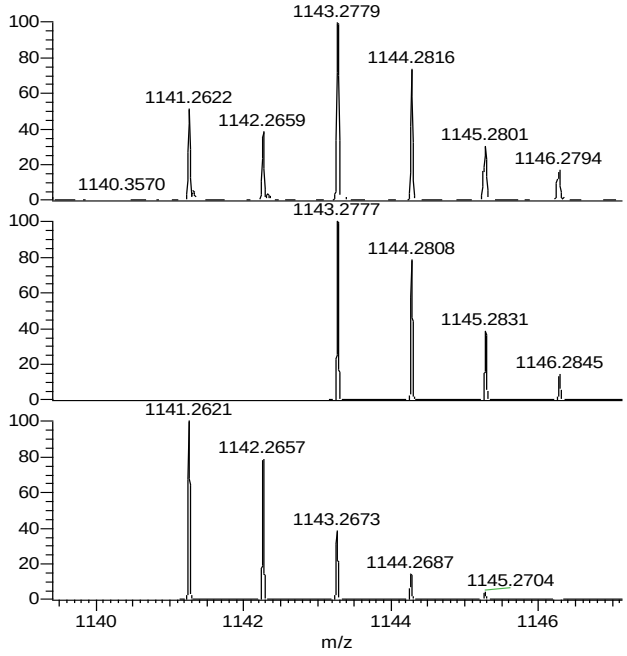

Figure S27. Experimental (top) *versus* simulated high-resolution ESI mass spectrum for **12HO-CPP** in the as-synthesized form (middle) and with one of the dicatechol-substituted phenylene units oxidized by air to the corresponding 2,5-dihydroxy-1,4-benzoquinone (bottom), ($[M_{unox}+K]^+$, $C_{72}H_{48}O_{12}K$; $[M_{ox}+K]^+$, $C_{72}H_{46}O_{12}K$). The addition of KCl was used to promote ionization. Data was collected immediately following removal of a solution of as-synthesized **12HO-CPP** from the glovebox.

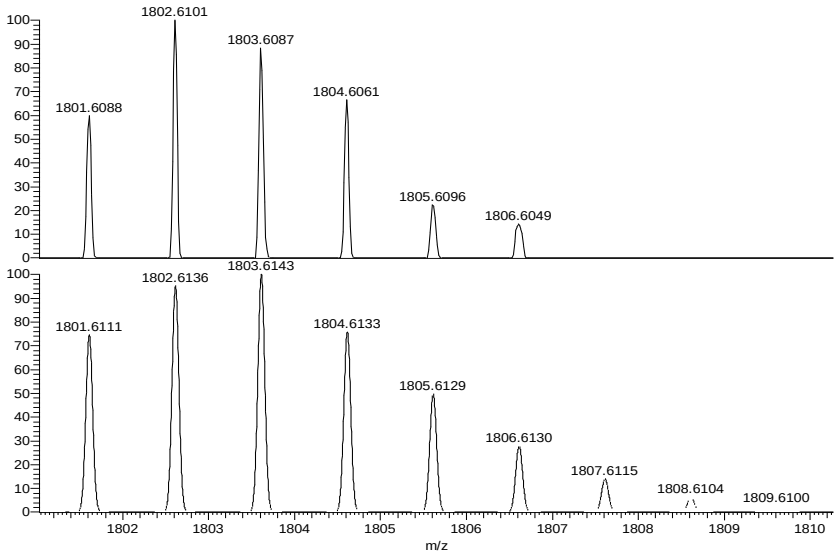

Figure S28. Experimental (top) *versus* simulated (bottom) high-resolution ESI mass spectrum of **12iPrS-CPP** ($[M+H]^+$, $C_{108}H_{120}S_{12}H$).

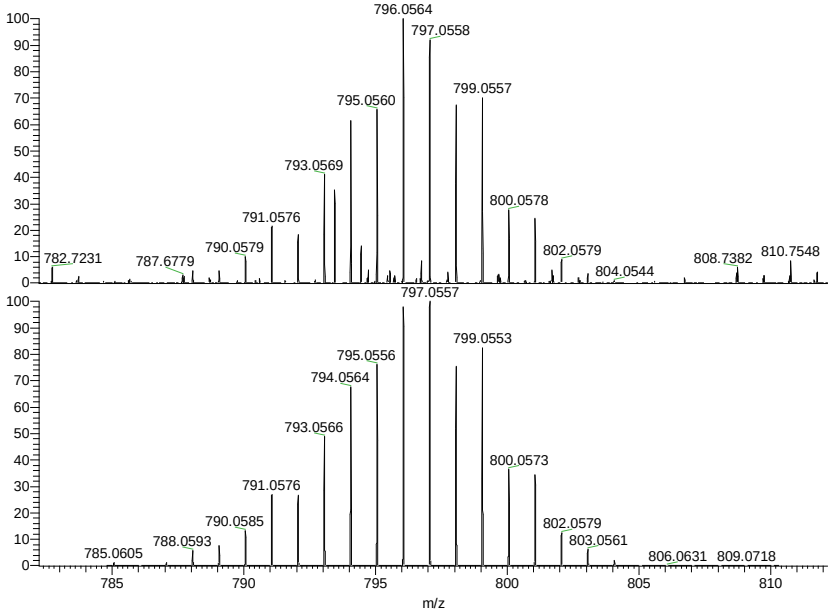

Figure S29. Experimental (top) *versus* simulated (bottom) high-resolution ESI mass spectrum of **Ru_2(Ph$_2$dhbq)** ($[M–Cl]^+$, $C_{38}H_{38}ClO_4Ru_2$).

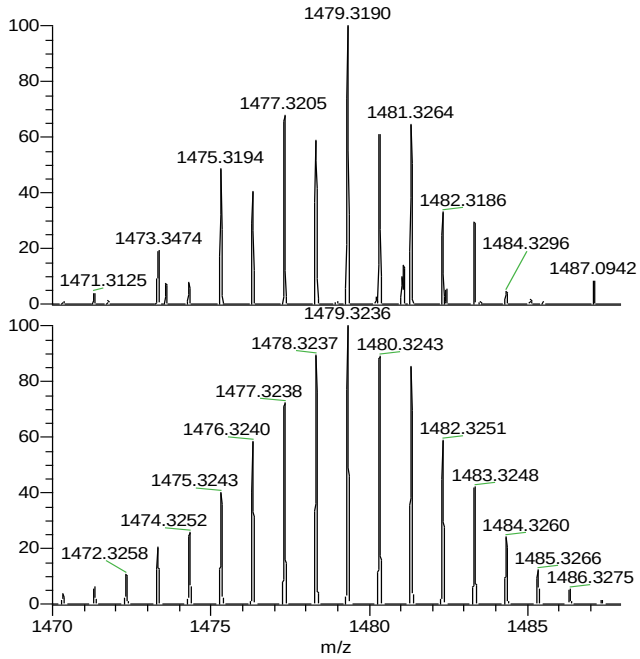

Figure S30. Experimental (top) *versus* simulated (bottom) high-resolution ESI mass spectrum of **Ru_2(4O-CPP)** ($[M–Cl]^+$, $C_{92}H_{72}O_4ClRu_2$).

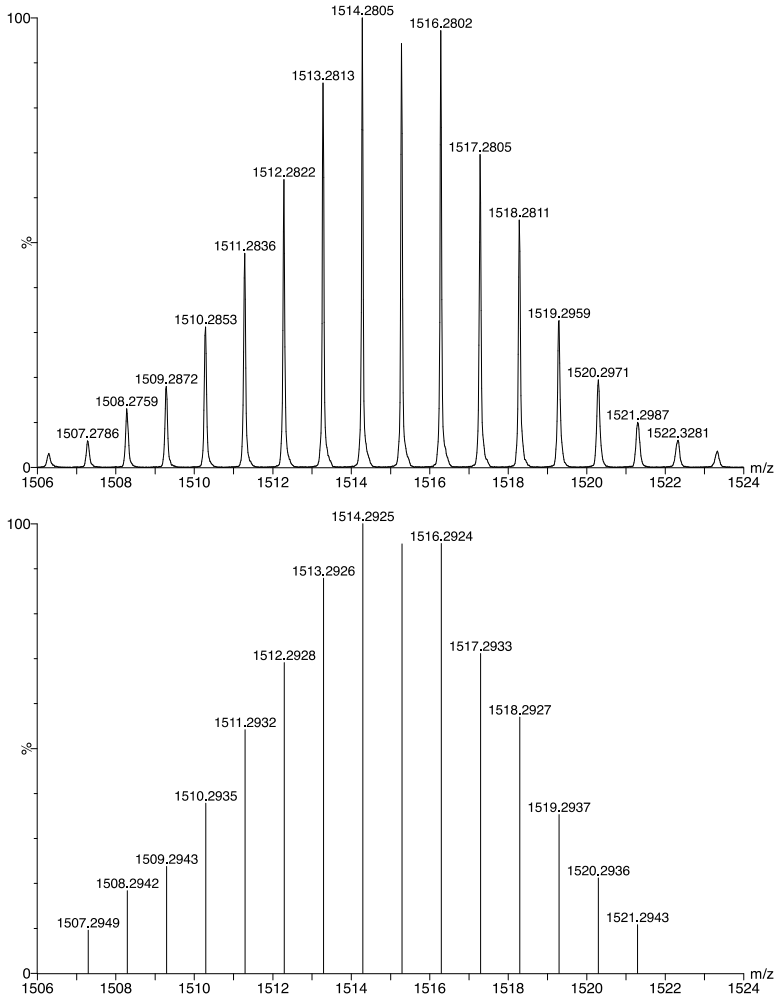

Figure S31. Experimental (top) *versus* simulated (bottom) high-resolution MALDI-TOF mass spectrum of **Ru_2(4O-CPP)** ($[M]^+$, $C_{92}H_{72}O_4Cl_2Ru_2$).

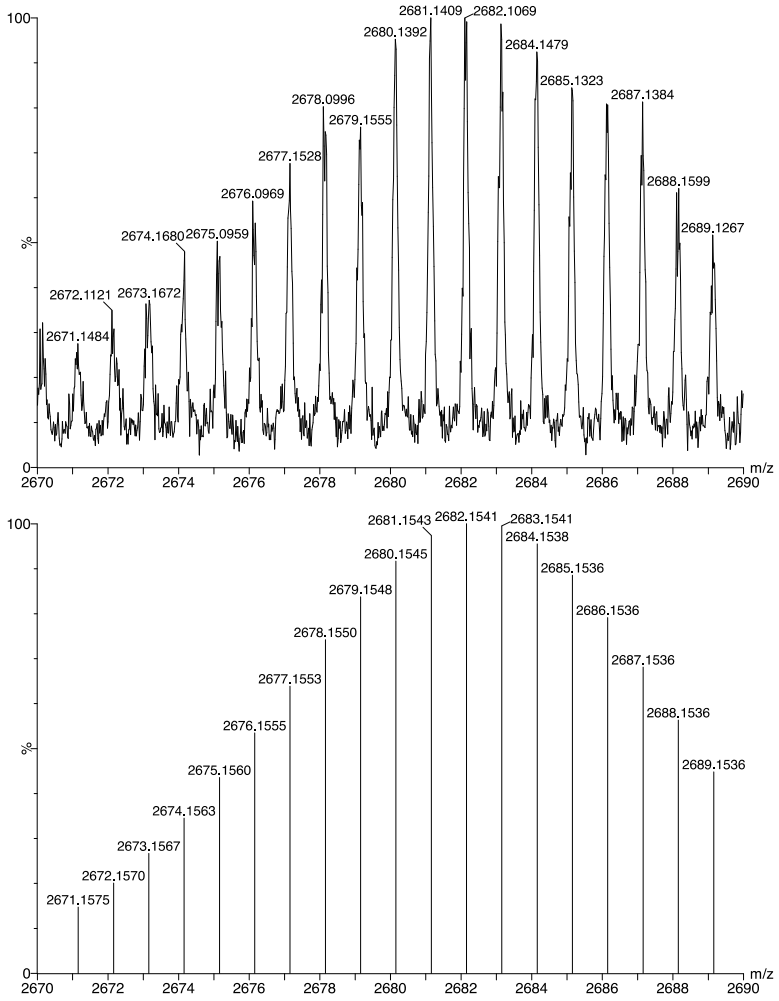

Figure S32. Experimental (top) *versus* simulated (bottom) high-resolution MALDI-TOF mass spectrum of **Ru_6(12O-CPP)** ($[M–Cl]^+$, $C_{132}H_{120}O_{12}Cl_5Ru_6$).

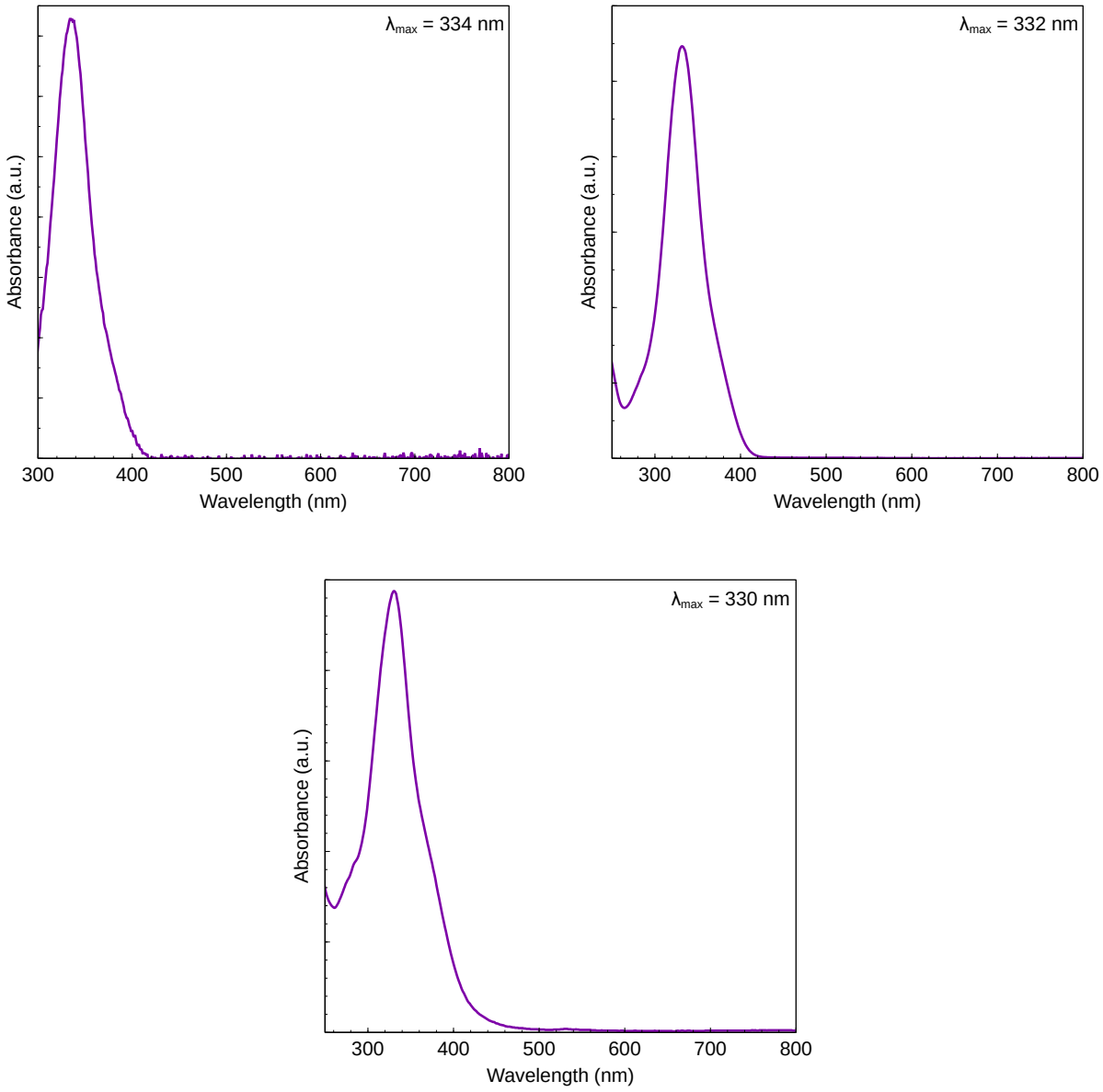

Figure S33. UV-vis spectra of **4F-CPP** (left), **4MeO-CPP** (right), and **4HO-CPP** (bottom) in DCM.

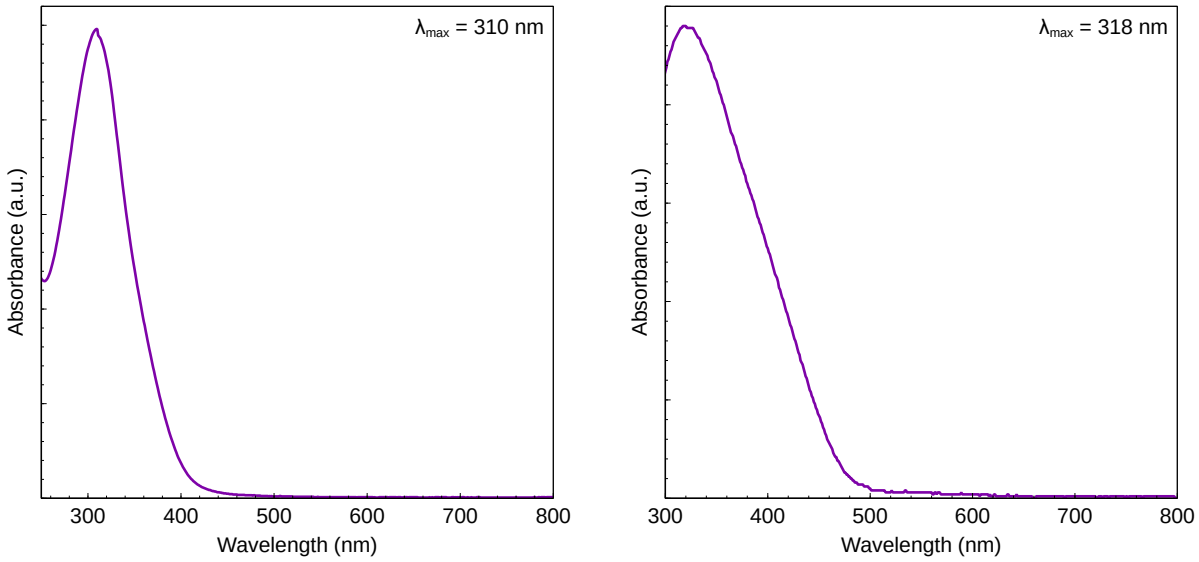

Figure S34. UV-vis spectra of **12MeO-CPP** (left) in DCM and **12HO-CPP** (right) in DMF.

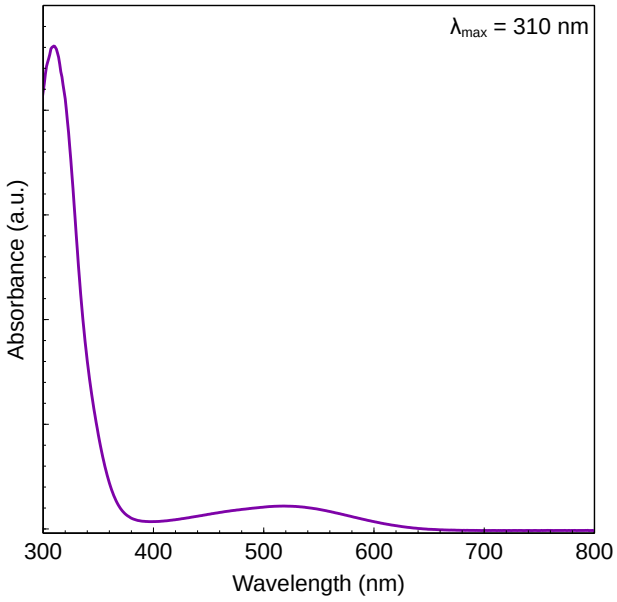

Figure S35. UV-vis spectrum of **H_4Ph_2dhbq** in DMF.

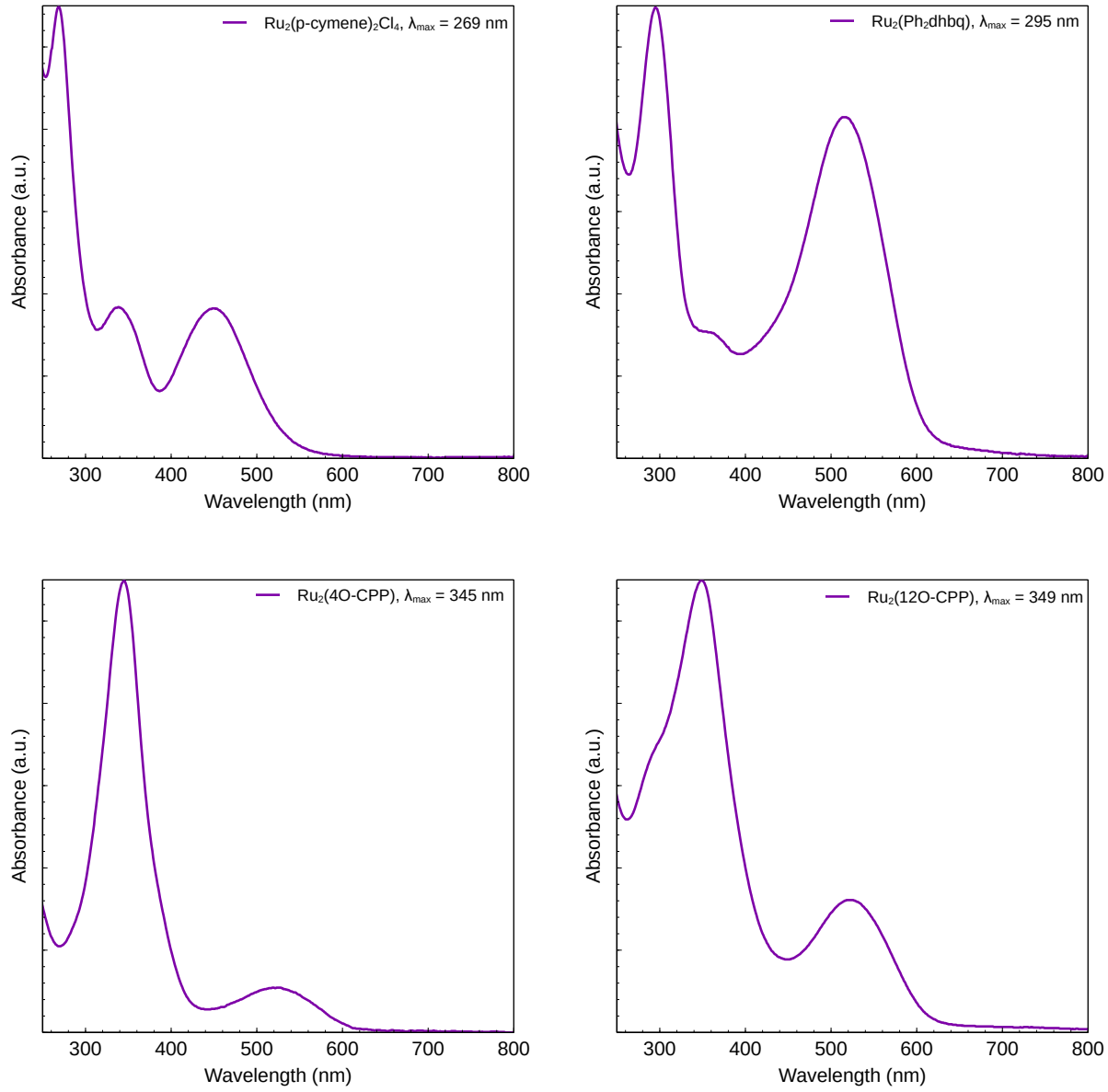

Figure S36. UV-vis spectra of Ru_2(*p*-cymene)$_2Cl_4$ (top left), **Ru_2(Ph$_2$dhbq)** (top right), **Ru_2(4O-CPP)** (bottom left), and **Ru_6(12O-CPP)** (bottom right), in DCM.

6. Supplementary DFT Optimized Geometries:

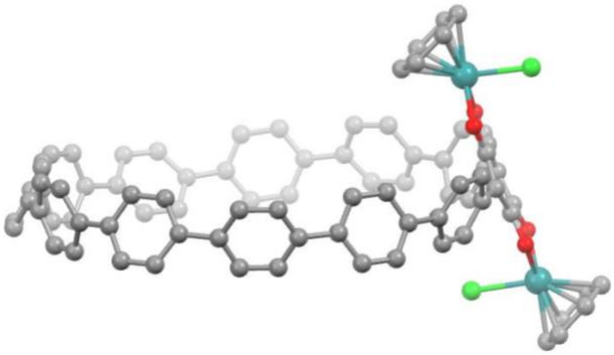

Figure S37. Optimized structure of **Ru_2(4O-CPP)** with Cl atoms in the *trans* configuration. Protons omitted for clarity. Ru, Cl, O, and C atoms are represented as dark green, light green, red, and gray, respectively.

148
E(RB3LYP): –4643.8065 Hartree

H	5.05268	6.23067	38.17191
H	6.55589	8.16412	38.00699
O	6.87487	1.95444	38.43014
C	5.98451	2.41309	39.22505
C	5.32191	1.36781	40.09966
C	5.66598	3.77857	39.31866
O	5.74329	0.17553	39.91102
C	4.35648	1.70153	41.06715
C	4.52908	4.06651	40.10237
C	6.57259	4.86030	38.85829
C	4.04570	0.84164	42.23714
C	3.87243	3.02477	40.98049
O	4.05786	5.24530	40.24249
C	7.95606	4.72527	39.08420
C	6.10357	6.10673	38.40699
C	2.80611	0.88194	42.90212
C	5.09008	0.12050	42.84922
O	2.94516	3.48234	41.73045
H	8.35588	3.77277	39.41702
C	8.80223	5.82471	39.00132
C	6.95848	7.20474	38.32254
H	1.96294	1.37592	42.43447
C	2.66581	0.35984	44.18724
H	6.05573	0.05173	42.35993
C	4.94132	-0.40330	44.12805
H	9.84217	5.70585	39.29188
C	8.31265	7.10553	38.68592
H	1.70809	0.45106	44.69415
C	3.75030	-0.23164	44.85639
H	5.80254	-0.85514	44.61247
C	9.15547	8.29661	38.95743
C	3.76122	-0.45180	46.32387
C	8.58271	9.43042	39.56053
C	10.55698	8.27876	38.83127
C	3.20965	0.52795	47.16751
C	4.49015	-1.48672	46.93715
H	7.50436	9.48178	39.67974
C	9.37153	10.42096	40.13524
H	11.03691	7.45418	38.31102
C	11.34716	9.27178	39.40431
H	2.64037	1.34379	46.73122
C	3.50108	0.55927	48.52627
H	4.87879	-2.29965	46.32931
C	4.76918	-1.46351	48.30143
H	8.88790	11.21889	40.69119
C	10.77490	10.33093	40.13307
H	12.42825	9.20260	39.31691
H	3.15433	1.40586	49.11050
C	4.34794	-0.39611	49.11782
H	5.36245	-2.26759	48.72801
C	11.56636	11.18693	41.05199
C	4.93562	-0.13180	50.45623
C	11.14694	12.47540	41.43334
C	12.66177	10.63973	41.74357
C	4.32874	0.73541	51.38415
C	6.24080	-0.56481	50.75652

H	10.35247	12.96718	40.87841	H	11.53720	4.37749	54.73160
C	11.69378	13.11435	42.54301	C	11.55859	6.51520	54.77903
H	13.01465	9.64574	41.48543	H	11.65264	13.52555	51.80906
C	13.21236	11.28033	42.84845	C	12.99484	11.84695	51.58729
C	5.04826	1.28240	52.44298	H	14.48343	10.38372	51.04181
H	3.29745	1.04420	51.23959	H	8.86535	8.48762	55.36802
H	6.74615	-1.25540	50.08852	C	10.82157	7.71076	54.86896
C	6.95187	-0.03682	51.82773	H	12.61739	6.55220	54.54140
H	11.31321	14.08986	42.83467	C	12.49599	11.05014	52.73581
C	12.69195	12.49833	43.31983	C	11.40341	8.98365	54.37134
H	13.98060	10.77054	43.42265	C	11.10842	10.92223	52.92049
H	4.57228	2.03426	53.06624	C	13.32548	10.21989	53.51123
C	6.40534	0.97104	52.64313	C	10.57637	9.91210	53.71304
H	7.97460	-0.36472	51.99014	C	12.79134	9.21607	54.31568
C	13.02982	12.95168	44.69208	H	10.43395	11.54356	52.33852
C	7.26852	1.82618	53.49550	H	14.40491	10.33281	53.45023
C	12.00500	13.41803	45.53386	H	9.49989	9.77387	53.72161
C	14.29043	12.73162	45.27688	H	13.46846	8.57290	54.87102
C	8.58596	2.08642	53.07696	H	5.84626	-2.48790	38.25570
C	6.79531	2.55679	54.60172	C	6.75894	-1.99687	37.93431
H	11.01616	13.59664	45.12161	C	6.71559	-1.08333	36.84625
C	12.18714	13.51126	46.90911	H	5.78420	-0.89235	36.32616
H	15.12817	12.43758	44.64992	C	7.87499	-0.31184	36.55508
C	14.47440	12.83167	46.65362	H	7.81473	0.48578	35.82191
H	8.98786	1.56357	52.21517	C	9.09076	-0.51431	37.26908
C	9.34335	3.09684	53.65176	C	9.11955	-1.46297	38.32636
H	5.80541	2.34944	54.99976	H	9.99956	-1.53003	38.95552
C	7.55577	3.57363	55.17840	C	7.96500	-2.21656	38.66262
H	11.33319	13.75778	47.53277	H	7.97329	-2.87650	39.52135
C	13.40491	13.14880	47.51217	H	9.95120	0.11396	37.07454
H	15.45415	12.61692	47.07182	Ru	7.43711	-0.02749	38.71795
H	10.31150	3.32954	53.22008	Cl	8.65075	0.80270	40.64494
C	8.82807	3.90828	54.67859	H	-0.20229	5.26796	42.99723
H	7.14013	4.13502	56.01124	C	0.64322	5.91416	42.79614
C	13.44740	12.88820	48.97340	C	0.60008	6.83610	41.71711
C	9.54422	5.16317	55.01797	H	-0.27412	6.86368	41.07696
C	12.58942	13.53933	49.88006	C	1.73854	7.61034	41.37320
C	14.19214	11.80156	49.46579	H	1.72217	8.24773	40.49774
C	8.83705	6.35104	55.27827	C	2.94174	7.44170	42.12045
C	10.93803	5.27406	54.86244	C	2.99654	6.56105	43.23456
H	12.05341	14.43121	49.56694	H	3.92622	6.40996	43.77057
C	12.36393	13.02774	51.15502	C	1.85695	5.76294	43.52827
H	14.86525	11.26835	48.80120	H	1.93144	4.98502	44.28102
C	13.97419	11.29550	50.74300	H	3.84535	7.94733	41.79611
H	7.76274	6.31229	55.43524	Ru	2.32758	5.43625	41.37838
C	9.46260	7.59313	55.21561	Cl	1.17189	4.54282	39.45532

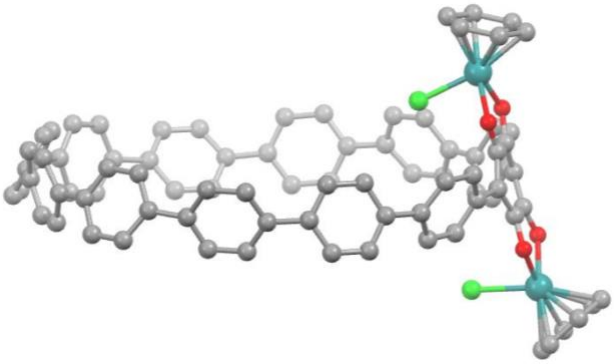

Figure S38. Optimized structure of **Ru$_2$(4O-CPP)** with Cl atoms in the *cis* configuration, both pointing inwards. Protons omitted for clarity. Ru, Cl, O, and C atoms are represented as dark green, light green, red, and gray, respectively.

148
E(RB3LYP): –4643.8018 Hartree

H	5.02205	6.31393	38.26217
H	6.53574	8.23899	38.13974
O	6.87881	2.01583	38.53496
C	5.96132	2.46909	39.30215
C	5.29797	1.42391	40.17404
C	5.61575	3.83170	39.36740
O	5.74618	0.23750	40.00929
C	4.30198	1.75034	41.11627
C	4.42057	4.08871	40.07062
C	6.52658	4.92023	38.93480
C	4.00227	0.91059	42.30293
C	3.75892	3.04247	40.94743
O	3.83175	5.22187	40.06914
C	7.90817	4.77606	39.17228
C	6.07013	6.17673	38.49876
C	2.77945	0.97426	42.99701
C	5.05073	0.18337	42.90348
O	2.70911	3.45316	41.54819
H	8.30100	3.82006	39.50151
C	8.76083	5.87084	39.10986
C	6.93136	7.27129	38.43816
H	1.93431	1.48035	42.54860
C	2.66146	0.47062	44.29149
H	6.00701	0.10009	42.39992
C	4.92284	-0.32426	44.19027
H	9.79722	5.74269	39.40888
C	8.28198	7.15846	38.80679
H	1.71895	0.58773	44.82094
C	3.75068	-0.12973	44.94260
H	5.78919	-0.78016	44.66151
C	9.13363	8.33974	39.09169
C	3.78822	-0.33977	46.41097
C	8.57365	9.46057	39.72949
C	10.53220	8.32005	38.93902
C	3.28963	0.66583	47.25692
C	4.49181	-1.39697	47.01525
H	7.49866	9.50669	39.87691
C	9.37583	10.43956	40.30563
H	10.99961	7.50261	38.39635
C	11.33537	9.30205	39.51314
H	2.75005	1.50351	46.82467
C	3.60372	0.69068	48.61079
H	4.84215	-2.22453	46.40366
C	4.79324	-1.37928	48.37499
H	8.90514	11.22533	40.88917
C	10.77873	10.34957	40.27006
H	12.41455	9.23307	39.40397
H	3.30179	1.55344	49.19616
C	4.42081	-0.29558	49.19329
H	5.36476	-2.20183	48.79631
C	11.59077	11.19373	41.18194
C	5.02966	-0.05233	50.52608
C	11.18339	12.48005	41.58269
C	12.69849	10.63723	41.84580
C	4.45049	0.82020	51.46638
C	6.32817	-0.51569	50.80894
H	10.37768	12.97773	41.04964
C	11.75624	13.10866	42.68505
H	13.04145	9.64373	41.57283
C	13.27475	11.26733	42.94367

C	5.19118	1.34104	52.52374	C	13.23932	11.78430	51.68875
H	3.42557	1.15392	51.33214	H	14.70322	10.31148	51.10372
H	6.81172	-1.20991	50.12853	H	9.14172	8.43272	55.50798
C	7.06069	-0.01270	51.87789	C	11.08007	7.63953	54.96678
H	11.38462	14.08263	42.99298	H	12.85614	6.46429	54.59422
C	12.76921	12.48368	43.43501	C	12.75342	10.98274	52.83954
H	14.05251	10.75001	43.49798	C	11.66752	8.91157	54.47363
H	4.73821	2.09812	53.15775	C	11.36804	10.86793	53.04785
C	6.54260	0.99757	52.70861	C	13.58742	10.13601	53.59197
H	8.07843	-0.36208	52.02672	C	10.83918	9.85564	53.83965
C	13.13865	12.92671	44.80249	C	13.05669	9.12976	54.39576
C	7.43038	1.82532	53.56270	H	10.69002	11.50140	52.48344
C	12.13423	13.39215	45.66899	H	14.66680	10.23760	53.51245
C	14.41082	12.69841	45.35842	H	9.76164	9.72839	53.86500
C	8.74620	2.07123	53.13085	H	13.73648	8.47328	54.93200
C	6.98298	2.54581	54.68609	H	5.94641	-2.46161	38.40222
H	11.13699	13.57538	45.27978	C	6.85152	-1.95159	38.08908
C	12.34688	13.47755	47.04031	C	6.80488	-1.05745	36.98475
H	15.23330	12.40396	44.71172	H	5.87914	-0.90056	36.44363
C	14.62525	12.79009	46.73138	C	7.94878	-0.26071	36.70230
H	9.12800	1.55580	52.25552	H	7.88253	0.52296	35.95472
C	9.52643	3.06141	53.71046	C	9.15685	-0.42134	37.44036
H	5.99482	2.34792	55.09325	C	9.19092	-1.35254	38.51233
C	7.76655	3.54189	55.26791	H	10.06089	-1.38730	39.15780
H	11.50753	13.72293	47.68389	C	8.04944	-2.12960	38.84110
C	13.57619	13.10742	47.61459	H	8.05911	-2.77509	39.71072
H	15.61277	12.56831	47.12719	H	10.00446	0.22566	37.25095
H	10.49174	3.28660	53.26856	Ru	7.46785	0.04618	38.85374
C	9.03695	3.86509	54.75588	Cl	8.62716	0.91364	40.79147
H	7.37031	4.09717	56.11422	H	-0.35877	4.22492	41.66089
C	13.64840	12.83879	49.07316	C	0.11409	5.19594	41.55634
C	9.77450	5.10554	55.10252	C	0.40616	5.69545	40.25789
C	12.81522	13.49183	50.00129	H	0.14255	5.12271	39.37642
C	14.39380	11.74292	49.54356	C	1.18612	6.87814	40.14276
C	9.08630	6.29811	55.39076	H	1.53440	7.19507	39.16518
C	11.16695	5.20193	54.92645	C	1.57893	7.61645	41.29736
H	12.28023	14.38983	49.70429	C	1.23290	7.12153	42.58210
C	12.61106	12.97391	51.27725	H	1.63687	7.60499	43.46389
H	15.04800	11.20791	48.86171	C	0.49560	5.91673	42.72549
C	14.19698	11.23022	50.82159	H	0.31072	5.50311	43.70916
H	8.01413	6.27029	55.56371	H	2.21391	8.48840	41.20054
C	9.72576	7.53333	55.33467	Ru	2.32085	5.49966	41.47643
H	11.75295	4.30020	54.77320	Cl	4.10494	5.70535	43.08041
C	11.80111	6.43665	54.84937				
H	11.91704	13.47325	51.94846				

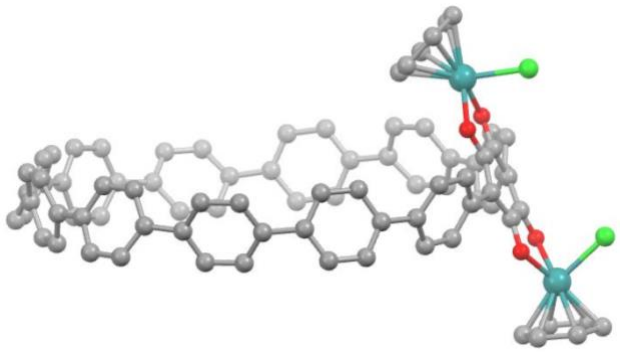

Figure S39. Optimized structure of **Ru$_2$(4O-CPP)** with Cl atoms in the *cis* configuration, both pointing outwards. Protons omitted for clarity. Ru, Cl, O, and C atoms are represented as dark green, light green, red, and gray, respectively.

148
E(RB3LYP): –4643.8001 Hartree

H	4.92540	6.22779	38.24347
H	6.39475	8.18050	38.03225
O	6.84399	1.96896	38.50313
C	5.91339	2.41861	39.25635
C	5.25962	1.37040	40.13633
C	5.60280	3.78677	39.36495
O	5.73094	0.19135	39.98653
C	4.31158	1.70518	41.12397
C	4.50299	4.08319	40.19619
C	6.48433	4.87377	38.86974
C	3.98624	0.83374	42.28137
C	3.85622	3.04035	41.07844
O	4.06220	5.26871	40.37443
C	7.87752	4.75957	39.03373
C	5.98526	6.11706	38.44043
C	2.75230	0.90281	42.95623
C	5.00345	0.06522	42.88001
O	2.96648	3.50492	41.86875
H	8.30237	3.80773	39.33329
C	8.70822	5.86868	38.92607
C	6.82207	7.22591	38.32882
H	1.92135	1.42464	42.49791
C	2.60351	0.37289	44.23655
H	5.95613	-0.04413	42.37474
C	4.84951	-0.46549	44.15547
H	9.76122	5.76164	39.17130
C	8.19034	7.14505	38.64168
H	1.65135	0.48847	44.74868
C	3.67252	-0.25727	44.89596
H	5.69662	-0.95547	44.62804
C	9.02416	8.34582	38.89752
C	3.68854	-0.48011	46.36283
C	8.45208	9.46609	39.52618
C	10.42208	8.34912	38.73442
C	3.16354	0.51133	47.20993
C	4.40027	-1.52959	46.97195
H	7.37655	9.50243	39.67267
C	9.24213	10.46113	40.09112
H	10.89950	7.53824	38.19069
C	11.21362	9.34618	39.29878
H	2.60709	1.33800	46.77766
C	3.46595	0.53788	48.56623
H	4.76458	-2.35288	46.36286
C	4.69163	-1.51006	48.33388
H	8.76227	11.24725	40.66672
C	10.64606	10.38918	40.05404
H	12.29299	9.29318	39.18286
H	3.14027	1.39131	49.15259
C	4.29876	-0.43324	49.15202
H	5.27116	-2.32576	48.75745
C	11.44722	11.24352	40.96604
C	4.90270	-0.17617	50.48450
C	11.02184	12.52295	41.37039
C	12.56028	10.69932	41.63125
C	4.31483	0.69847	51.41760
C	6.20648	-0.62247	50.77092
H	10.21320	13.01354	40.83523
C	11.58116	13.15331	42.47868
H	12.91923	9.71275	41.35349
C	13.12260	11.33103	42.73542
C	5.05186	1.24009	52.46701
H	3.28503	1.01702	51.28400

H	6.69630	-1.32031	50.09872	C	13.00395	11.79816	51.49014
C	6.93535	-0.09913	51.83260	H	14.48739	10.34244	50.91146
H	11.19622	14.12137	42.78865	H	8.93375	8.42697	55.32205
C	12.59730	12.53697	43.23178	C	10.87945	7.64623	54.78913
H	13.90564	10.82188	43.28988	H	12.66723	6.48419	54.43141
H	4.59061	1.99761	53.09443	C	12.52256	10.99203	52.63959
C	6.40825	0.91620	52.65155	C	11.45484	8.91872	54.28315
H	7.95659	-0.43674	51.98438	C	11.13798	10.86334	52.84504
C	12.95027	12.97502	44.60524	C	13.36379	10.15700	53.39702
C	7.28909	1.76720	53.48991	C	10.61802	9.84999	53.64141
C	11.93355	13.42584	45.46517	C	12.84191	9.14980	54.20532
C	14.21898	12.75407	45.17200	H	10.45469	11.48810	52.27721
C	8.60181	2.01867	53.05170	H	14.44216	10.26993	53.31974
C	6.83584	2.50405	54.60031	H	9.54170	9.71271	53.66706
H	10.93885	13.60467	45.06745	H	13.52739	8.50401	54.74720
C	12.13215	13.50382	46.83902	H	6.95751	-2.11566	36.11814
H	15.05070	12.47247	44.53146	C	7.57889	-1.75441	36.92932
C	14.41926	12.83826	46.54758	C	8.42696	-0.63475	36.71048
H	8.98860	1.48971	52.18666	H	8.47377	-0.16707	35.73484
C	9.37230	3.02800	53.61096	C	9.11150	-0.05945	37.81865
H	5.85089	2.30314	55.01362	H	9.67635	0.85607	37.67665
C	7.60966	3.51926	55.16170	C	9.00749	-0.62430	39.12079
H	11.28498	13.73933	47.47602	C	8.11469	-1.70981	39.32169
C	13.35895	13.14033	47.42277	H	7.91695	-2.06106	40.32910
H	15.40509	12.62361	46.95132	C	7.41717	-2.30301	38.22632
H	10.33529	3.25400	53.16440	H	6.70258	-3.09840	38.39891
C	8.87566	3.84661	54.64128	H	9.50674	-0.15948	39.96295
H	7.20906	4.08557	55.99851	Ru	6.94195	-0.10394	38.31432
C	13.42043	12.86469	48.88053	Cl	4.91466	0.09312	37.03160
C	9.60051	5.10090	54.96415	H	-0.09067	5.34417	43.28500
C	12.57324	13.50571	49.80434	C	0.76445	5.97274	43.06918
C	14.17299	11.77443	49.35255	C	0.70935	6.91927	42.01203
C	8.90010	6.29047	55.23483	H	-0.18478	6.98322	41.40281
C	10.99147	5.20925	54.78325	C	1.85626	7.66930	41.64453
H	12.03206	14.39977	49.50675	H	1.82768	8.32481	40.78288
C	12.36556	12.98190	51.07730	C	3.07918	7.45353	42.34698
H	14.83850	11.24910	48.67411	C	3.14719	6.54982	43.44128
C	13.97255	11.25590	50.62770	H	4.08933	6.36502	43.94395
H	7.82874	6.25403	55.41118	C	1.99760	5.77426	43.75605
C	9.52655	7.53132	55.15959	H	2.07597	4.97902	44.49008
H	11.58696	4.31154	54.64369	H	3.98426	7.94300	42.00257
C	11.61258	6.44925	54.68717	Ru	2.38422	5.48146	41.58402
H	11.66280	13.47280	51.74558	Cl	1.12932	4.66403	39.69744

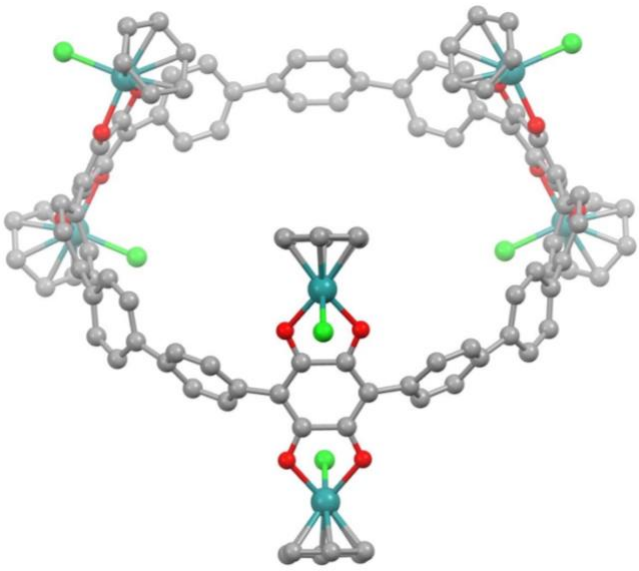

Figure S40. Optimized structure of **Ru$_6$(12O-CPP)** with Cl atoms in the higher symmetry configuration (contains a C_3 axis of rotation). Protons omitted for clarity. Ru, Cl, O, and C atoms are represented as dark green, light green, red, and gray, respectively.

204
E(RB3LYP): –8386.3157 Hartree

H	4.76727	6.28397	38.30000
H	6.09649	8.34358	38.17083
O	6.99090	2.17968	38.37793
C	6.07468	2.52484	39.20002
C	5.54462	1.39643	40.06113
C	5.62017	3.84831	39.33754
O	6.09000	0.26109	39.84262
C	4.56596	1.60497	41.04914
C	4.46706	3.99301	40.13666
C	6.41393	5.02621	38.90507
C	4.38007	0.69688	42.20907
C	3.93718	2.86630	40.99552
O	3.87274	5.11081	40.31045
C	7.80831	5.00534	39.10287
C	5.82990	6.24288	38.51010
C	3.14855	0.53502	42.86834
C	5.52288	0.13954	42.81513
O	2.97375	3.20060	41.76570
H	8.29647	4.08183	39.39670
C	8.55498	6.17509	39.04118
C	6.58663	7.41286	38.44608
H	2.24079	0.90655	42.40689
C	3.08590	-0.04037	44.13746
H	6.48920	0.23357	42.33054
C	5.45368	-0.42849	44.08089
H	9.60699	6.13607	39.30839
C	7.95305	7.41889	38.77543
H	2.12175	-0.11880	44.63397
C	4.24608	-0.47437	44.80170
H	6.37510	-0.74641	44.56000
C	8.70837	8.66581	39.05417
C	4.27929	-0.76694	46.25646
C	8.07118	9.74618	39.68996
C	10.10458	8.74885	38.89926
C	3.48981	-0.01330	47.14312
C	5.22912	-1.63476	46.82658
H	6.99421	9.72031	39.83072
C	8.80236	10.77982	40.26699
H	10.62945	7.96965	38.35313
C	10.83603	9.78290	39.47651
H	2.74578	0.66999	46.74323
C	3.73501	-0.01745	48.51274
H	5.81290	-2.28654	46.18217
C	5.47445	-1.63888	48.19672
H	8.27905	11.53659	40.84474
C	10.20826	10.78616	40.23783
H	11.91743	9.79041	39.36959
H	3.17670	0.66271	49.14995

C	4.78230	-0.77544	49.06602	C	8.92553	6.20242	55.82026
H	6.24493	-2.29372	48.59476	C	10.57579	4.97123	54.57215
C	10.96510	11.67675	41.15274	H	11.89434	14.55729	50.04177
C	5.25621	-0.49110	50.44355	C	12.25578	12.92607	51.38871
C	10.50180	12.94715	41.53621	H	14.36022	11.36251	48.55154
C	12.08946	11.17158	41.83140	C	13.64628	11.15540	50.55702
C	4.39888	-0.06231	51.47153	H	8.00192	6.24045	56.38639
C	6.63896	-0.44728	50.70061	C	9.65676	7.37369	55.62284
H	9.67623	13.40344	40.99539	H	10.93208	4.04992	54.12300
C	11.04790	13.61903	42.62982	C	11.29694	6.14222	54.37619
H	12.47448	10.18974	41.57181	H	11.66694	13.37860	52.18289
C	12.64095	11.83705	42.91889	C	12.82466	11.65569	51.58398
C	4.89843	0.50692	52.64289	H	14.09839	10.17367	50.66397
H	3.32230	-0.13963	51.34016	H	9.29213	8.30235	56.05515
H	7.33662	-0.76142	49.92975	C	10.82402	7.38372	54.83988
C	7.14348	0.11464	51.86650	H	12.19091	6.10648	53.76041
H	10.63165	14.57379	42.93015	C	12.43141	10.76049	52.70065
C	12.08622	13.04502	43.38467	C	11.43522	8.63315	54.32188
H	13.45202	11.37012	43.46807	C	11.10196	10.75092	53.15884
H	4.20748	0.87499	53.39263	C	13.28470	9.75641	53.19462
C	6.28227	0.66756	52.83426	C	10.61634	9.71388	53.94922
H	8.21796	0.20792	51.98600	C	12.79886	8.71889	53.98519
C	12.45992	13.51859	44.74140	H	10.41041	11.50817	52.80013
C	6.85950	1.57151	53.86104	H	14.33646	9.76617	52.92145
C	11.48063	13.90971	45.67809	H	9.55707	9.68581	54.18905
C	13.75554	13.38406	45.27094	H	13.48090	7.93918	54.31352
C	8.12058	1.36098	54.44651	C	7.17096	-0.77731	36.70007
C	6.28846	2.83187	54.13415	C	8.27319	0.09252	36.45900
O	10.26679	14.15204	45.36047	C	9.56907	-1.02067	38.21797
C	11.74549	13.90672	47.16725	C	8.47201	-1.87103	38.50404
O	14.79497	13.21169	44.54681	H	8.51524	-2.55779	39.34051
C	14.02100	13.38162	46.76265	H	10.29747	0.66054	37.03701
O	8.70768	0.22551	54.45863	Ru	7.77371	0.26724	38.61933
C	8.91705	2.48758	55.07274	Cl	8.92130	1.19468	40.54179
O	5.11724	3.16714	53.74836	H	-0.37376	4.65021	43.04611
C	7.08373	3.95657	54.75889	C	0.42017	5.36936	42.88701
O	10.71588	14.14724	47.88487	C	0.31689	6.33325	41.84697
C	12.98750	13.51277	47.70705	H	-0.55008	6.32085	41.19657
O	15.24628	13.20802	47.08322	C	1.39394	7.20676	41.55323
O	10.06234	2.14125	55.52315	H	1.33752	7.87926	40.70608
C	8.44268	3.81080	55.10702	C	2.60066	7.09806	42.30930
O	6.46596	5.07421	54.80608	C	2.71220	6.17604	43.38339
C	13.10502	13.03383	49.10751	H	3.64635	6.07047	43.92261
C	9.33677	4.98850	55.24175	C	1.63382	5.27872	43.62626
C	12.39004	13.60275	50.17639	H	1.76248	4.47394	44.34266
C	13.78784	11.82569	49.34862	H	3.46572	7.68486	42.01815

Ru	2.15127	5.08618	41.47429	C	7.54681	13.04287	47.06156
Cl	1.06090	4.13064	39.54307	H	7.79340	11.99320	46.95230
Ru	4.44789	5.05210	54.31126	Cl	10.09953	16.91695	46.69848
Ru	10.71245	0.23080	55.01900	Cl	15.47838	10.47076	45.72959
Ru	9.00330	14.77366	46.88800	H	17.47164	13.96880	43.06417
Ru	16.53053	12.64633	45.54473	H	18.06715	11.54299	43.21153
H	8.16388	0.90821	35.75186	C	3.64713	7.14485	54.54397
C	9.48581	-0.03980	37.19052	C	2.35601	5.30689	53.51498
H	6.23743	-0.64040	36.16692	H	3.20427	4.49781	51.68294
H	10.43973	-1.04023	38.86321	H	5.08155	6.14972	51.55593
C	7.26490	-1.72140	37.75605	C	4.56102	7.09802	53.45046
H	6.38819	-2.29367	38.04101	H	3.83853	7.79241	55.39070
H	18.73950	11.98422	47.47663	H	1.93301	6.17896	55.45335
C	18.55540	12.43124	46.50731	H	5.45852	7.70717	53.48020
C	18.22001	13.81662	46.40452	C	2.55433	6.23864	54.56722
H	18.14081	14.41312	47.30739	C	4.35805	6.20721	52.36076
C	17.90892	14.40151	45.15026	C	3.28352	5.27910	52.43178
H	17.61226	15.44199	45.08771	H	1.57073	4.56416	53.58296
C	17.84247	13.56240	43.99940	H	12.22714	0.91527	57.47408
C	18.17433	12.18298	44.07856	C	12.01944	0.08027	56.81311
C	18.52091	11.62629	45.34289	H	13.66529	0.53906	55.46268
H	18.64834	10.55374	45.43290	H	10.23670	-0.54639	57.90993
H	8.06644	13.12841	49.16637	C	12.83637	-0.12603	55.67085
C	7.68913	13.68930	48.31757	C	10.87855	-0.74131	57.05870
C	7.42251	15.08499	48.46294	C	12.47208	-1.13432	54.73076
H	7.58142	15.57627	49.41505	C	10.51552	-1.71284	56.09285
C	7.07057	15.84118	47.31705	C	11.32382	-1.93513	54.93379
H	6.99392	16.91957	47.39462	H	13.01655	-1.20963	53.79666
C	6.96683	15.22649	46.03898	H	9.57932	-2.25068	56.19978
H	6.78301	15.82757	45.15709	H	11.00815	-2.64170	54.17578
C	7.23856	13.83410	45.91853	Cl	4.09304	4.09051	56.49777
H	7.27276	13.38112	44.93308	Cl	11.11761	1.16312	52.81882

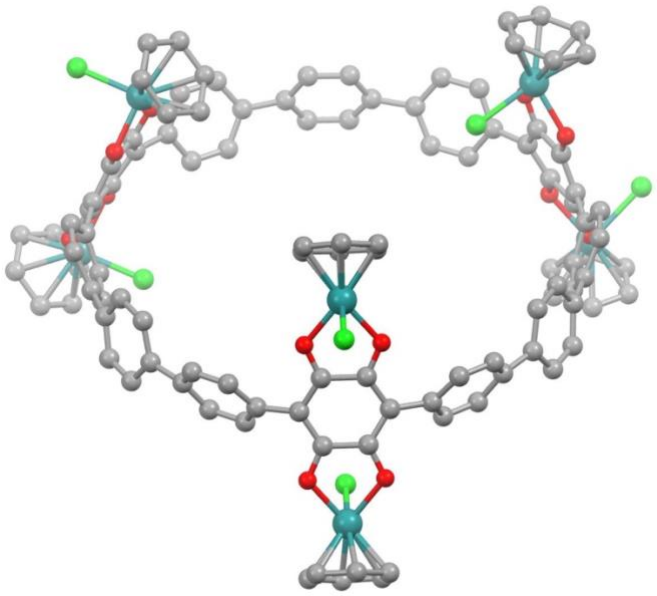

Figure S41. Optimized structure of **Ru$_6$(12O-CPP)** with Cl atoms in the lower symmetry configuration. Protons omitted for clarity. Ru, Cl, O, and C atoms are represented as dark green, light green, red, and gray, respectively.

204
E(RB3LYP): –8386.3109 Hartree

H	4.61048	6.23169	38.36768
H	5.90381	8.31341	38.22906
O	6.87534	2.15394	38.32622
C	5.98510	2.48295	39.18352
C	5.49012	1.34027	40.04650
C	5.52813	3.80142	39.35291
O	6.03577	0.21091	39.79689
C	4.54072	1.52876	41.06546
C	4.41127	3.93418	40.20465
C	6.29401	4.99134	38.90315
C	4.38291	0.59784	42.21148
C	3.91575	2.79330	41.06460
O	3.82794	5.04917	40.42309
C	7.69423	4.98770	39.05357
C	5.67993	6.20376	38.54247
C	3.16007	0.40703	42.87828
C	5.53960	0.04905	42.79777
O	2.98837	3.11474	41.88201
H	8.20442	4.06708	39.31785
C	8.42111	6.16986	38.98597
C	6.41630	7.38597	38.47268
H	2.24273	0.77220	42.43039
C	3.11767	-0.18738	44.13904
H	6.49915	0.16428	42.30389
C	5.49113	-0.53660	44.05691
H	9.48163	6.14374	39.21927
C	7.79155	7.40809	38.76169
H	2.15939	-0.28790	44.64271
C	4.29101	-0.60956	44.78799
H	6.42175	-0.84617	44.52363
C	8.53137	8.66253	39.04791
C	4.33869	-0.91240	46.24029
C	7.89203	9.71002	39.73463
C	9.91972	8.77965	38.85112
C	3.53376	-0.18384	47.13410
C	5.31091	-1.76029	46.80259
H	6.82163	9.65468	39.91125
C	8.61855	10.74314	40.31799
H	10.44259	8.02704	38.26690
C	10.64703	9.81353	39.43424
H	2.77281	0.48444	46.74102
C	3.78179	-0.19154	48.50279
H	5.90915	-2.39340	46.15279
C	5.55923	-1.76792	48.17245
H	8.09911	11.46817	40.93804
C	10.02201	10.78095	40.24265
H	11.72416	9.84901	39.29322
H	3.20856	0.47092	49.14522

C	4.84777	-0.92815	49.04931	C	8.80850	6.12985	55.83129
H	6.34636	-2.40667	48.56410	C	10.51425	4.92343	54.63442
C	10.78678	11.66245	41.15867	H	11.70906	14.48107	50.02508
C	5.31357	-0.64065	50.42899	C	12.07476	12.87412	51.39321
C	10.31800	12.91718	41.58178	H	14.27618	11.33114	48.63121
C	11.93396	11.16132	41.79949	C	13.51804	11.12669	50.61542
C	4.44342	-0.22925	51.45350	H	7.86978	6.15313	56.37284
C	6.69414	-0.57068	50.69210	C	9.52031	7.31427	55.64364
H	9.47066	13.37159	41.07439	H	10.89957	4.00610	54.20124
C	10.88285	13.57558	42.67332	C	11.21667	6.10769	54.44853
H	12.32658	10.19127	41.50819	H	11.45564	13.32199	52.16652
C	12.50084	11.81396	42.88546	C	12.66455	11.61938	51.61871
C	4.92652	0.35311	52.62489	H	13.98948	10.15671	50.74536
H	3.36922	-0.32836	51.31796	H	9.12553	8.23874	56.05797
H	7.40111	-0.87233	49.92470	C	10.70514	7.34250	54.88825
C	7.18238	0.00321	51.85957	H	12.12674	6.08657	53.85594
H	10.45810	14.51570	43.00070	C	12.26952	10.73021	52.73868
C	11.94668	13.00462	43.39683	C	11.29537	8.60077	54.36756
H	13.33527	11.35058	43.39788	C	10.92834	10.68708	53.15839
H	4.22530	0.71056	53.37048	C	13.13983	9.76165	53.27212
C	6.30575	0.54248	52.82067	C	10.45393	9.64862	53.95340
H	8.25431	0.11757	51.98535	C	12.66457	8.72226	54.06689
C	12.35110	13.46132	44.74911	H	10.22330	11.41276	52.76307
C	6.85669	1.46494	53.84553	H	14.19823	9.80090	53.02800
C	11.42681	13.97910	45.67966	H	9.38949	9.58972	54.16209
C	13.64020	13.25311	45.28200	H	13.36023	7.96901	54.42718
C	8.10612	1.27391	54.46019	C	7.00729	-0.76779	36.59781
C	6.26962	2.72591	54.07997	C	8.10508	0.10257	36.33684
O	10.28308	14.44515	45.35368	C	9.45055	-1.04457	38.03573
C	11.69317	13.97173	47.17307	C	8.36020	-1.89617	38.34125
O	14.65299	12.93891	44.56726	H	8.42675	-2.59705	39.16438
C	13.90649	13.24666	46.77294	H	10.14817	0.65414	36.86062
O	8.70643	0.14522	54.49233	Ru	7.67331	0.24218	38.51393
C	8.87336	2.41347	55.09907	Cl	8.88952	1.14849	40.40488
O	5.11056	3.04762	53.65036	H	-0.28497	4.58213	43.35357
C	7.03655	3.86387	54.71522	C	0.51456	5.29103	43.17740
O	10.73298	14.43161	47.87876	C	0.38238	6.28534	42.16903
C	12.88196	13.44758	47.72121	H	-0.51350	6.30651	41.55933
O	15.10380	12.92841	47.09003	C	1.46136	7.14667	41.84976
O	10.01074	2.08301	55.58170	H	1.37929	7.84390	41.02498
C	8.38371	3.73108	55.11269	C	2.69890	6.99697	42.54744
O	6.41131	4.97755	54.72638	C	2.84159	6.04318	43.58862
C	12.97144	12.97949	49.12608	H	3.79676	5.90784	44.08246
C	9.25733	4.92138	55.26964	C	1.75824	5.15862	43.85702
C	12.22352	13.54120	50.17795	H	1.90422	4.33255	44.54530
C	13.67078	11.78800	49.40469	H	3.56046	7.57782	42.23488

Ru	2.17169	5.01521	41.67847	C	6.79333	15.18328	47.43574
Cl	0.96730	4.11412	39.78852	H	6.11480	14.37059	47.66716
Ru	4.41580	4.94287	54.14651	Cl	8.54679	12.47921	46.95556
Ru	10.69313	0.17594	55.11060	Cl	16.27881	15.33779	45.58784
Ru	8.94783	14.85838	46.89554	H	18.10250	13.04559	43.00316
Ru	16.49346	12.93297	45.54054	H	16.76561	10.95408	43.34136
H	7.97663	0.93053	35.64741	C	3.62519	7.04750	54.29106
C	9.33915	-0.04620	37.02737	C	2.35257	5.18809	53.27800
H	6.05803	-0.61854	36.09671	H	3.24985	4.31950	51.49792
H	10.34076	-1.07769	38.65311	H	5.14099	5.95713	51.37788
C	7.13060	-1.73000	37.63381	C	4.57116	6.96316	53.22668
H	6.26108	-2.30411	37.93650	H	3.79533	7.71969	55.12302
H	17.60549	11.08009	47.57424	H	1.87732	6.12117	55.17602
C	17.79387	11.44923	46.57143	H	5.47082	7.56867	53.26388
C	18.55463	12.64061	46.39839	C	2.52584	6.15023	54.30804
H	18.94702	13.16963	47.25804	C	4.39506	6.04127	52.15956
C	18.68123	13.19448	45.09581	C	3.31183	5.12216	52.22548
H	19.14717	14.16559	44.97530	H	1.56010	4.45289	53.34420
C	18.07356	12.57129	43.97642	H	12.16540	0.90484	57.57870
C	17.31706	11.37750	44.17440	C	11.96892	0.05801	56.92947
C	17.21583	10.77783	45.45786	H	13.63738	0.49164	55.59984
H	16.61025	9.89109	45.60449	H	10.16569	-0.54732	58.00543
H	7.50276	15.37481	49.48190	C	12.80498	-0.16964	55.80623
C	7.59255	15.73663	48.46491	C	10.82247	-0.75864	57.16962
C	8.60315	16.68858	48.12442	C	12.45632	-1.19521	54.87781
H	9.28500	17.03871	48.89240	C	10.47615	-1.74804	56.21669
C	8.77644	17.12317	46.78604	C	11.30468	-1.99138	55.07554
H	9.57207	17.81335	46.53061	H	13.01712	-1.28777	53.95502
C	7.98993	16.51807	45.76289	H	9.53816	-2.28394	56.31727
H	8.20710	16.73964	44.72315	H	11.00148	-2.71147	54.32516
C	6.97673	15.57247	46.07836	Cl	3.96943	4.02449	56.33548
H	6.42151	15.08010	45.28970	Cl	11.15624	1.09572	52.91574

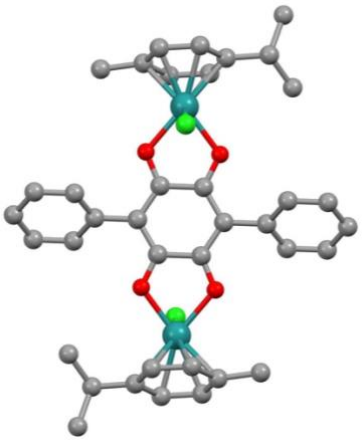

Figure S42. Optimized structure of **Ru$_2$(Ph$_2$dhbq)**. Protons omitted for clarity. Ru, Cl, O, and C atoms are represented as dark green, light green, red, and gray, respectively.

84
E(RB3LYP): –2880.135513 Hartree

C	7.20434	-2.42039	-2.51177
C	4.86701	0.04775	-2.39864
C	4.65942	1.42555	-2.16933
C	-0.74346	-4.74707	-2.10114
C	4.72612	-2.97606	-2.41279
C	0.24340	-5.58188	-1.57238
C	-0.80433	-3.40373	-1.72944
C	5.88832	-2.24358	-1.72422
C	5.63439	-0.76341	-1.48930
C	1.17139	-5.06113	-0.66777
C	5.17751	2.05924	-0.98692
C	0.12529	-2.86973	-0.82099
C	4.83879	3.49514	-0.68997
C	1.11483	-3.71802	-0.29480
C	1.20591	-0.62335	-0.38749
C	0.06255	-1.44174	-0.41776
C	6.15496	-0.12020	-0.34238
C	5.93996	1.27231	-0.09067
C	1.14382	0.82443	0.04389
C	-1.14382	-0.82443	-0.04389
C	-5.93996	-1.27231	0.09066
C	-6.15496	0.12020	0.34237
C	-0.06255	1.44173	0.41776
C	-1.20591	0.62334	0.38750
C	-1.11483	3.71802	0.29481
C	-4.83880	-3.49514	0.68996
C	-0.12529	2.86973	0.82099
C	-5.17752	-2.05924	0.98692
C	-1.17139	5.06112	0.66778
C	-5.63439	0.76341	1.48929
C	-5.88831	2.24359	1.72421
C	0.80433	3.40373	1.72945
C	-0.24340	5.58188	1.57239
C	-4.72611	2.97606	2.41278
C	0.74346	4.74706	2.10115
C	-4.65943	-1.42555	2.16933
C	-4.86702	-0.04775	2.39863
C	-7.20434	2.42040	2.51175
H	7.12817	-1.97113	-3.50964
H	4.37045	-0.42061	-3.24079
H	4.01761	1.98943	-2.83842
H	4.60714	-2.65904	-3.45645
H	-1.46775	-5.14045	-2.81031
H	7.42744	-3.48550	-2.64014
H	0.28888	-6.62861	-1.86253
H	8.05145	-1.95497	-1.99547
H	4.93075	-4.05207	-2.42809
H	-1.57217	-2.75974	-2.14598
H	3.77856	-2.81254	-1.89201
H	5.32838	4.15885	-1.41341
H	3.75753	3.65465	-0.75325
H	1.94059	-5.70297	-0.24523
H	-6.27317	-1.69905	-0.84817
H	6.02576	-2.69364	-0.73264
H	-6.64221	0.71619	-0.42176
H	1.83644	-3.31999	0.41172

H	-5.16568	-3.77789	-0.31394	H	-7.42744	3.48552	2.64013
H	5.16568	3.77789	0.31393	H	1.46775	5.14045	2.81031
H	-1.83644	3.31998	-0.41171	H	-4.60714	2.65904	3.45644
H	6.64222	-0.71619	0.42175	H	-4.01762	-1.98943	2.83842
H	-6.02575	2.69364	0.73262	H	-4.37046	0.42061	3.24079
H	6.27317	1.69906	0.84816	H	-7.12817	1.97114	3.50963
H	-1.94060	5.70297	0.24524	O	2.36112	-1.01631	-0.76817
H	-3.75754	-3.65466	0.75325	O	2.26031	1.44484	-0.01526
H	-5.32840	-4.15885	1.41340	O	-2.26031	-1.44484	0.01527
H	-3.77856	2.81254	1.89200	O	-2.36112	1.01631	0.76817
H	1.57218	2.75974	2.14598	Cl	-3.72864	0.46658	-1.92586
H	-4.93074	4.05207	2.42808	Cl	3.72865	-0.46658	1.92586
H	-8.05145	1.95498	1.99546	Ru	3.95335	0.27990	-0.37339
H	-0.28888	6.62861	1.86254	Ru	-3.95335	-0.27990	0.37339

7. Supplementary Crystallographic Data:

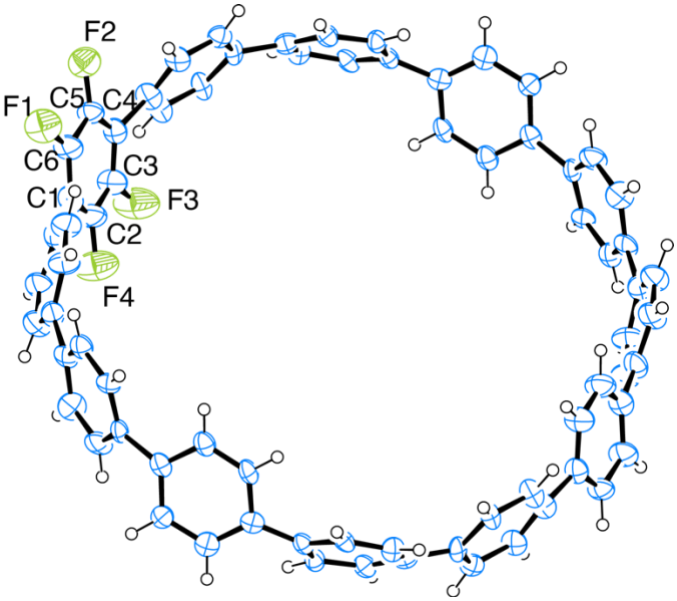

Figure S43. ORTEP of the single crystal structure of **4F-CPP**. Disorder and solvent are omitted for clarity. Thermal ellipsoids are rendered at the 50% probability level.

Table S2. Crystallographic parameters for the single crystal structure of **4F-CPP**.

Empirical formula	C72 H44 F4	
Formula weight	985.07	
Temperature	100(2) K	
Wavelength	0.7288 Å	
Crystal system	Monoclinic	
Space group	P $2_1/c$	
Unit cell dimensions	a = 19.7037(19) Å	α = 90˚
	b = 8.3789(8) Å	β = 108.289(3)˚
	c = 21.004(2) Å	γ = 90˚
Volume	3292.4(6) $Å^3$	
Z	2	
Density (calculated)	0.994 Mg/m^3	
Absorption coefficient	0.068 mm^{-1}	
F(000)	1024	
Crystal size	0.300 x 0.090 x 0.040 mm^3	
Theta range for data collection	2.041 to 27.106˚	
Index ranges	$-24 \leq h \leq 22, 0 \leq k \leq 10, 0 \leq l \leq 26$	

Reflections collected	6324
Independent reflections	6324 [R_{int} = 0.0408]
Completeness to theta = 25.930˚	98.8%
Refinement method	Full-matrix least-squares on F^2
Data / restraints / parameters	6324 / 180 / 362
Goodness-of-fit on F^2	1.033
Final R indices [I>2sigma(I)]	R1 = 0.0706, wR2 = 0.2148
R indices (all data)	R1 = 0.0802, wR2 = 0.2240
Largest diff. peak and hole	0.592 and –0.362 e $Å^{-3}$

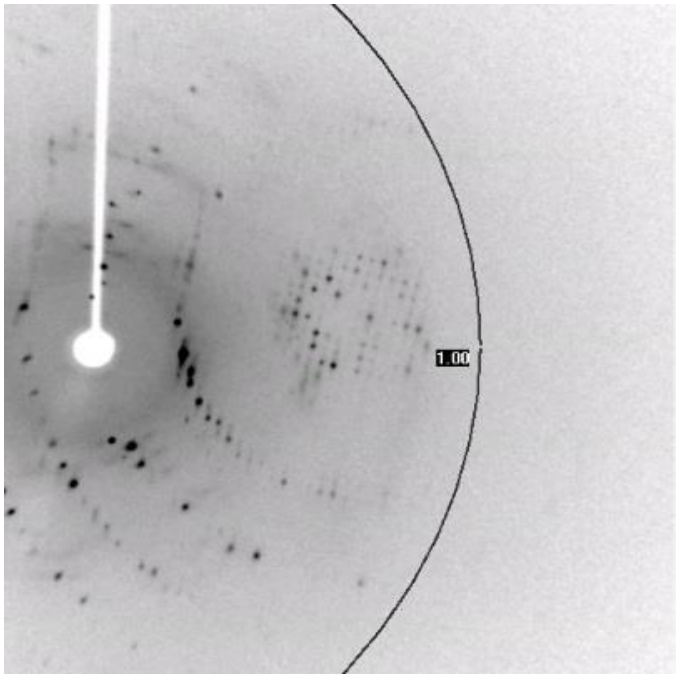

Figure S44. Example of the diffraction pattern observed while collecting the single crystal structure of **4MeO-CPP**.

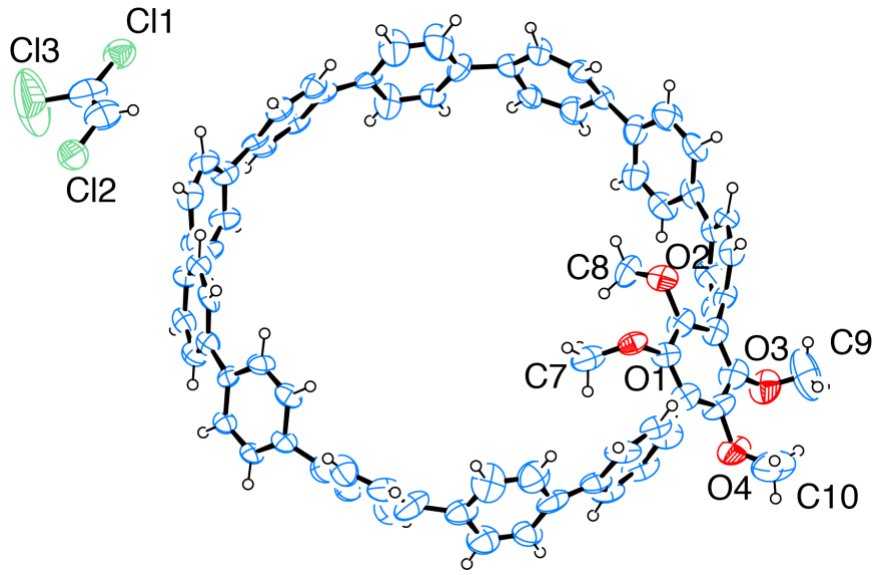

Figure S45. ORTEP of the single crystal structure of **4MeO-CPP** with one refined trichloroethylene solvent molecule. Thermal ellipsoids are rendered at the 50% probability level.

Table S3. Crystallographic parameters for the single crystal structure of **4MeO-CPP**.

Empirical formula	C78 H57 Cl3 O4 [+ solvent]	
Formula weight	1164.58	
Temperature	100(2) K	
Wavelength	0.71073 Å	
Crystal system	Orthorhombic	
Space group	F d d 2	
Unit cell dimensions	a = 57.683(4) Å	α = 90˚
	b = 12.1111(8) Å	β = 90˚
	c = 50.915(3) Å	γ = 90˚
Volume	35569(4) $Å^3$	
Z	16	
Density (calculated)	0.870 Mg/m^3	
Absorption coefficient	0.139 mm^{-1}	
F(000)	9728	
Crystal size	0.600 x 0.150 x 0.090 mm^3	
Theta range for data collection	2.027 to 25.027˚	
Index ranges	$-68 \leq h \leq 68$, $-14 \leq k \leq 14$, $-60 \leq l \leq 60$	
Reflections collected	101139	
Independent reflections	15535 [R_{int} = 0.1097]	
Completeness to theta = 25.027˚	99.2 %	
Refinement method	Full-matrix least-squares on F^2	
Data / restraints / parameters	15535 / 1003 / 786	
Goodness-of-fit on F^2	1.050	
Final R indices [I>2sigma(I)]	R1 = 0.1202, wR2 = 0.3064	
R indices (all data)	R1 = 0.1800, wR2 = 0.3545	
Absolute structure parameter	0.6(2)	
Largest diff. peak and hole	0.430 and –0.472 e $Å^{-3}$	

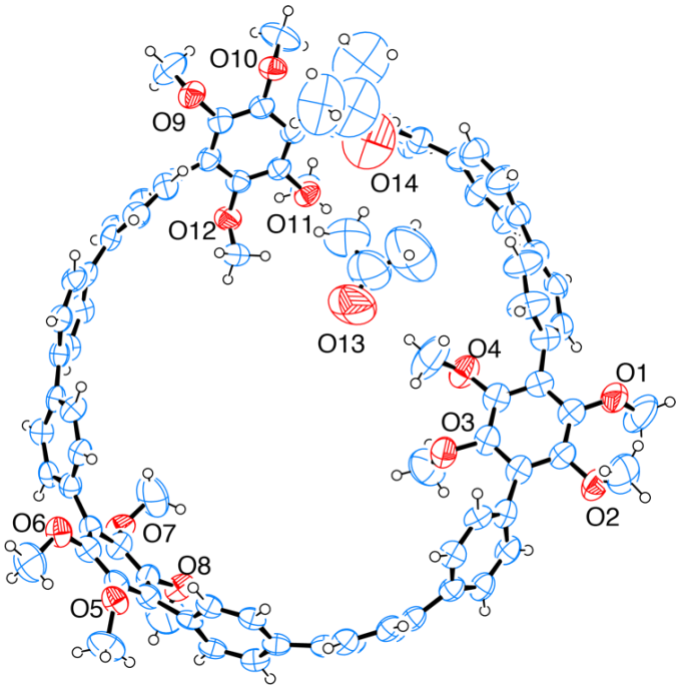

Figure S46. ORTEP of the single crystal structure of **12MeO-CPP** with two refined acetone solvent molecules. Disorder of one acetone (O14…) is omitted for clarity. Thermal ellipsoids are rendered at the 50% probability level.

Table S4. Crystallographic parameters for the single crystal structure of **12MeO-CPP**.

Empirical formula	C90 H84 O14	
Formula weight	1389.57	
Temperature	100(2) K	
Wavelength	0.7288 Å	
Crystal system	Monoclinic	
Space group	P $2_1/n$	
Unit cell dimensions	a = 20.514(3) Å	α = 90°
	b = 9.4966(13) Å	β = 104.097(5)°
	c = 39.416(6) Å	γ = 90°
Volume	7447.4(18) $Å^3$	
Z	4	
Density (calculated)	1.239 Mg/m^3	
Absorption coefficient	0.086 mm^{-1}	
F(000)	2944	
Crystal size	0.200 x 0.100 x 0.100 mm^3	
Theta range for data collection	2.456 to 25.709°	

Index ranges	$-24 \leq h \leq 23, -11 \leq k \leq 11, 0 \leq l \leq 46$
Reflections collected	25207
Independent reflections	13026 [R_{int} = 0.0251]
Completeness to theta = 25.709˚	99.0 %
Refinement method	Full-matrix least-squares on F^2
Data / restraints / parameters	13026 / 639 / 969
Goodness-of-fit on F^2	1.062
Final R indices [I>2sigma(I)]	R1 = 0.1274, wR2 = 0.2752
R indices (all data)	R1 = 0.1445, wR2 = 0.2820
Extinction coefficient	0.0276(17)
Largest diff. peak and hole	0.488 and –0.362 e $Å^{-3}$

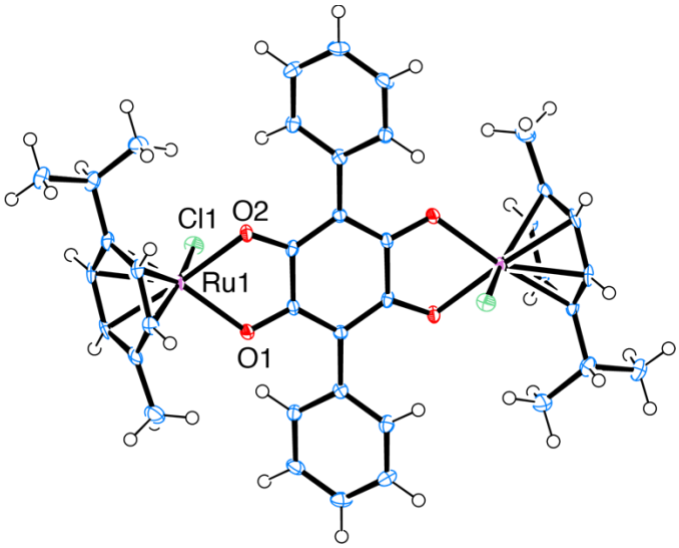

Figure S47. ORTEP of the single crystal structure of **Ru_2(Ph_2dhbq)**. Thermal ellipsoids are rendered at the 50% probability level.

Table S5. Crystallographic parameters for the single crystal structure of **Ru_2(Ph_2dhbq)**.

Empirical formula	C38 H38 Cl2 O4 Ru2	
Formula weight	831.72	
Temperature	100(2) K	
Wavelength	0.71073 Å	
Crystal system	Monoclinic	
Space group	P 21/n	
Unit cell dimensions	a = 11.6451(7) Å	α = 90˚
	b = 10.9012(6) Å	β = 109.990(3)˚
	c = 14.0135(7) Å	γ = 90˚
Volume	1671.77(16) $Å^3$	
Z	2	
Density (calculated)	1.652 Mg/m^3	
Absorption coefficient	1.104 mm^{-1}	
F(000)	840	
Crystal size	0.090 x 0.060 x 0.050 mm^3	
Theta range for data collection	1.972 to 28.357˚	
Index ranges	$-15 \le h \le 15$, $-14 \le k \le 14$, $-18 \le l \le 18$	
Reflections collected	16214	
Independent reflections	4178 [R_{int} = 0.0744]	

Completeness to theta = 25.000˚	100.0 %
Refinement method	Full-matrix least-squares on F^2
Data / restraints / parameters	4178 / 0 / 211
Goodness-of-fit on F^2	1.015
Final R indices [I>2sigma(I)]	R1 = 0.0307, wR2 = 0.0582
R indices (all data)	R1 = 0.0525, wR2 = 0.0653
Largest diff. peak and hole	0.576 and –0.972 e $Å^{-3}$

8. References:

(1) Leonhardt, E. J.; Van Raden, J. M.; Miller, D.; Zakharov, L. N.; Alemán, B.; Jasti, R. A Bottom-Up Approach to Solution-Processed, Atomically Precise Graphitic Cylinders on Graphite. *Nano Lett.* **2018**, *18* (12), 7991–7997. https://doi.org/10.1021/acs.nanolett.8b03979.

(2) Van Raden, J. M.; Leonhardt, E. J.; Zakharov, L. N.; Pérez-Guardiola, A.; Pérez-Jiménez, A. J.; Marshall, C. R.; Brozek, C. K.; Sancho-García, J. C.; Jasti, R. Precision Nanotube Mimics via Self-Assembly of Programmed Carbon Nanohoops. *J. Org. Chem.* **2020**, *85* (1), 129–141. https://doi.org/10.1021/acs.joc.9b02340.

(3) C. Lovell, T.; E. Colwell, C.; N. Zakharov, L.; Jasti, R. Symmetry Breaking and the Turn-on Fluorescence of Small, Highly Strained Carbon Nanohoops. *Chemical Science* **2019**, *10* (13), 3786–3790. https://doi.org/10.1039/C9SC00169G.

(4) Kamin, A. A.; Moseley, I. P.; Oh, J.; Brannan, E. J.; Gannon, P. M.; Kaminsky, W.; Zadrozny, J. M.; Xiao, D. J. Geometry-Dependent Valence Tautomerism, Magnetism, and Electrical Conductivity in 1D Iron–Tetraoxolene Chains. *Chem. Sci.* **2023**. https://doi.org/10.1039/D2SC06392A.

(5) Garci, A.; Mbakidi, J.-P.; Chaleix, V.; Sol, V.; Orhan, E.; Therrien, B. Tunable Arene Ruthenium Metallaprisms to Transport, Shield, and Release Porphin in Cancer Cells. *Organometallics* **2015**, *34* (16), 4138–4146. https://doi.org/10.1021/acs.organomet.5b00555.

(6) Morisaki, Y.; Tsuji, Y.; Chujo, Y. Synthesis of Cyclic Compounds Consisting of Face-to-Face p-Oligophenyls. *Tetrahedron Letters* **2014**, *55* (9), 1631–1634. https://doi.org/10.1016/j.tetlet.2014.01.093.

(7) Bruker (2007). APEX2 (Version 2.1-4), SAINT (Version 7.34A), SADABS (Version 2007/4). BrukerAXS Inc., Madison, Wisconsin, USA.

(8) Sheldrick, G. M. A Short History of SHELX. *Acta Cryst A* **2008**, *64* (1), 112–122. https://doi.org/10.1107/S0108767307043930.

(9) Sheldrick, G. M. SHELXT – Integrated Space-Group and Crystal-Structure Determination. *Acta Cryst A* **2015**, *71* (1), 3–8. https://doi.org/10.1107/S2053273314026370.

(10) SHELDRICK, G. M. SHELXL-97, Program for the Solution of Crystal Structures. *University of Göttingen, Germany.* **1997**.

(11) Sheldrick, G. M. Crystal Structure Refinement with SHELXL. *Acta Cryst C* **2015**, *71* (1), 3–8. https://doi.org/10.1107/S2053229614024218.

(12) Waasmaier, D.; Kirfel, A. New Analytical Scattering-Factor Functions for Free Atoms and Ions. *Acta Cryst A* **1995**, *51* (3), 416–431. https://doi.org/10.1107/S0108767394013292.

(13) Spek, A. L. Single-Crystal Structure Validation with the Program PLATON. *J Appl Cryst* **2003**, *36* (1), 7–13. https://doi.org/10.1107/S0021889802022112.

(14) Spek, A. L. Structure Validation in Chemical Crystallography. *Acta Cryst D* **2009**, *65* (2), 148–155. https://doi.org/10.1107/S090744490804362X.

(15) van der Sluis, P.; Spek, A. L. BYPASS: An Effective Method for the Refinement of Crystal Structures Containing Disordered Solvent Regions. *Acta Cryst A* **1990**, *46* (3), 194–201. https://doi.org/10.1107/S0108767389011189.

(16) Gaussian 16, Revision B.01. M.J. Frisch et al. Gaussian, Inc. Wallingford CT, 2016.

(17) Becke, A. D. Density-functional Thermochemistry. III. The Role of Exact Exchange. *J. Chem. Phys.* **1993**, *98* (7), 5648–5652. https://doi.org/10.1063/1.464913.

(18) Stephens, P. J.; Devlin, F. J.; Chabalowski, C. F.; Frisch, M. J. Ab Initio Calculation of Vibrational Absorption and Circular Dichroism Spectra Using Density Functional Force Fields. *J. Phys. Chem.* **1994**, *98* (45), 11623–11627. https://doi.org/10.1021/j100096a001.
(19) Lee, C.; Yang, W.; Parr, R. G. Development of the Colle-Salvetti Correlation-Energy Formula into a Functional of the Electron Density. *Phys. Rev. B* **1988**, *37* (2), 785–789. https://doi.org/10.1103/PhysRevB.37.785.
(20) Hertwig, R. H.; Koch, W. On the Parameterization of the Local Correlation Functional. What Is Becke-3-LYP? *Chemical Physics Letters* **1997**, *268* (5), 345–351. https://doi.org/10.1016/S0009-2614(97)00207-8.
(21) Dunning, Thom. H.; Hay, P. J. Gaussian Basis Sets for Molecular Calculations. In *Methods of Electronic Structure Theory*; Schaefer, H. F., Ed.; Springer US: Boston, MA, 1977; pp 1–27. https://doi.org/10.1007/978-1-4757-0887-5_1.
(22) Hay, P. J.; Wadt, W. R. Ab Initio Effective Core Potentials for Molecular Calculations. Potentials for the Transition Metal Atoms Sc to Hg. *J. Chem. Phys.* **1985**, *82* (1), 270–283. https://doi.org/10.1063/1.448799.
(23) Hay, P. J.; Wadt, W. R. Ab Initio Effective Core Potentials for Molecular Calculations. Potentials for K to Au Including the Outermost Core Orbitals. *J. Chem. Phys.* **1985**, *82* (1), 299–310. https://doi.org/10.1063/1.448975.
(24) Hehre, W. J.; Ditchfield, R.; Pople, J. A. Self—Consistent Molecular Orbital Methods. XII. Further Extensions of Gaussian—Type Basis Sets for Use in Molecular Orbital Studies of Organic Molecules. *J. Chem. Phys.* **1972**, *56* (5), 2257–2261. https://doi.org/10.1063/1.1677527.
(25) Hariharan, P. C.; Pople, J. A. Accuracy of AH n Equilibrium Geometries by Single Determinant Molecular Orbital Theory. *Molecular Physics* **1974**, *27* (1), 209–214. https://doi.org/10.1080/00268977400100171.
(26) Francl, M. M.; Pietro, W. J.; Hehre, W. J.; Binkley, J. S.; Gordon, M. S.; DeFrees, D. J.; Pople, J. A. Self-consistent Molecular Orbital Methods. XXIII. A Polarization-type Basis Set for Second-row Elements. *J. Chem. Phys.* **1982**, *77* (7), 3654–3665. https://doi.org/10.1063/1.444267.
(27) Rassolov, V. A.; Ratner, M. A.; Pople, J. A.; Redfern, P. C.; Curtiss, L. A. 6-31G* Basis Set for Third-Row Atoms. *Journal of Computational Chemistry* **2001**, *22* (9), 976–984. https://doi.org/10.1002/jcc.1058.
(28) Weigend, F.; Ahlrichs, R. Balanced Basis Sets of Split Valence, Triple Zeta Valence and Quadruple Zeta Valence Quality for H to Rn: Design and Assessment of Accuracy. *Phys. Chem. Chem. Phys.* **2005**, *7* (18), 3297–3305. https://doi.org/10.1039/B508541A.